The Institute of Paper Chemistry

Appleton, Wisconsin

Doctor's Dissertation

An Investigation of the Streaming Current Method for Determining the Zeta Potential of Fibers

John A. Ciriacks

June, 1967

AN INVESTIGATION OF THE STREAMING CURRENT METHOD FOR DETERMINING THE ZETA POTENTIAL OF FIBERS

A thesis submitted by

John A. Ciriacks

B.S.(Ch.E.) 1958, University of Wisconsin
M.S. 1964, Lawrence University

in partial fulfillment of the requirements
of The Institute of Paper Chemistry
for the degree of Doctor of Philosophy
from Lawrence University,
Appleton, Wisconsin

June, 1967

TABLE OF CONTENTS

SUMMARY

A relationship between the zeta potential and the streaming current from mats of cylindrical fibers was derived using the flow model developed by Happel (31). Applying experimental data to this relationship resulted in constant values for the zeta potential at various mat porosities (void fractions) in the range 0.60 to 0.85 and at electrolyte concentrations of 1-4 x 10^{-4} molar KCl and 0.5-2 x 10^{-4} M $CaCl_2$. The new streaming current relationship represents an improvement over the usual capillary-flow-model approach to the streaming current phenomenon in fiber mats. With the latter approach, a systematic increase in calculated zeta potentials as a function of increasing porosity was noted in this study, as well as in the streaming current studies of Neale and Peters (21) and Mason and coworkers (22, 26).

The major assumptions used to develop the new streaming current model were as follows:

(1) The Gouy-Chapman theory for the diffuse portion of the electric double layer at equilibrium conditions can be applied to the nonequilibrium conditions of electrokinetics;

(2) The flow equations developed by Happel from a free-surface model give an adequate description of the velocity very close to the surface of cylindrical fibers which are arranged in concentrated assemblages and are oriented perpendicular to the approaching velocity;

(3) The dominant means of counter-ion transport in the fiber mats is by liquid flow (i.e., the rate of charge transport to the fiber surfaces from the bulk of the liquid by ion migration in an electric field, or by ion diffusion is small compared to the rate of charge transport by liquid flow).

An analysis was made of the counter-ion transport process. Calculations based on several simplifying assumptions regarding mat geometry, ion migration, and ion diffusion indicated that liquid flow was the dominant means of transport.

A reproducible experimental system was developed using silver-silver chloride electrodes to measure the streaming current produced by liquid permeation of 3-inch diameter mats of dacron fibers. Results indicated that zeta potential changes as a function of electrolyte concentration were similar to those reported in the literature.

Reproducibility between runs was not obtained with mats of nylon fibers, although the zeta potentials calculated within a run were as consistent as those with dacron fiber mats. The reason for this variability with nylon fibers is not clear; there were indications that it might relate to the length of time the fibers equilibrated in the dilute electrolyte solutions. Even with the reproducible dacron-fiber system, low streaming current readings were observed during the first two runs with electrodes which were newly anodized or had been idle for several weeks. These low current readings may indicate a lack of equilibrium conditions in the structure of the Ag-AgCl electrodes during the first two runs in a series of 6 to 14 runs with a particular pair of electrodes.

The streaming current data appeared to be quite sensitive to fiber orientation in the mat. Fiber orientation was used to explain the difference in the extent of zeta potential variation as a function of porosity between this study and studies which used 1-inch diameter fiber mats (22, 26). The sensitivity to fiber orientation emphasizes the anisotropic character of fiber mats. Happel and Brenner (25) concluded that the capillary-model (Kozeny-Carman) concept can be applied only to isotropic porous media, where orientation effects are absent.

Suggestions for future work include additional experimental methods of testing the new streaming current model, a possible first step to extend the present approach to the streaming current phenomenon to noncylindrical fibers, and work to further establish the effect of fiber orientation on the streaming current.

INTRODUCTION

Scientific inquiry of electrokinetic effects dates back as far as 1808 when Reuss (1) observed that water began to flow through a porous plug of wet clay or sand if a potential difference was maintained across the plug. In addition to this electroosmotic effect observed by Reuss, electrokinetics includes the streaming potential/current effect, in which a potential develops due to an imposed liquid flow at solid-liquid interfaces.

One requirement for a quantitative approach to electrokinetic phenomena is an accurate description of the ion distribution within the electric double layer which develops in the liquid at the solid-liquid interface. Most solid materials which contact a liquid develop an electrical charge at the surface due to mechanisms such as ionization of the solid or ion adsorption from the liquid. In order to compensate for the charged surface, a layer of oppositely charged counter ions forms within a very thin (several hundred Ångström units thick) region in the liquid at the interface. These two layers of opposite charge constitute the electric double layer.

A second requirement for a sound theoretical approach to electrokinetics calls for a valid model to describe flow past the solid-liquid interface. Both of these requirements are analyzed in the Literature Review. The need for an adequate flow model is the primary argument in the present investigation, where the Happel model for flow perpendicular to assemblages of cylinders is used to revise the usual capillary-model approach to the analysis of streaming currents from fiber mats.

A brief introduction to the zeta or electrokinetic potential is in order since the variation of this often mentioned, sometimes maligned, quantity with

fiber-mat porosity will be used to judge the adequacy of streaming current models. The potential drop across that portion of the electric double layer known as the diffuse layer will be represented by ψ_δ. The experimentally determined zeta potential (ζ) will be equal to or less than ψ_δ depending upon the validity of the particular electrokinetic model, as will be discussed later.

Controversy over the zeta potential arises when its application to practical systems is discussed, as well as when the theoretical model or experimental technique is examined. Considerable success has been achieved in qualitatively relating the stability of colloidally dispersed hydrophobic particles to the zeta potential of the particles. A high ζ for colloidal particles of like charge denotes a large repulsive energy barrier between particles, and, therefore, a stable dispersion with a very slow rate of coagulation (flocculation).

Sennett and Olivier (2), who give a good review of electrokinetic effects and the concept of the zeta potential, discuss several cases where the zeta potential has been related to properties of practical systems, e.g., flotation of mineral particles and clarification of water. However, it should be noted that the behavior of these and other practical systems may be influenced by factors which are not necessarily reflected as zeta potential changes, e.g., adsorption of a nonionic polymer.

LITERATURE REVIEW

The comment has been made that electrokinetic effects are among the easiest to detect and the most difficult to interpret (3). This literature review is directed at interpretations of streaming current results from fiber mats. The present concept of the electric double layer is examined. Then a review of streaming current studies with fiber plugs is presented with emphasis on the variation in calculated zeta potentials as the void fraction (porosity) of the fiber mat is changed; the zeta potential is a function of the charge on a solid surface and should not change as the porosity of a given fiber mat is varied.

The zeta or electrokinetic potential (ζ) will be defined as the experimentally obtained value for the potential drop across the diffuse layer portion of the electric double layer. The relation of ζ to ψ_δ depends upon the validity of the models used to derive the electrokinetic equations. In other words, meaningful zeta potentials can be calculated when the equations describing both charge distribution near the solid-liquid interface and fluid velocity in the same region are valid with respect to the system being examined.

ELECTRIC DOUBLE LAYER

DOUBLE LAYER MODEL

It will be helpful to examine the present concept of the electric double layer. Several recent reviews of electric-double-layer theory are available (2, 4-6). Briefly, the theoretical development started in 1879 with the Helmholtz capacitor model, which pictured a layer of counter ions parallel to a charged surface (7). A model which described a diffuse layer of mobile counter ions was proposed independently by Gouy (8) and Chapman (9). In 1924 Stern (10) modified

the theory to include an immobile, inner region of adsorbed ions. The Gouy-Chapman-Stern model is the basis of the present electric-double-layer concept. In the intervening years, however, some modification of the theory has been made particularly with respect to the immobile Stern layer (11-13).

The electric double layer representation in Fig. 1 is based on the Grahame-Devanthan (11, 12) model as described by Levine, Mingins, and Bell (14) in 1965. The Stern layer of adsorbed ions lies between the charged surface and the outer Helmholtz plane (O.H.P.), which is defined as the mean plane of closest approach of diffuse-layer ions to the interface. Thus, the diffuse layer of mobile ions extends from the O.H.P. out to the bulk solution, where the concentrations of anions and cations are such that the region is electrically neutral. Theoretically, the distance is infinite since the potential (ψ) vs. distance curve is exponential. However, in this study the diffuse layer thickness (τ) is designated as the distance at which $\psi = 0.001\psi_\delta$, where ψ_δ is the mean potential at the O.H.P. The mean potential at the interface is represented by ψ_o. The distance (δ) between the interface and the O.H.P. depends on factors such as the ion concentration, the type of counter ions, and the magnitude of ψ_o (14).

The preceding discussion provides a foundation for evaluating the meaning of the zeta potential calculated from electrokinetic data. Obviously, if the hydrodynamic shear plane coincides with the outer Helmholtz plane and if the electrokinetic equations are valid, $\zeta = \psi_\delta$. However, a number of factors, some of which are not well understood, may cause a discrepancy between the calculated ζ and ψ_δ of the model. The largest differences between ζ and ψ_δ occur when the surface potential is high and electrolyte concentration (c) is also large ($c > 10^{-3}$ moles per liter for a 1-1 electrolyte), according to Haydon (4) and Lyklema and Overbeek (15). Reasons for differences between ζ and ψ_δ are discussed below.

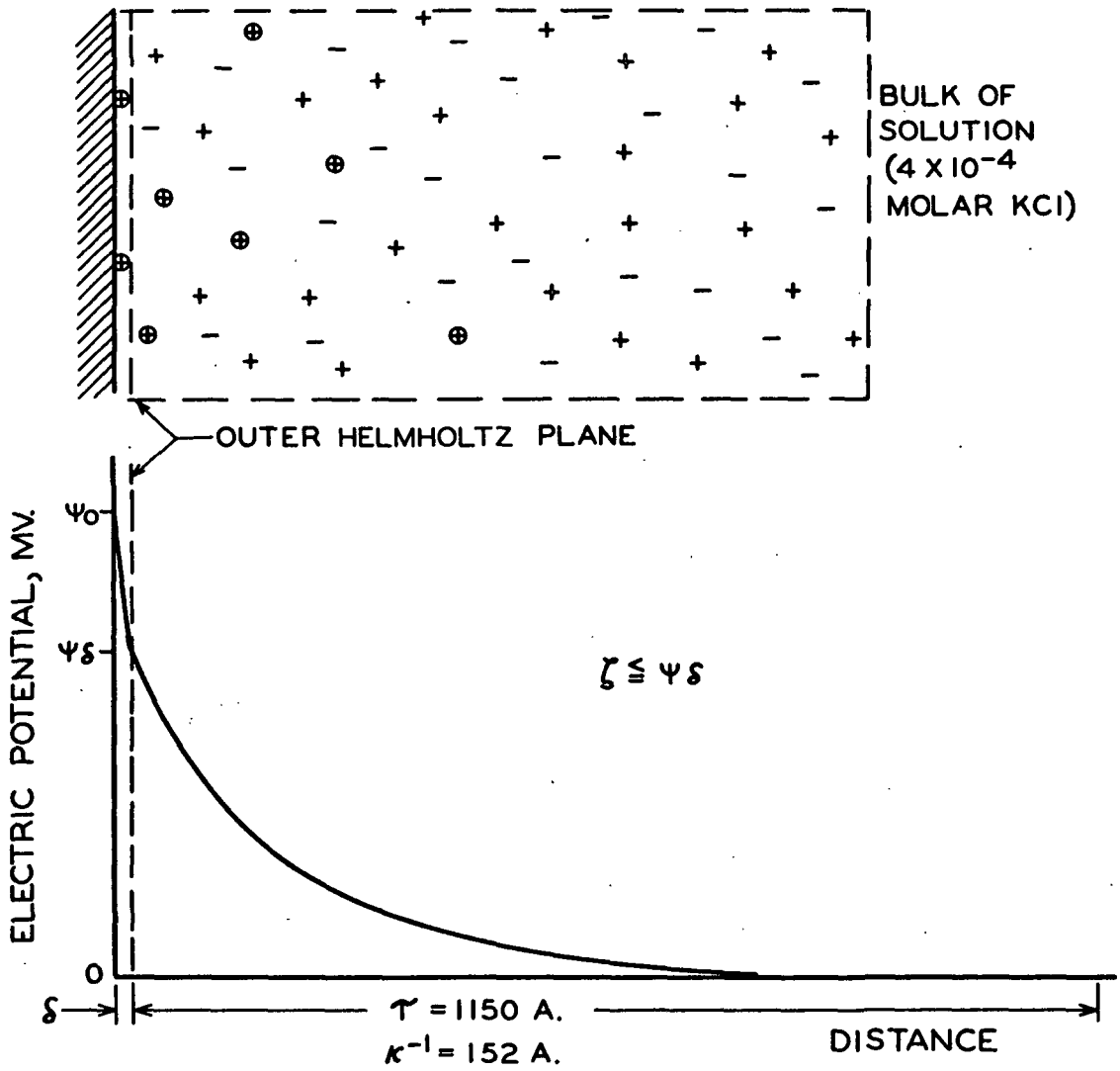

ψ_δ = POTENTIAL AT PLANE OF CLOSEST APPROACH OF COUNTER ION CENTERS ≥ ZETA POTENTIAL (ζ)

ψ_o = POTENTIAL AT SOLID SURFACE

δ = THICKNESS OF IMMOBILE STERN LAYER

τ = THICKNESS OF DIFFUSE LAYER (SEE DEFINITION ON P. 7)

κ = DEBYE-HÜCKEL CONSTANT

Figure 1a. Ions Within Electric Double Layer at a Solid Surface (400 A. x 400 A.) Which has a Negative Charge. The Counter Ions (Circled Positive Ions) Correspond in Number to the Negative Charges on the Solid Surface. The Boltzmann Equation [Eq. (11)] was used to Calculate the Number of Positive and Negative Ions for ψ_δ = -13 mv.

Figure 1b. Potential vs. Distance from the Solid Surface; Refer to Equation (19) for ψ vs. r within the diffuse layer

CONDITIONS FOR MEANINGFUL ZETA POTENTIALS

The experimental conditions under which the calculated zeta potentials have meaning in relation to the electric-double-layer model will be covered by examining (1) viscosity variation near the interface, (2) liquid immobilization at the interface, (3) the validity of the equations used to calculate ζ, and (4) nonequilibrium double layers.

Viscosity Variation Within the Diffuse Layer

Variable viscosity of water in the diffuse layer due to the electric field strength was used by Lyklema and Overbeek (15) to correct zeta potentials calculated from electrophoresis data. However, these corrections became important only at high electrolyte concentration. At $c < 10^{-3}$ moles per liter of a 1-1 electrolyte and $\psi_\delta < 100$ mv., the calculated $\zeta \cong \psi_\delta$. Thus, the usual assumption that the diffuse layer viscosity equals that of the bulk solution appears valid at low potentials and low salt concentrations.

The fact that there are no data for the viscosity of water in the presence of an electric field (15) indicates that viscosity corrections to electrokinetic data are in an early stage of evolution. Viscoelectric constants for organic liquids were used by Lyklema and Overbeek (15) to estimate the constant for water. Stigter (15a) concluded that Lyklema and Overbeek's viscoelectric effect was overestimated. Davies and Rideal (6) also discuss viscosity changes within the electric double layer, although not as extensively as Lyklema and Overbeek.

Liquid Immobilization at Interface

It is possible that several layers of water are immobilized at the solid-liquid interface. In this case, the hydrodynamic shear layer would be located at a greater distance from the interface than the outer Helmholtz plane.

Lyklema and Overbeek (15) treated this case assuming a distance of 10 A. between the shear layer and the O.H.P. for a 1-1 electrolyte and also assuming that there is no specific adsorption of ions in the Stern layer. Calculations showed that $\zeta \cong \psi_\delta$ at $\underline{c} < 10^{-3}\underline{M}$ and $\psi_\delta < 50$ mv.

Validity of the Poisson-Boltzmann Equation

In the Gouy-Chapman-Stern model for the electric double layer, the Poisson-Boltzmann equation is used to describe the distribution of ions in relation to the mean potential. Despite several limiting assumptions, the Poisson-Boltzmann equation appears to be a reasonable approximation for 1-1 electrolyte concentrations $< 0.01\underline{M}$ if $\psi_\delta < 100$ mv., or $\underline{c} < 0.1\underline{M}$ if $\psi_\delta < 50$ mv. (14, 4).

The limitations of the Poisson-Boltzmann equation include the following assumptions: (1) Ions are point charges, i.e., no allowance needs to be made for ion volume; (2) the dielectric properties are uniform throughout the diffuse layer; (3) the self-atmosphere effect is negligible; (4) ion-polarization effects are negligible. Haydon (4) discusses these limitations.

For $\underline{c} > 0.01\underline{M}$ and $\psi_\delta > 100$ mv., the ionic volume correction will probably become larger than the other corrections, and the size of the ion volume correction depends on which ion radius is assumed, e.g., 2 to 6 A. (4). Dielectric saturation may also increase rapidly under these conditions (4, 15). The corrections work in a positive direction, i.e., ψ_δ is greater than predicted from the Poisson-Boltzmann equation.

The self-atmosphere effect of the counter ions in the diffuse layer accounts for the free energy of interaction between neighboring ions. This effect, which reduces the potential from the Poisson-Boltzmann equation prediction, becomes less important at high electrolyte concentrations (4).

An extra energy term in the Boltzmann equation must be considered if ion polarization is significant. An ion becomes polarized when it is transferred from the bulk phase where the external electric field is zero to a point of finite electric field in the diffuse layer (4). The effect of both ion-polarization and self-atmosphere reduces the potential from the Poisson-Boltzmann equation prediction, while ionic volume and dielectric saturation cause increased potential.

In addition to a valid model for the distribution of counter ions within the electric double layer, it must be reemphasized that an accurate model for liquid flow in the same region is needed if ζ is to approximate ψ_δ. The capillary model for flow through porous media will be examined later in a section on streaming current measurements.

Nonequilibrium Double Layer

Before leaving the Gouy-Chapman approach to the diffuse layer, it should be noted that this approach is for a diffuse layer at equilibrium. Delahay (5) reviewed the literature on nonequilibrium double layers in which current was flowing. It was concluded that the double-layer structure was changed very little by current flow, except at very high current (5). Sparnaay (16) reached a similar conclusion based on calculations for the two cases of liquid flow perpendicular to a porous electrode and current flowing through the diffuse layer.

Résumé

In summary, it appears at this stage in the development of electric-double-layer theory that the uncorrected Poisson-Boltzmann equation is a reasonable approximation for 1-1 electrolyte concentrations (c) < 0.01 mole per liter and ψ_δ < 100 mv. (14, 4). The application of the present theory to the nonequilibrium condition of current flowing through the diffuse layer appears valid, but application to the case of liquid flowing through the diffuse layer is less certain. In addition,

the possible effects of viscosity variation within the diffuse layer and liquid immobilization near the outer Helmholtz plane may require that c be less than 0.01 molar and ψ_δ be less than 50 mv. in order that ζ calculated from classical electrokinetic equations approximate ψ_δ (15, 15a).

The comment of Delahay (5) concerning the present double-layer theory is an appropriate conclusion of this section. He pointed out that a fundamentally new approach may be better than repeated modification of the Gouy-Chapman theory. Buff and Stillinger's (17) work on a statistical mechanical theory of double-layer structure and properties was cited by Delahay as a step in this direction.

STREAMING CURRENT MEASUREMENTS

It is important that a valid hydrodynamic flow model be applied to the analysis of electrokinetic phenomena. The flow equations are well established for simple systems such as uniform-diameter capillaries, but hydrodynamic theory is still evolving for fluid transport through plugs of particles, e.g., fiber mats. A review of streaming current studies with fiber mats follows. The generally accepted streaming current model, which is based on the capillary flow model, will be examined in order to explain the unexpected variation of the calculated zeta potential as the void fraction of the fiber mat is changed.

COMPARISON OF THE STREAMING CURRENT AND STREAMING POTENTIAL METHODS

The streaming current method employs a low resistance galvanometer to measure the current flowing between electrodes, while a high resistance potentiometer is placed across the electrodes during streaming potential measurements. The latter method is still used with plugs of particles by some workers (18, 19). The advantage of the method is that very little current flows through the electrodes. It is necessary, however, to accurately determine the electrical resistance of the

plug when the streaming potential method is used. And in establishing the resistance, it is impossible to theoretically calculate a correction for surface conductance in a plug with "pores" of varying shape (20).

The plug resistance can be measured when liquid flow is stopped at the completion of a streaming potential determination. However, it must be assumed that the back conductance through the plug, including surface conductance which is important at 1-1 electrolyte concentrations less than 10^{-3} molar, is the same under static conditions as it is under the dynamic conditions of streaming potential measurements.

Neale and Peters (21) used a method which measured the electrical resistance of fiber plugs under dynamic conditions. The streaming potential method was abandoned, however, in favor of streaming current measurements, which simplified the experimental procedure. Since experimental simplification was the only reason given, it is implied that the dynamically measured resistance could be used to calculate comparable currents in both the streaming potential and the streaming current methods.

Current passing through the electrodes did not cause electrode problems according to Neale and Peters (21). The silver-silver chloride electrodes in the 1.23-cm. diameter cell did not "polarize excessively" and gave reproducible readings.

Goring and Mason (22) adopted the streaming current method because it was more sensitive than the streaming potential procedure at low plug resistances. Comparing results from the same fiber mat, Goring and Mason concluded that the current calculated from streaming potential data (I = potential/plug resistance) equaled that measured with the streaming current method, provided that a direct

current (d.c.) technique was used to find the mat resistance. When measuring the resistance of sulfite pulp fiber mats with a 1000-cycle per second resistance bridge method, a dispersion effect produced resistance values which were too low. It should be noted that subsequent work by Mossman and Mason (23) showed that no low-frequency dispersion effect existed (i.e., $\underline{R}_{1000\ c.p.s.} = \underline{R}_{d.c.}$) for nylon, orlon, dacron, and glass fibers, which exhibit little or no swelling in water.

It is concluded that the streaming current and streaming potential methods yield comparable results when the experimental technique for measuring electrical resistance is chosen carefully.

DISCREPANCIES BETWEEN THEORY AND EXPERIMENT

The primary concern of the present study involves the variation of calculated zeta potentials as the void fraction of a fiber mat is changed. In the classical approach to the streaming current/potential phenomenon with porous media, the streaming current produced by liquid flow through a uniform-diameter capillary is used to estimate the total current from the numerous pores or capillaries in a porous bed (refer to discussion in 24, 22, 20). In other words, it is assumed that the Kozeny-Carman concept of a porous bed as a bundle of capillaries with a common radius ($\underline{m}$) can be applied to electrokinetic phenomena in porous media. The mean hydraulic radius ($\underline{m}$) equals the ratio of the volume filled with liquid to the wetted surface area (25).

The following streaming current equation was derived using the capillary-model or mean-hydraulic-radius approach (see Appendix I for derivation).

$$In L/(\Delta PD) = -\{A\zeta/[4\pi(L_e/L)^2]\}(1-\alpha c_1) \qquad (1),$$

where

$\underline{I}$ = streaming current,

η = viscosity of the bulk of the permeant,

$\underline{L}$ = mat thickness,

$\Delta\underline{P}$ = overall frictional pressure drop across mat,

$\underline{D}$ = dielectric constant of the bulk of the permeant,

$\underline{A}$ = cross-sectional area of mat,

ζ = zeta potential $\leq \psi_\delta$ in Fig. 1,

$(\underline{L}_e/\underline{L})^2$ = tortuosity factor, which is assumed to be independent of porosity and $\cong 2.0$,

α = specific volume of fibers, cc./g.,

$\underline{c}_1$ = mat concentration, g./cc., and

$(1-\alpha\underline{c}_1)$ = void fraction or porosity (ϵ) of porous medium.

If the streaming current model used to obtain Equation (1) is valid for all porous media, the calculated zeta potential ($\zeta_{\underline{c}}$) for the fibers in a particular mat should not change as the porosity of the mat is varied (refer back to p. 6).

Neale and Peters (21) found that the calculated value of the zeta potential was not constant, but decreased as the fiber plug was compressed, i.e., as the porosity was decreased. It was hypothesized that the capillary or pore radii in the plugs became very small at low porosity and were of the same order of magnitude as the thickness of the diffuse layer. The reduced streaming current that would result at low porosities was given as the cause of the smaller $\zeta_{\underline{c}}$.

A similar decrease in the calculated zeta potential with decreasing mat porosity was obtained by Goring and Mason (22).

Streaming current results may be examined by an alternative method to calculating zeta potentials at each porosity. According to Equation (1), a plot of $[I\eta L/(\Delta PD)]$ vs. c_1 should yield a straight line assuming that ζ, α, and $(L_e/L)^2$ are not functions of c_1.

Using the alternative method, Mason and coworkers (22, 26) observed two discrepancies: (1) The value for the specific volume (α) in Equation (1) was about 1.5 times that calculated from permeability data with the same fiber mats. (2) At porosities greater than about 0.80 and less than 0.60, the plot of $(I\eta L/\Delta PD)$ vs. c_1 did not follow a straight line as predicted by Equation (1). A sample plot is given in Fig. 2.

Analysis of Streaming Current Theory

Goring and Mason (22) pointed out that the large specific volume discrepancy indicates a serious weakness in electrokinetic theory. Their analysis of the problem involved the following areas: (1) the assumption that the thickness of the diffuse layer is much smaller than the radius of the hypothetical capillary through which flow occurs in a fiber mat; (2) the effect of the capillary wall curvature on the simplified, flat-surface form of the Poisson equation; (3) the pore size distribution, and (4) the model for the electric double layer at the surface of cellulose fibers. It was concluded that the first three factors could not account for the specific volume discrepancy. A model consisting of partially dissolved, charged cellulose chains extending out from the surface to distances considerably larger than the diffuse layer thickness was proposed to explain the large specific volume values from streaming current data.

In subsequent work, Biefer and Mason (26) found that a similar specific volume discrepancy existed for smooth, nonfibrillated fibers such as nylon and dacron.

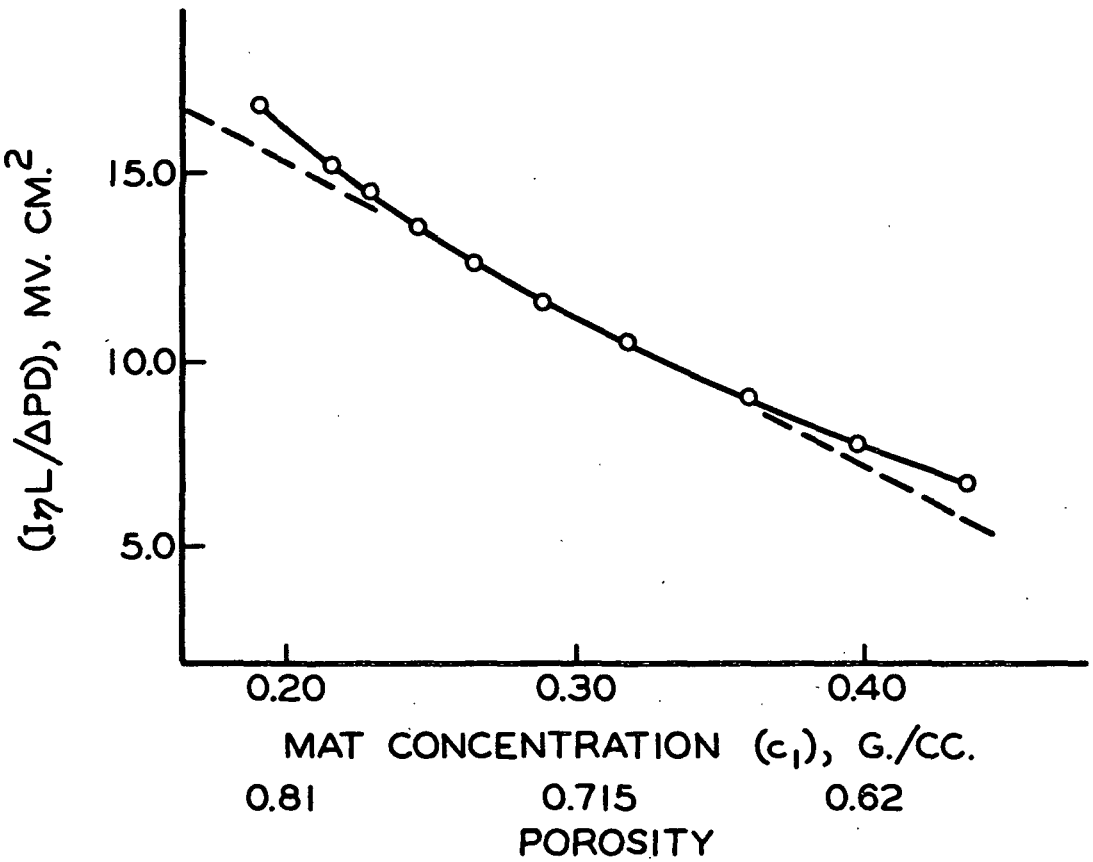

Figure 2. Biefer and Mason's (26) Streaming Current Data for Cellulose Acetate Fibers (α = 0.95) and 2 x 10^{-5}M KCl

Therefore, a new explanation based on tortuosity variation was proposed to account for the specific volume discrepancy. An empirical fit of experimental data indicated that a straight line was obtained at porosities less than 0.80 and that the specific volume discrepancy disappeared if the tortuosity factor in Equation (1) was assumed to vary with porosity according to the following equation:

$$(L_e/L)^{-2} = b\epsilon^h \qquad (2),$$

where exponent h equals 1.5, ϵ equals porosity, and b is a constant which was arbitrarily set equal to 1.0 at $\epsilon < 0.80$. Modifying Equation (1) with Equation (2) produces the relation

$$[I\eta L/(\Delta P D)]^{0.4} = -[A\zeta b/(4\pi)]^{0.4}(1 - \alpha c_1) \qquad (3).$$

Biefer and Mason (26) emphasized that b was arbitrarily set equal to 1.0 since the absolute value of the zeta potential of fibers could not be determined from present electrokinetic theory. In addition, it was proposed that a value of b less than 1.0 at $\epsilon > 0.80$ might explain why the $[I\eta L/(\Delta P D)]^{0.4}$ vs. c_1 plot according to Equation (3) remained nonlinear at $\epsilon > 0.80$.

Tortuosity Variation with Porosity

Biefer and Mason (26) could not offer an explanation for a tortuosity variation with porosity in the streaming current equation, while the tortuosity factor in the permeability equation is considered constant at porosities < 0.80 for randomly packed cylindrical particles according to Sullivan and Hertel (27). In Brown's (28) studies of air flowing perpendicular to glass-wool fibers, L_e/L equaled 1.47 $\pm$ 0.04 over the porosity range 0.95 to 0.74. The lower limit was 0.74 because appreciable fiber breakage occurred at porosities < 0.70.

In addition to streaming current and permeability tortuosity factors, a third tortuosity factor has to be considered. On the basis of conductance data

through the same fiber mats used for streaming current measurements, Biefer and Mason (26) found that

$$1/q = a_1 \epsilon \qquad (4),$$

where

q = the orientation or tortuosity factor for electrical conductance through a porous medium,

a_1 = constant = 0.95, and

ϵ = mat porosity.

Comparison of Equation (4) with Equation (2) shows that q varied with porosity in a different manner from the streaming current tortuosity in Equation (2).

Carman (29) concluded that there is no clear understanding of the relationship between q from conductance and $(L_e/L)^2$ in permeability since viscous flow is a quite different process. However, one finds it more difficult to describe a difference between the permeability tortuosity factor and that in streaming current work since, in the latter case, liquid flow creates the current by transporting counter ions to the downstream electrode. Back-conductance through the porous medium represents only a small fraction of the total streaming current. Biefer and Mason (26) proposed an alternative approach to the problem by referring to Scheidegger's (30) criticism of applying the simple capillary model of the Kozeny-Carman equation to the pore system in porous media.

Happel and Brenner (25) in an analysis of flow relative to particle assemblages of complex geometry concluded that the "Carman-Kozeny" concept can be applied only to isotropic porous media where orientation effects are absent. The fiber mats discussed here are definitely anisotropic. Thus, the capillary model is very likely inadequate for describing the streaming current phenomenon in fiber mats. An alternative flow model proposed by Happel (25, 31) is discussed in a later section.

RELATED WORK IN RECENT LITERATURE

In the last ten years, there have been several other papers on electrokinetics in porous media, but none adequately explains the discrepancies found with capillary-model-based electrokinetic theory for fiber mats. Boyack and Giddings (32) place the relationship for conductance in Equation (4) on a firmer theoretical basis using paper electrophoresis studies. Nevertheless, tortuosity variation with porosity in streaming current work remains uncertain.

An attempt to explain the results of Biefer and Mason (26) on the basis of surface conductance was made by Ghosh and coworkers (33, 34). As was discussed previously, however, the conductance of current back through the fiber mat is negligible in streaming current measurements. This includes surface conduction of current. Therefore, some explanation other than surface conductance is needed.

In a later paper on electroosmosis with diaphragms of quartz and glass particles, Ghosh, Moulik, and Sengupta (35) were able to estimate the true zeta potential by applying a correction for surface conductance. What makes the work relevant to the present discussion is the fact that their estimated ζ agreed fairly well with the ζ others had found with capillaries of similar material and at comparable electrolyte concentrations. There is always the uncertainty of whether experimental conditions, particularly with respect to adsorbed material, are the same when electrokinetic data are compared. Nevertheless, the implication from the work of Ghosh, et al. (35) is that the capillary model used in the classical Helmholtz-Smoluchowski equation adequately describes the charge transport in plugs of approximately spherical particles. The preceding is supported by the previously mentioned conclusion of Happel and Brenner (25) that the capillary model can be applied only to isotropic porous media.

Stigter (36) conducted electroosmosis studies with wet wool plugs. There is considerable scatter in the electrokinetic data as a function of porosity, which makes it difficult to establish how well the results fit the classical capillary-model-based theory.

In streaming current work with pulp fibers, Jacquelin and Bourlas (37) used Biefer and Mason's modified equation [refer to Equation (3)] but did not contribute to the theory. Hastbacka and Nordman (38) conducted streaming current measurements with pulp fibers but did not analyze the theory nor use Biefer and Mason's modified equation. This should not detract from the qualitative nature of these studies. However, it is evident that zeta potentials reported for fiber mats have only a qualitative value.

PRESENTATION OF THE PROBLEM

The conclusion from the literature review is that there remains a need to adequately explain the discrepancies found in streaming current studies. It has been shown that the classical streaming current/potential theory, which is based on the capillary model, does not agree with experimental data from fiber mats (21, 22, 26). The discrepancies are noted as either (1) a continually decreasing calculated zeta potential with decreasing porosity or (2) excessively large specific volume values and nonlinear $[I\eta L/(\Delta P D)]$ vs. c_1 curves [see Equation (1) and Fig. 2]. The latter method of treating the data was used by Mason and coworkers (22, 26) as an alternative to calculating the zeta potential at each mat porosity.

The hypothesis of Biefer and Mason (26) that the streaming current tortuosity factor varies with porosity is questionable. In the first place, it is difficult to visualize a difference between tortuosity in permeability and that in the streaming current phenomenon since, in the latter case, liquid flow creates the current by transporting counter ions to the downstream electrode. The paths for both liquid and charge transport should be very similar. The tortuosity factor in permeability was shown to be constant over a relatively large porosity range (0.95 to 0.74) in Brown's (28) studies of air flowing perpendicular to glass fiber mats.

Secondly, it appears that the capillary model does not always give an adequate description of flow through porous media (25, 30, 39), particularly through anisotropic assemblages such as fiber mats in which the fibers are oriented perpendicular to the flowing fluid (25).

The objective of the present study is to develop a streaming current relationship which is based on a more adequate flow model, namely, the Happel model (31), and thus improve upon the usual capillary-model approach to the streaming current phenomenon with fiber mats.

DEVELOPMENT OF STREAMING CURRENT RELATIONSHIP USING HAPPEL MODEL

HAPPEL MODEL

In 1959, Happel (31) proposed a model for slow flow perpendicular to an array of cylinders. The creeping motion equations for two-dimensional flow around cylinders were derived from the equation of motion; inertial terms were assumed negligible. Conceptually, the Happel-model approach to flow through fiber mats is superior to that of the capillary model, which assumes that flowing fluid follows a tortuous path through channels or capillaries in the porous bed.

The unit-cell approach used by Happel to solve the equation of motion should be especially useful in predicting the streaming current from a fiber mat. The cell model has its greatest applicability in concentrated assemblages, where the container wall influence can be neglected (25). Secondly, the flow equations developed by Happel are good approximations of actual average flow patterns close to the particle surface ($r \cong a$ in Fig. 3) in real physical systems (25). The velocity patterns of interest for streaming current predictions are very close (within about 0.2 μm.) to the solid-liquid interface in comparison to the lateral distance between fibers (at least one fiber diameter, or > 17 μm., in the present study).

The Happel approach produces relatively good agreement between the theoretically predicted Kozeny factor, k, and k from experimental data (31). It is concluded that the Happel model for flow perpendicular to assemblages of cylinders should be an improvement over the capillary model for predicting the streaming current from mats of cylindrical fibers.

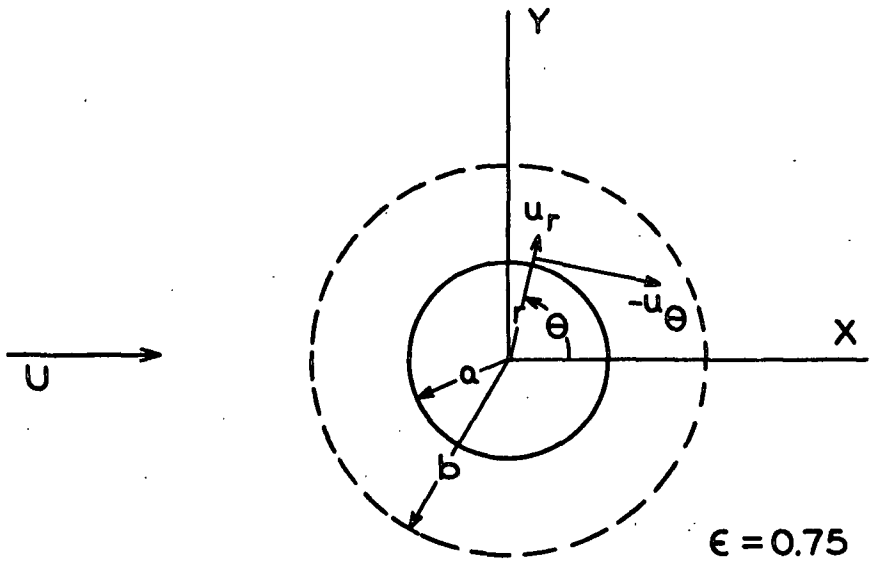

a = RADIUS OF CYLINDER

b = RADIUS OF FLUID ENVELOPE

U = FLUID VELOCITY APPROACHING CYLINDER

ϵ = CELL POROSITY = $(b^2 - a^2)/b^2$

Figure 3. Free-Surface Model for Flow Perpendicular to One Cylinder

In Happel's approximation of flow through cylindrical-fiber mats, it is assumed that the two concentric circular cylinders represented in Fig. 3 can serve as model for flow through an assemblage of cylinders. The outer cylinder of radius $\underline{b}$ is assumed to be a frictionless surface (zero shear stress). The void or liquid fraction of the cell model is equated to the overall void fraction of the assemblage of cylinders. The particular Happel velocity equation which will be used can be expressed in cylindrical coordinates as follows:

$$u_\theta = U(\sin\theta) - v_\theta = -\sin\theta\{U - [3Cr^2/8 + D_1 \ln (r)/2 + D_1/4 + E - F/r^2]\} \quad (5)$$

where

$\underline{u}_\theta$ = theta component of velocity vector for the case of fluid moving to a stationary cylinder,

$\underline{U}$ = fluid velocity approaching the cylinder, or superficial approach velocity above a porous bed,

$\underline{v}_\theta$ = fluid angular velocity for the case of a solid cylinder moving perpendicular to its axis in a fluid cell of radius $\underline{b}$,

$\underline{r}$ = radial distance from axis of cylinder,

θ = angular displacement from positive x-axis, and

$\underline{C}$, $\underline{D}_1$, $\underline{E}$, and $\underline{F}$ = constants which vary with the porosity of the unit cell (or fiber mat).

Happel solved the equation of motion for the case of a solid cylinder moving perpendicular to its axis in a fluid. Therefore, for fluid moving perpendicular to a stationary cylinder, $[\underline{U}(\sin\theta) - \underline{v}_\theta]$ represents the angular velocity, $\underline{u}_\theta$.

Creeping flow of a constant-density, constant-viscosity fluid is assumed in the application of the equation of motion. As discussed previously (p. 9), Lyklema and Overbeek (15) concluded that the viscosity in the diffuse layer can be assumed equal to that in the bulk solution at 1-1 electrolyte concentrations $< 10^{-3}\underline{M}$ and $\psi_\delta < 100$ mv., and even these conditions may be too restrictive according to Stigter (15a).

The free-surface model makes no allowance for the effect of cylinders in physical contact, nor for any bending of the cylinders that might occur as a fiber mat is compressed to low void fractions. It is not necessary, however, to assume any particular fiber orientation in the y-z plane. The only orientation specification is that all the fibers be in this y-z plane which is perpendicular to the x-direction flow.

In addition, Happel's model is considered applicable only at void fraction greater than 0.4 to 0.5 (25, 31). This limitation will present no problem in the present study, where the lowest porosity was about 0.65.

THEORETICAL DEVELOPMENT OF STREAMING CURRENT EQUATION

It is necessary to theoretically determine the quantity of charge per unit time swept from the diffuse layer surrounding each fiber. The total streaming current, I, passing a plane, S, perpendicular to flow (Fig. 4) can be represented as follows:

$$I = \iint_S \rho \vec{u} \cdot d\vec{S} \qquad (6)$$

where

ρ = excess charge (i.e., counter ions) per unit volume, or charge density, and

$\vec{u}$ = velocity vector.

For the case of an assemblage of cylinders (Fig. 4), $\vec{u}$ may be approximated by Happel's (31) equations. If the plane S is located at the center of the cylinders ($\theta = \pi/2$ and $3\pi/2$), only the u_θ component of velocity need be considered.

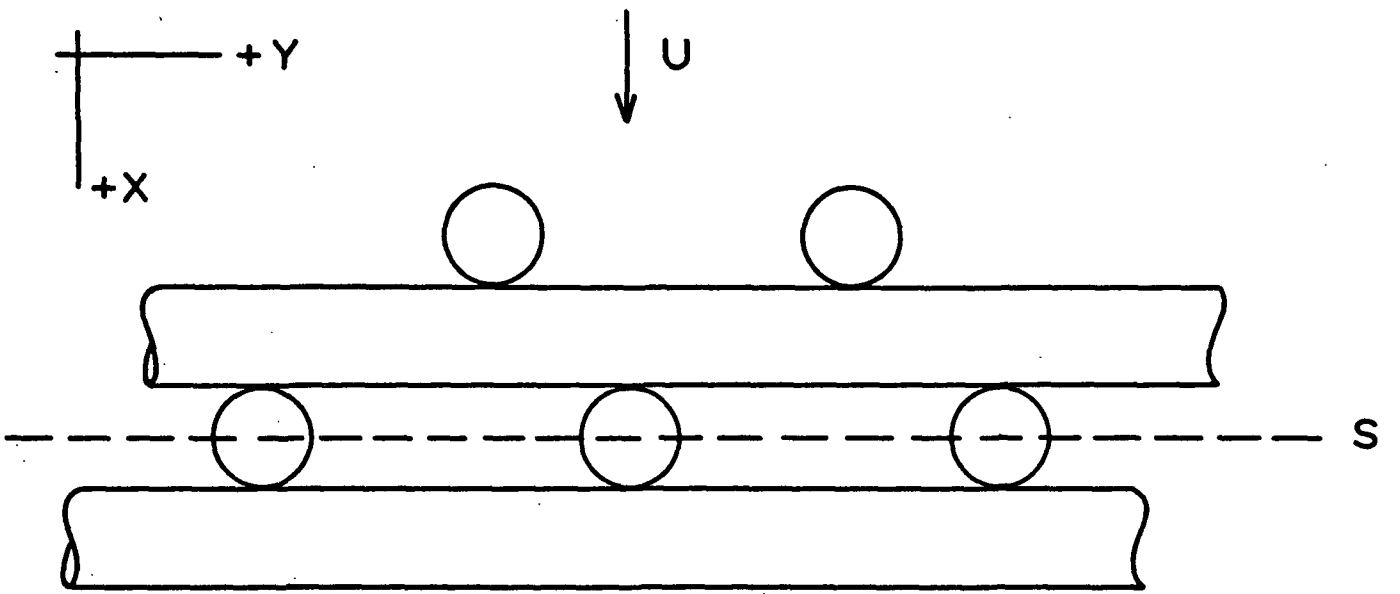

Figure 4. An Idealized View into a Mat of Cylindrical Fibers

NUMBER OF FIBERS CONTRIBUTING TO TOTAL CURRENT

The number of cylinders contributing to the total streaming current, $\underline{I}$, passing plane $\underline{S}$ must be determined. The physical number of cylinders intersected by plane $\underline{S}$ can be estimated from geometric considerations (see p. 99). However, it is also necessary to count the number of cylinders which are not intersected by plane $\underline{S}$, but which still contribute to $\underline{I}$. In other words, the same counter ions passing through the diffuse layers in one layer of cylinders do not necessarily flow through the diffuse layers in the next downstream layer of cylinders. A fairly large lateral separation (average > $2\underline{a}$ depending on mat porosity) exists between fibers in the mats of this study. Therefore, a relatively strong driving force would be required to laterally transport counter ions located midway between fibers to the fiber surfaces. Mass transport of counter ions within the fiber mats will be examined next.

Three processes by which counter ions can be transported to the electric double layer surrounding each fiber are: (1) liquid flow, i.e., the flowing electrolyte solution which is permeating the fiber mat, (2) ion migration in an electric field caused by the charged fiber surface, and (3) diffusion of counter ions due to a concentration gradient. Analysis of the ion-transport process is difficult since there is no clear understanding of the effect of liquid flow on the equilibrium model for the electric double layer (refer to page 11-12). Another factor complicating the analysis is fiber orientation in a fiber mat; the model in Fig. 4 is highly simplified.

A more thorough discussion of counter-ion transport is given in Appendix II. On the basis of an analysis which required several simplifying assumptions regarding mat geometry, ion migration, and ion diffusion, it was concluded that ion transport by liquid flow around the fibers was the dominant means of ion transport.

An estimate of N, the number of fibers contributing to the total streaming current across plane S can now be made. It will be assumed that the counter ions swept from a fiber by liquid flow do not diffuse out of the downstream projection of that fiber. Since the bulk of the liquid will have a fairly uniform counter-ion density if liquid flow is the dominant method of ion transport, no concentration gradient would exist to cause counter-ion diffusion from the liquid under the downstream projection; hence, the preceding assumption.

As a first approximation of N, it is assumed that all fiber segments which are "visible" in the upstream projection from plane S contribute to the total streaming current across S. Thus,

$$N = A/2a\ell \tag{7}$$

where

A = cross-sectional area of the fiber mat

a = radius of the swollen cylindrical fiber, and

ℓ = fiber length.

It should be noted that N is independent of mat porosity. This independence of porosity is essential to the new streaming current model, as will be demonstrated when experimental results are discussed on page 40 (refer also to page 99 for a discussion of results if N is assumed to be a function of porosity).

Nonetheless, it can be concluded from the preceding discussion of the assumptions made in order to estimate N that the true value for N could be either greater or less than that given in Equation (7), depending upon the extent of counter-ion diffusion and migration within the fiber mat. Thus, the relative nature of calculations based on the Equation (7) estimate of N should be understood [i.e., ζ values computed from Equation (23) are not necessarily the true or absolute zeta potentials].

Substituting $-u_\theta$ (velocity at $\theta = \pi/2$) and Equation (7) into Equation (6) results in the following streaming current expression:

$$I = -\frac{A}{a\ell} \int_0^{\ell} \int_a^{(a+\tau)} \rho\, u_\theta \, dr\, dz \qquad (8).$$

ION DISTRIBUTION WITHIN DIFFUSE LAYER

An expression for the excess charge density, ρ, as a function of the potential, ψ, will be obtained for the convex side of a cylindrical surface. The derivation to establish the ρ vs. ψ relationship is similar to that of Gouy (8) and Chapman (9) and resembles that of the Debye-Hückel (40) theory for strong electrolytes. Henry (41) used equations similar to Equations (19) and (20), which follow, in a study on the electrophoresis of suspended spheres and cylinders.

The relationship between the average electric potential, ψ, and ρ at any point is given by the Poisson equation,

$$\nabla^2 \psi = -4\pi\rho/D \qquad (9)$$

where ∇^2 is the Laplace operator and D equals the dielectric constant, which is assumed to be uniform throughout the liquid. Since it is assumed that the counter-ion distribution is also uniform at all fiber surfaces, ψ will not be a function of the θ- or z-cylindrical coordinates; and Equation (9) becomes:

$$\frac{1}{r} \frac{\partial}{\partial r} \left[r \frac{\partial \psi}{\partial r} \right] = -4\pi\rho(r)/D \qquad (10).$$

The Boltzmann equation is used to relate the concentration, $n_i(r)$, of ions of type i at a distance r to the potential and the ion concentration, $n_i(\infty)$, in the bulk of the solution:

$$n_i(r) = n_i(\infty) \exp[-z_i\, e\, \psi(r)/(k_1\, T)] \qquad (11),$$

where

$\underline{z_i}$ = ion valency,

$\underline{e}$ = electronic charge,

$\underline{k_1}$ = Boltzmann constant, and

$\underline{T}$ = absolute temperature.

The value for the excess charge density, ρ, at distance $\underline{r}$ results from a summation:

$$\rho(r) = \sum_i z_i \, e \, n_i(r) \qquad (12).$$

For a 1-1 electrolyte (e.g., KCl), Equation (12) becomes

$$\rho(r) = -2n_i(\infty) \, e \, \sinh[e \, \psi(r)/(k_1 \, T)] \qquad (13),$$

assuming that $\underline{n_i}(\infty)$ for the positive ions equals $\underline{n_i}(\infty)$ for the negative ions.

If $\underline{e} \, \psi \ll \underline{k_1} \, \underline{T}$, which means $\psi < 10$ mv. at $\underline{T} = 298°K.$,

$$\sinh[e \, \psi/(k_1 \, T)] \cong e \, \psi/(k_1 \, T) \qquad (14).$$

Rice and Whitehead (42) state that the approximation of Equation (14) results in a ψ vs. $\underline{r}$ distribution at a single plane surface which agrees with that calculated from the exact solution for a 1-1 electrolyte and $\psi_\delta < 50$ mv. The specification of a plane surface applies to the present case since the diffuse layer thickness, τ, $\ll$ than the fiber radius.

Substituting for ρ in Equation (10) yields the Poisson-Boltzmann equation for a cylindrical surface:

$$\frac{1}{r} \frac{d}{dr} \left[r \frac{d\psi(r)}{dr} \right] = \kappa^2 \psi \qquad (15),$$

where κ is the Debye-Hückel constant and

$$\kappa^2 = 8\pi \, n_i(\infty) \, e^2/(D \, k_1 \, T) \qquad (16).$$

The desired solution of Equation (15) can be represented in terms of Bessel functions. Since ψ approaches zero as $\underline{\kappa r} \rightarrow \infty$,

$$\psi = C_2 \, I_o(\kappa r) + C_2 \, K_o \, (\kappa r) \tag{17}$$

will be finite providing that $\underline{C}_1 = 0$. Therefore,

$$\psi = C_2 \, K_o \, (\kappa r) \tag{18},$$

where $\underline{C}_2$ is a constant and $\underline{K}_o$ is the symbol for the zero-order modified Bessel function of the second kind.

Using the boundary condition that $\psi = \psi_\delta$ at $\underline{r} \cong \underline{a}$ to eliminate $\underline{C}_2$ from Equation (18),

$$\psi = \psi_\delta \, K_o \, (\kappa r)/K_o \, (\kappa a) \tag{19}.$$

Combining Equations (10), (15), and (19) yields the equation,

$$\rho(r) = -[D \, \kappa^2 \, \psi_\delta/(4\pi)] \, [K_o(\kappa r)/K_o(\kappa a)] \tag{20}.$$

STREAMING CURRENT EQUATION

An expression for the streaming current caused by flow perpendicular to the axes of cylindrical fibers is obtained by substituting Equations (5) and (20) into Equation (8) and performing the integration with respect to $\underline{z}$:

$$I = - \frac{A \, D \, \kappa^2 \, \zeta_c}{4a \, \pi \, K_o \, (\kappa a)} \int_a^{(a+\tau)} K_o(\kappa r)[U - (3C \, r^2/8 + D_1 \, \ln(r)/2 + D_1/4 + E - F/r^2)] \, dr \tag{21}$$

where $\underline{\zeta_c}$ is the experimentally determined estimate of ψ_δ at each mat porosity.

Since $[\int_{\underline{a}}^{(\underline{a}+\tau)} 3\underline{C}\ \underline{K}_o(\kappa\underline{r})\ \underline{r}^2/8\ d\underline{r}]$ was the only term for which the exact integral could be determined, numerical integrations were performed using Newton-Cotes quadrature. The magnitude of $\kappa\underline{r}$ is very large (e.g., 8.7 μm./0.03 μm. = 290). For $\kappa\underline{r} \geq 10$, the Bessel function $\underline{K}_o$ can be approximated by the asymptotic expansion (43), and

$$K_o(\kappa r)/K_o(\kappa a) \cong (a/r)^{1/2} \exp(\kappa a - \kappa r) \qquad (22).$$

Combining Equations (21) and (22) and solving for $\zeta_{\underline{c}}$ gives Equations (23a) to (23i). The constants, $\underline{C}$, $\underline{D}_1$, $\underline{E}$, and $\underline{F}$, are expressed as a function of fiber radius, $\underline{a}$, and mat porosity, ε. Refer to Appendix IV for the Fortran language computer program which was used to calculate $\zeta_{\underline{c}}$.

$$\zeta_c = -4C_4\ \pi\ a\ \kappa^{-2}(I/U)/[AD(T_3 - 0.375CT_1 - 0.5D_1T_2 - T_3(E + 0.25D_1) + F\ T_4] \qquad (23a)$$

where

$$D_1 = -2/\ln[1/(1 - \varepsilon)^{0.5}] + 4[(1 - \varepsilon)^2 - 1]/[(1 - \varepsilon)^2 + 1] \qquad (23b),$$

$$F = D_1a^2/[4(1 - \varepsilon)^2 + 4] \qquad (23c),$$

$$C = -8F(1 - \varepsilon)^2/a^4 \qquad (23d),$$

$$E = 1 + F/a^2 - 0.5D_2\ (\ln a + 0.5) - 0.375C\ a^2 \qquad (23e),$$

$$T_1 = a^{0.5} \int_a^{a+\tau} \exp(\kappa a - \kappa r) r^{1.5}\ dr \qquad (23f),$$

$$T_2 = a^{0.5} \int_a^{a+\tau} [\exp(\kappa a - \kappa r)\ \ln r/r^{0.5}]dr \qquad (23g),$$

$$T_3 = a^{0.5} \int_a^{a+\tau} [\exp(\kappa a - \kappa r)/r^{0.5}]dr \qquad (23h),$$

$$T_4 = a^{0.5} \int_a^{a+\tau} [\exp(\kappa a - \kappa r)/r^{2.5}]dr \qquad (23i),$$

and $C_4 = 9.0$, a constant which converts units to the same system.

EXPERIMENTAL

One requirement for streaming current measurements is electrodes which do not polarize easily. Another experimental requisite, one peculiar to this study, is that the fibers be cylindrical and that they be assembled in porous mats with their axes perpendicular to the approaching fluid; mats of uniform porosity were also desired. A third requirement is a good flow system that is capable of constant-rate permeation of the fiber mats with deaerated electrolyte solutions. The experimental system is discussed in general terms in the next several pages, while details of experimental apparatus and calculations are given in the Appendix.

ELECTRODES

Although it is impossible to have an ideally nonpolarizable electrode, it is possible to approach this condition. One of the most common "nonpolarizable" electrodes is silver-silver chloride (44). The requirements for minimizing electrode polarization include: (1) solid phases that are present in adequate amounts and (2) a sufficiently high concentration of ions that are common to the electrode and the solution. Refer to Appendix III for details of preparing the 3-inch diameter, perforated silver disks to form silver-silver chloride (Ag-AgCl) electrodes. Two of these electrodes were used – one upstream and one downstream of the fiber mat. The two AgCl surfaces faced each other and were in direct contact with the mat.

The range of electrolyte concentrations was 0.2 to 4 x 10^{-4} M for potassium chloride and 0.5 to 2 x 10^{-4} M for calcium chloride. Electrolyte concentrations can decrease to a point (possibly 0.2 x 10^{-4} M KCl) which is too low to maintain reversible Ag-AgCl electrodes (44). However, Zucker (45) found that at concentrations greater than 1 x 10^{-5} M KCl the ion concentration was sufficient to give reliable data with Ag-AgCl electrodes.

FORMING FIBER MAT

The cylindrical fibers used to form the mats (4-28 grams) were either nylon or dacron. Trials with dacron fiber mats were more reproducible than the runs with nylon 66 fibers. Each mat was formed directly on the perforated bottom electrode (procedure in Appendix III).

Special attention was given to forming mats which would have the fiber axes oriented mainly in the y-z plane, i.e., oriented perpendicular to the approaching x-direction flow. In order to minimize edge effects, the mats were relatively large (3-inch diameter). Edge effects, which are discussed by Han (46, p. 141-3), exist because fibers close to the wall of the forming tube tend to drag themselves along the wall. The result is that some fibers around the circumference of the mat have an x-direction orientation.

Clearly, the edge effect on the average fiber orientation will be less for 3-inch diameter mats in comparison to 1-inch diameter fiber plugs, which have been used in previous streaming current studies (21, 22, 26). This subject is discussed further on page 53.

FLOW SYSTEM

A diagram of the flow system used for streaming current measurements is shown in Fig. 5. Provision was made for bleeding all the air from the system. Maintaining deaerated liquid is a requirement for reproducible results (21, 22).

PROCEDURE

All streaming current runs involved downflow of a dilute electrolyte solution through mats of synthetic fibers.

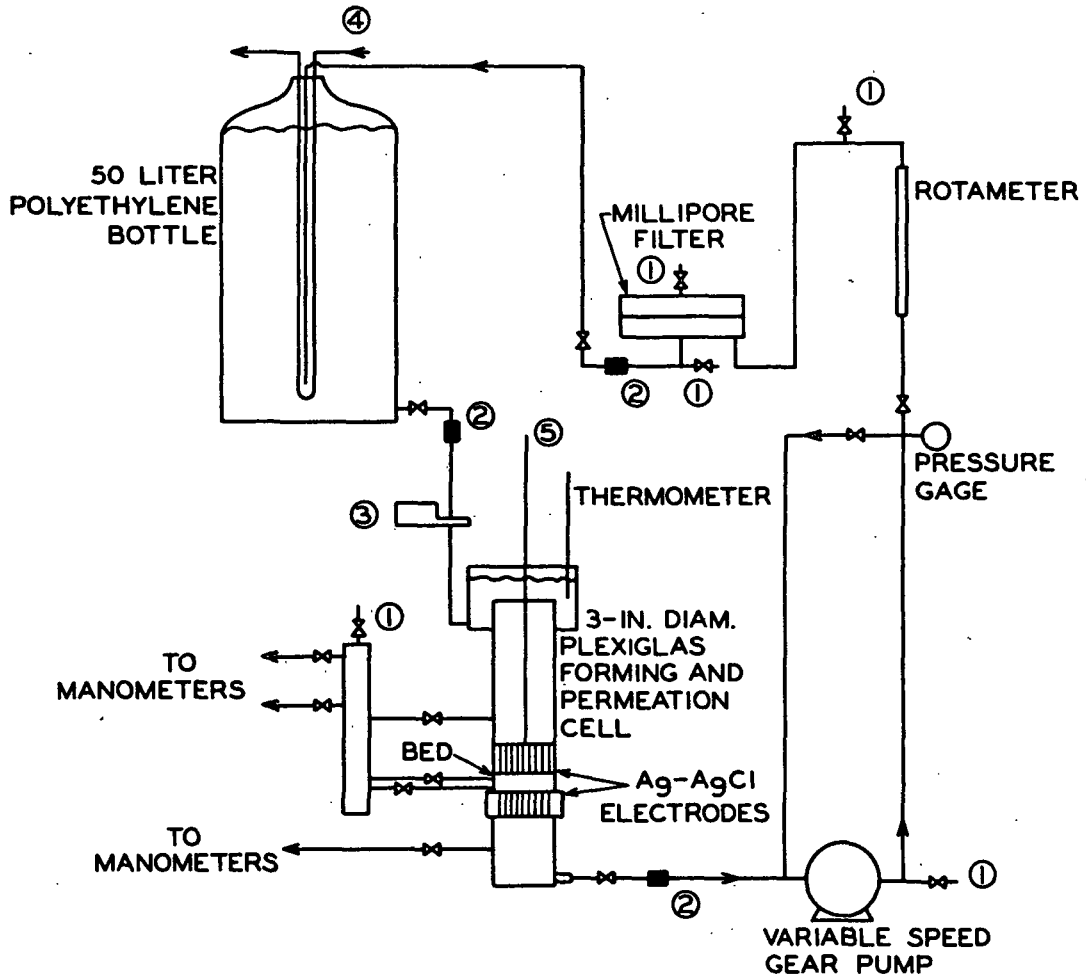

① VALVES TO REMOVE AIR FROM LINES
② DISCONNECTS TO CHANGE FROM DOWNFLOW TO UPFLOW THROUGH CELL (AN ADDITIONAL PUMP USED)
③ VALVE WITH SOLENOID CONTROLLED BY A FLOAT AT TOP OF PERMEATION CELL
④ HEAT EXCHANGER (STAINLESS STEEL TUBING) TO MAINTAIN CONSTANT TEMPERATURE
⑤ STAINLESS STEEL SHAFT TRANSMITTING LOAD FROM HYDRAULIC PRESS

Figure 5. Flow System for Streaming Current Measurements

About an hour before each run, the electrolyte solution was pumped through the cell at three or four flow rates. By measuring the current between the electrodes with no mat present, an estimate of the flow current I_f, was obtained (refer to discussion in Appendix IV). After forming the mat the top electrode was placed back in the Plexiglas permeation cell (Fig. 6 and 7) and attached to the stainless-steel shaft which transmitted compressive force to the mat. The porosity of the mat was changed by periodically increasing the pressure in a hydraulic ram located on top of the stainless-steel shaft.

The initial step at each porosity level was to determine the separation between electrodes by reading the two micrometers (Fig. 7). Following this, current and pressure drop readings were taken at each of three or four flow rates. This procedure was repeated for about seven different porosities. During several runs, pressure drop readings within the mat were taken at the three highest porosity levels. These readings indicated that a constant pressure gradient, and thus uniform porosity, was maintained within the mat as the flow rate increased (see Appendix III, page 90).

At the end of a run, the electrolyte solution was drained from the permeation cell. After the mat had been removed, the two electrodes were submerged in deaerated salt solution and shorted together during storage. Each fiber mat was dried at 105°C. to constant weight.

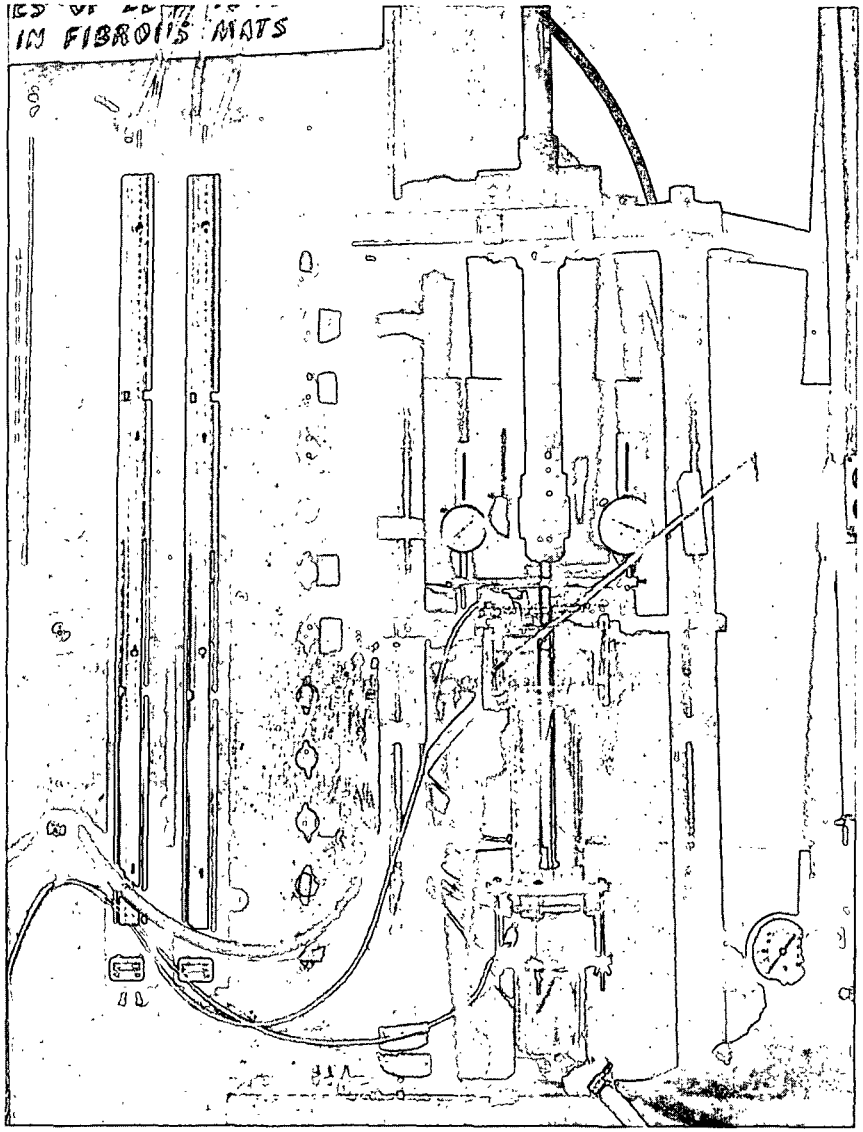

Figure 6. Streaming Current Apparatus

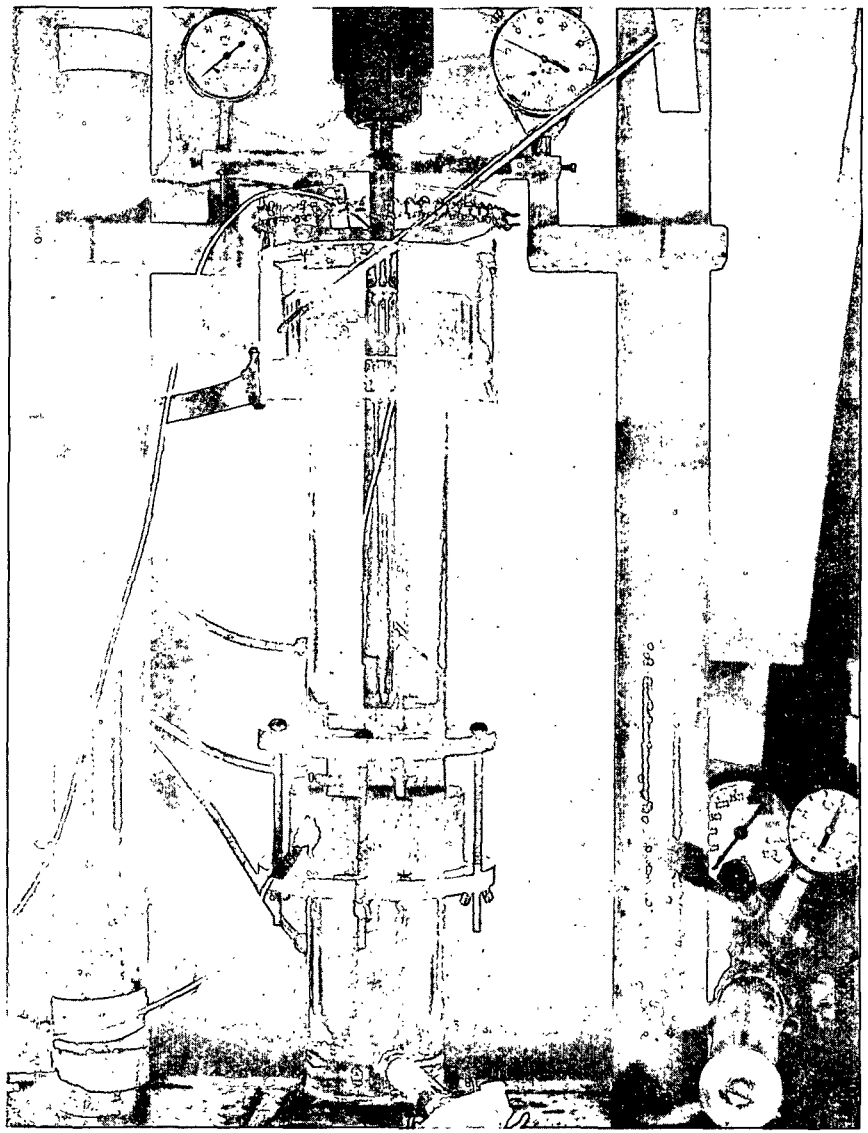

Figure 7. Plexiglas Cell Used to Form Fiber Mat and to Conduct Streaming Current Measurements

RESULTS AND DISCUSSION

APPLICATION OF NEW STREAMING CURRENT MODEL

A comparison of the new streaming current model [i.e., Equation (23)] with that based on the capillary model [Equation (1)] is given by the calculated zeta potential, ζ_c, vs. mat porosity plot presented in Fig. 8. Although ζ_c results from only one run are shown, they are representative of many other runs (see data presented in Table I and Appendix V).

A systematic increase in ζ_c with increasing porosity is produced when Equation (1) is applied (Fig. 8, Curve 1). However, when Equation (23) is used, a constant ζ_c value results (Curve 3).

Exceptions to the constant ζ_c value were noted for the initial one or two ζ_c values at the beginning of most runs, i.e., ζ_c at high porosity ($\epsilon \geq 0.85$). These low ζ_c values at high porosity will be discussed later (p. 57).

Now that an introduction has been given to an apparent improvement in treating streaming current data, the soundness of the experimental data used to test the new model must be evaluated. The results of zeta potential variation as a function of electrolyte concentration will be discussed with emphasis placed on the reproducibility of streaming current data. In addition, the sensitivity of streaming current data to the extent of fiber orientation in the direction of flow will be demonstrated. A listing of assumptions and experimental limitations concludes the discussion section.

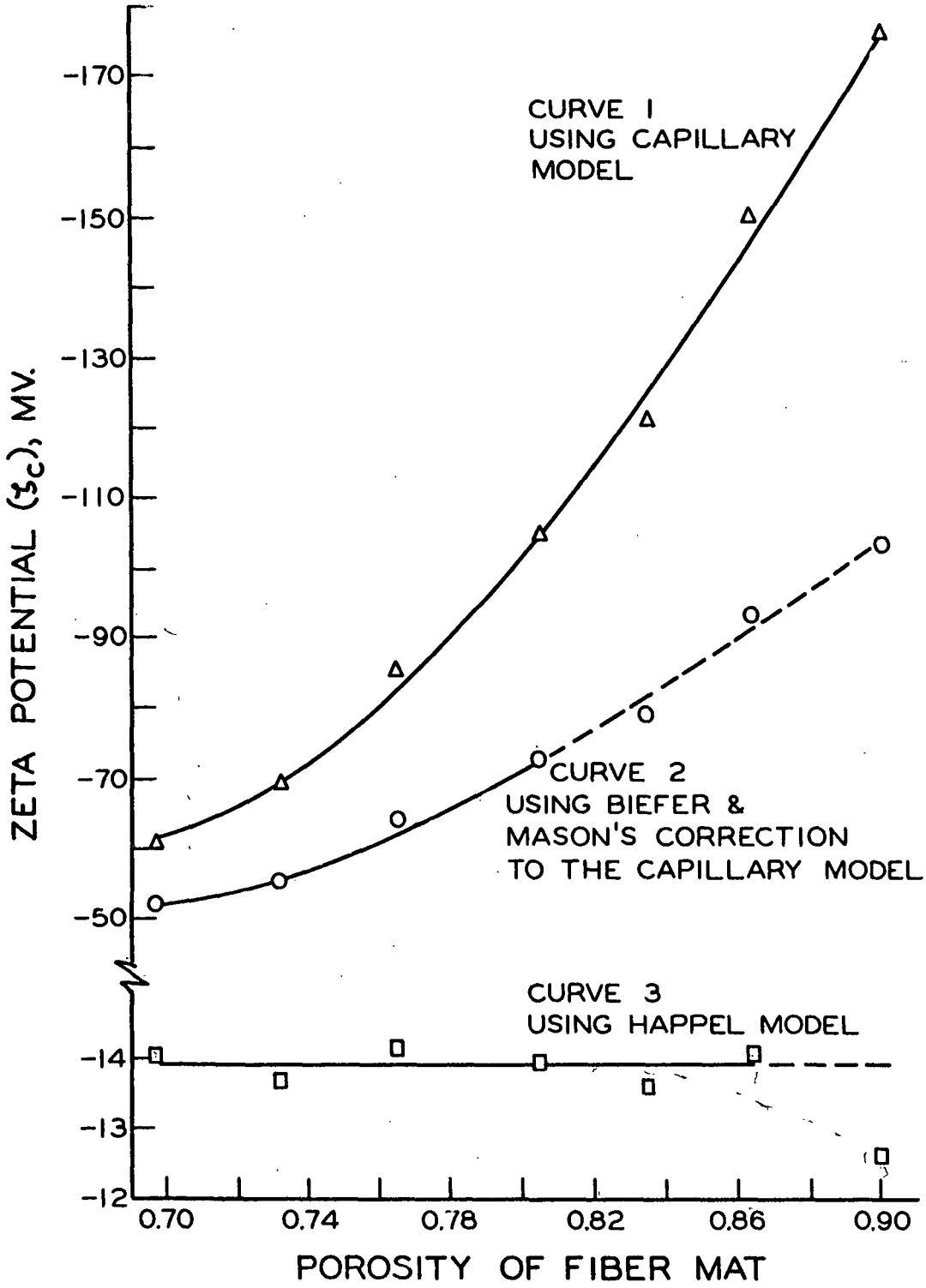

Figure 8. Comparison of Zeta Potential Variation as a Function of Porosity Using Two Different Models for Flow Through Fiber Mats; Run 10-10A Used as an Example – Dacron Fibers and 1.0 x 10^{-4} M KCl

TABLE I

STREAMING CURRENT RESULTS WITH DACRON FIBERS[a]

Key for Fig. 9 & 10	Run	Calc'd. Zeta Potential -ζ, mv.	Coeff. of Variation[b]	Empirical Exponent, h[c]	Permeant moles/l. x 10,000	Permeant -log (moles per liter)
Elec-	8-9-66	12.9[d] ±	4%	3.5	1.30	3.89 KCl
trode	8-10	13.5	7	4.0	1.30	
Pair	8-11	13.0	6	3.7	1.30	
No. 9	8-12	12.6	10	4.0	1.30	
1	8-30	11.2	8	5.2	1.20	3.92 KCl
2	8-31	11.8	14	4.6	1.20	3.92
3	9-2A	13.7	7	5.1	1.15	3.94
4	9-2B	8.7	12[e]	6.4[e]	3.9	3.41
5	9-5	9.5	13[e]	5.3[e]	3.9	
6	9-6	8.3	7[e]	4.7[e]	3.9	
7	9-7A	14.4	17	2.5	0.20	4.70
8	9-7B	13.8	18	2.9	0.20	
9	9-9	14.3	11	3.6	0.50	4.30
10	9-10	12.3	14	3.7	0.81	4.09
11	9-12	14.1	8	3.4	1.15	3.94
12	9-16A	13.0	11	3.6	0.72	4.14
13	9-16B	12.8	11	3.2	1.30	3.89
Pair No. 10						
1	9-22	9.0	9	3.5	1.45	3.84 KCl
2	9-23	9.6	9	3.3	1.45	
3	9-24	14.9	18	2.9	0.19	4.72
4	9-25	14.3	18	3.5	0.51	4.29
5	9-26A	14.4	12	3.3	0.79	4.10
6	9-26B	13.8	12	3.0	1.15	3.94
Pair No. 11						
1	9-30	12.4	11	3.8	0.48	4.32 KCl
2	10-1	12.1	4	4.0	1.16	3.94
3	10-2A	14.8	10	3.7	0.60	4.22
4	10-2B	14.0	5[e]	3.8[e]	1.15	3.94
5	10-3	12.7	4[e]	4.3[e]	2.20	3.66
6	10-4A	7.6	10[e]	5.5[e]	4.2	3.38
7	10-4B	18.5	11	3.5	0.48	4.32 KCl
8	10-5	8.5	4	3.3	4.2	3.38

See end of table for footnotes.

TABLE I (Continued)

STREAMING CURRENT RESULTS WITH DACRON FIBERS[a]

Key for Fig. 9 & 10	Run	Calc'd. Zeta Potential -ζ, mv.	Coeff. of Variation[b]	Empirical Exponent,[c] h	Permeant moles/l. x 10,000	Permeant -log (moles per liter)	
9	10-10A	13.9 ±	2%	3.7	1.04	3.98	
10	10-10B	8.5	8	4.6	3.7	3.43	
Pair No. 11 with $CaCl_2$							
1	10-12A	11.9	4	3.7	0.51	4.29	$CaCl_2$
2	10-12B	7.0	5	4.4	1.9	3.72	
3	10-14A	12.1	2	3.6	0.48	4.32	
4	10-14B	10.9	7	4.1	0.92	4.04	
			Average =	3.7[f]			

[a] No correction for the flow current was made for any run; only fibers for Runs 8-9 to 8-12 were extracted with ethanol prior to the run; for dacron fibers: diameter = 17.4 μm., $S_V = 4/2a = 2300$ cm.^{2}/cc., $\alpha = 0.67$ cc./g., length = 6.0 mm.

[b] Coefficient of variation = sigma x 100/ζ = sigma x 100/average ζ_c.

[c] Empirical exponent was determined for porosity ≤ 0.80; Biefer and Mason found that $h = 1.5$.

[d] Only ζ_c values at the four lowest porosities were used to determine ζ since ζ_c at the start of run were markedly lower (see Appendix V).

[e] Polarization was detected at end (last 2 or 3 porosity levels) of these five runs; thus, relatively large coefficients of variation and larger values for empirical exponent h.

[f] Values for runs mentioned above in which polarization occurred were omitted from average h.

ZETA POTENTIALS AS A FUNCTION OF ELECTROLYTE CONCENTRATION

A summary of results with dacron fiber mats is given by the zeta potential, ζ, vs. electrolyte concentration curves of Fig. 9. Either potassium chloride or calcium chloride solutions were used to permeate the mat.

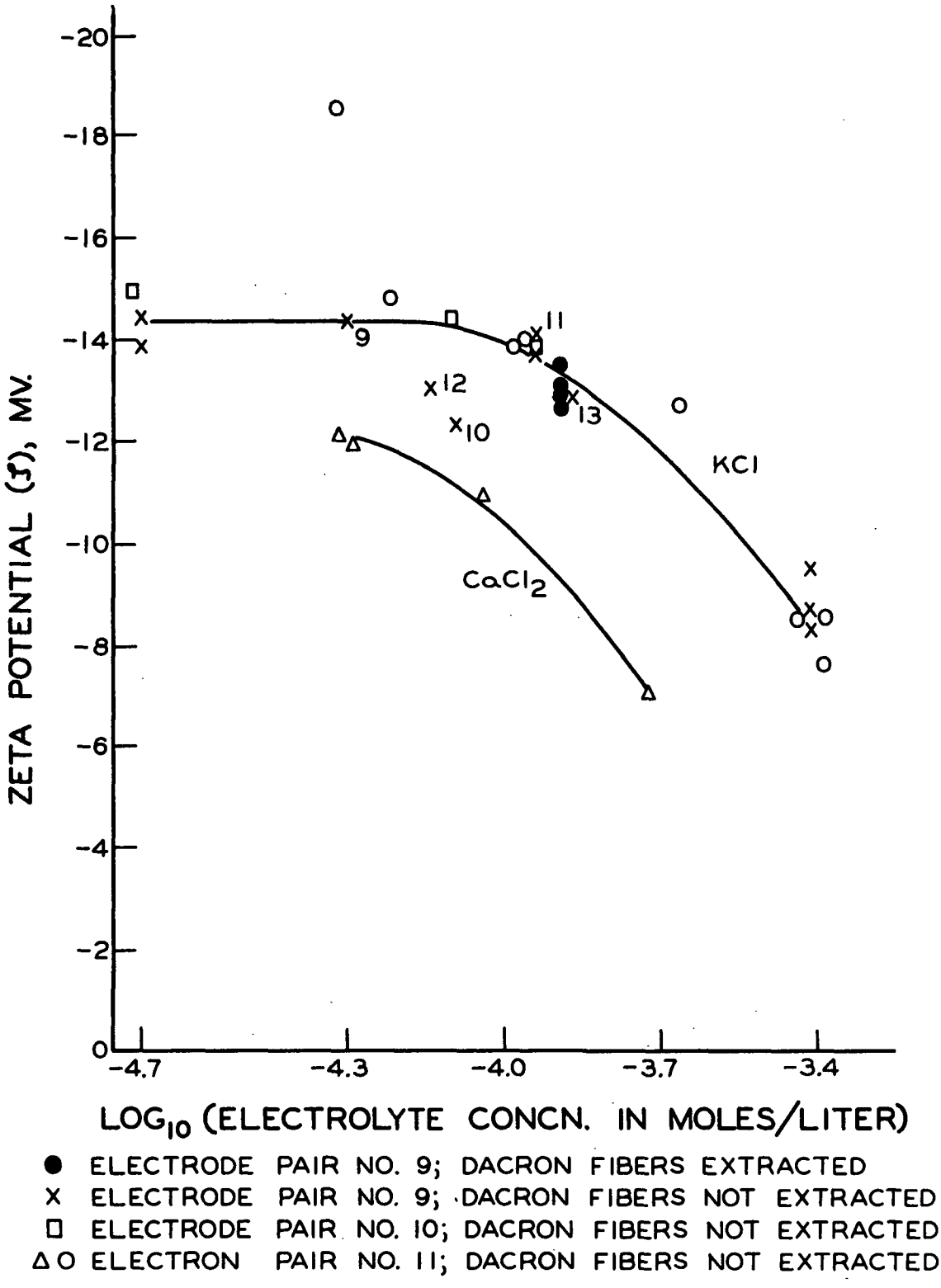

Figure 9. Zeta Potential as a Function of Electrolyte Concentration

REPRODUCIBILITY

Fairly good experimental reproducibility is indicated by the results with dacron fiber mats, particularly when consideration is given to the fact that the data with KCl solutions were gathered over a two-month period in which different batches of distilled water and three separately anodized sets of silver-silver chloride electrodes were used. However, in addition to one unusually high ζ value at 5×10^{-5} M KCl (Run 10-4B, Table I and Fig. 9), a distinct group of six low points exists as shown in Fig. 10.

The six low ζ values and experimental reproducibility in general will be discussed under the headings of electrode polarization, porous structure of silver chloride layer, variation in mat formation, and nonreproducibility with nylon fiber mats.

Electrode Polarization

The possibility of electrode polarization is raised by the six low zeta potentials in Fig. 10. The primary reason for using Ag-AgCl electrodes was their acceptance as the most common "nonpolarizable" electrode system (44). In theory it is impossible to have nonpolarizable, reversible electrodes for experimental measurements since the flow of electrons is associated with the time-dependent processes of chemical change and mass transport (44, 5).

Practically, however, electrode polarization can be minimized under favorable conditions, e.g., (1) if the solid phases are present in adequate amounts, and (2) when there is a sufficiently high concentration of ions that are common to the electrode and solution (Cl^- in this case) (44). Support for the first conditions was shown by the somewhat improved results using electrode pair no. 11 (see data given in Table I and Fig. 9), which was anodized to give six times more AgCl than with previous electrodes.

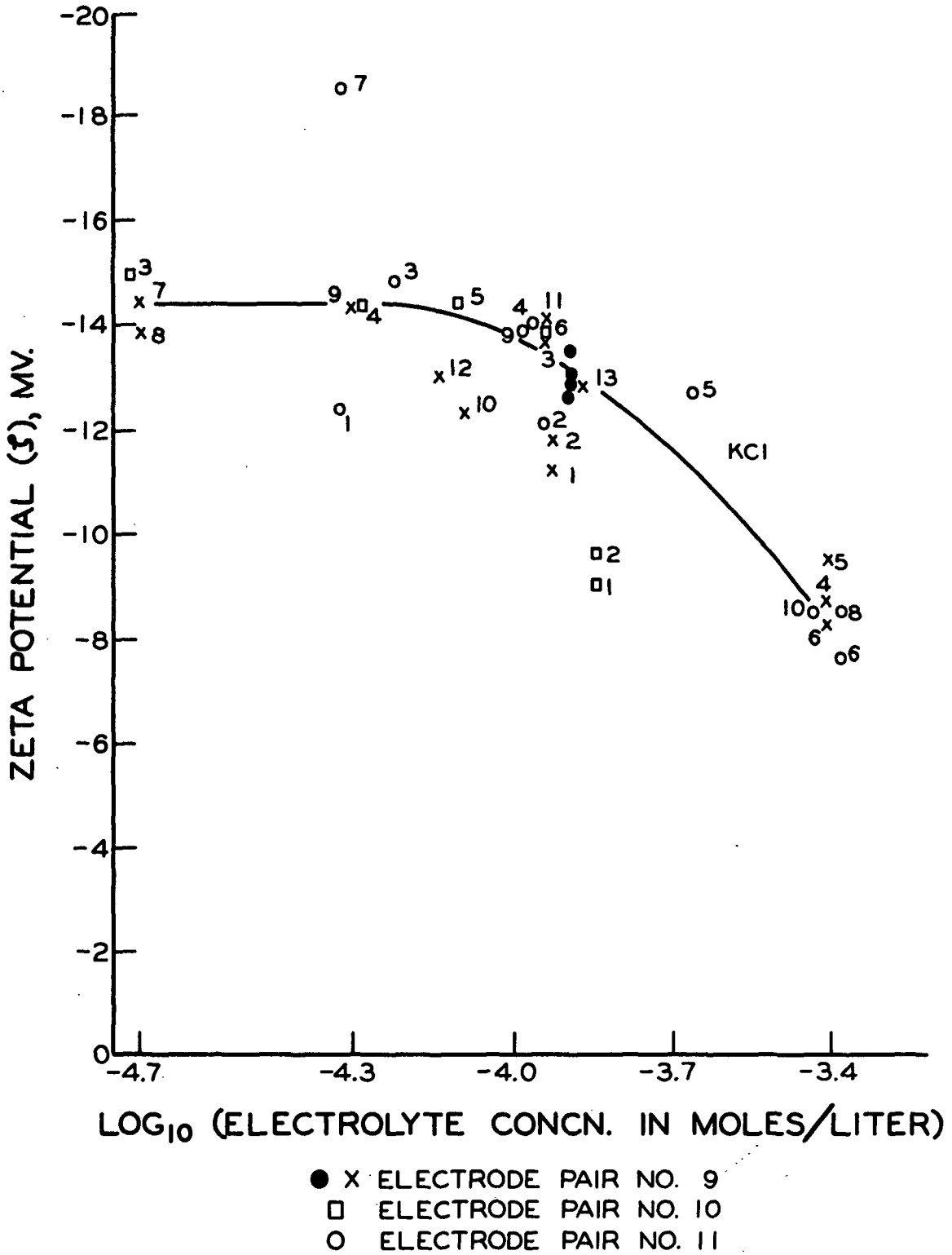

Figure 10. The same as Fig. 9 Except that the Initial Two Points with each Electrode Pair are Included and the Runs are Numbered (see Table I); Data with $CaCl_2$ Omitted

The importance of the second condition is emphasized by the discussion of Ives and Janz (44), who state that with decreasing ion concentration, "at some stage it will become mechanistically impossible for the ions to control the electrode potential." The result will be an unstable, indefinite potential, "not so much controlled by, as at the mercy of, dissolved oxygen and such other impurities as the solution may contain." The aforementioned should be considered when analyzing electrokinetic data at low electrolyte concentrations such as 2×10^{-5} M KCl, and very possibly 5×10^{-5} M KCl (Run 10-4B), in this study. However, Zucker (45) reported that $c > 1 \times 10^{-5}$ M KCl was sufficient to give reliable data with Ag-AgCl electrodes.

Experimental observations indicated that very little polarization occurred. The test for polarization involved a check of current direction immediately after flow was stopped. In no case was there a sharp reversal of current accompanied by decay back to 0.00 microamp. The only indications of polarization were relatively small current reversals with several of the runs at KCl concentrations greater than 2×10^{-4} molar and then only at low porosities (Runs 9-2B, 9-5, 9-6, 10-3, and 10-4A).

Note that none of these runs are included among the six low ζ trials in Fig. 10 (Runs 8-30, 8-31, 9-22, 9-23, 9-30, and 10-1 in Table I). Thus, electrode polarization is an unlikely explanation for these six ζ values.

Nonetheless, polarization did cause unusually large coefficients of variation in comparison to the coefficients in those runs at $c > 2 \times 10^{-4}$ M KCl in which polarization was not observed (Runs 10-5, 10-10B, and 10-12B in Table I and Appendix V).

Porous Structure of Silver Chloride Layer

The six points well below the curve in Fig. 10 still require explanation. It should be noted that these points were all from the initial two measurements with electrodes that were either freshly anodized (no. 10 and 11) or had been idle for 18 days (no. 9). The implication is that something in the nature of the Ag-AgCl electrodes must change before steady-state measurements are attained.

Porosity of the AgCl layer could be a factor. That portion of the AgCl layer formed toward the end of anodization lies beneath a relatively nonporous AgCl coating (44). It may take hours for the electrolyte concentration to increase in the AgCl layer after the ion depletion which accompanies anodization.

It is possible that low ζ values for the initial trials with new electrodes were caused by a lack of equilibrium conditions in the structure of the Ag-AgCl electrodes. However, the proposal is questionable since electrode pair no. 9 was not newly anodized and should have reached an equilibrium condition, although it is noted that pair no. 10, not 9, produced the largest discrepancy from the curve in Fig. 10.

Variation in Mat Formation

Special attention was given to the mat-forming technique in an attempt to eliminate this factor from the streaming current variation between runs. The Kozeny factor, k, which is a function of the overall frictional pressure drop, ΔP, across the mat, as well as other variables, was used to measure mat-forming reproducibility; it is calculated from the following relationship:

$$k = \Delta P\, \epsilon^3/[U\, L(1 - \epsilon)^2 \eta\, S_v^2] \qquad (24),$$

where

ε = porosity,

U = superficial approach velocity,

L = overall thickness of mat,

η = viscosity of bulk of the liquid, and

S_V = specific surface area per unit volume of fiber.

The value of k calculated at each porosity for dacron fiber mats was usually 2 to 4 times the generally accepted value of k, which was calculated from the Davis equation (46). In spite of the large values for k, the between-run variation in k was small, particularly between consecutive runs (refer to Appendix V).

The large discrepancy between experimental k and that of Davis was not observed with nylon fiber mats (runs prior to 8-9). There are several possible reasons for the difference between mats of nylon and dacron fibers: (1) The nylon fiber mats were at least twice as heavy as the dacron fiber mats; thus, less mat-septum (perforated electrodes) interaction would be expected. The nylon fiber mats were heavier because the consistency in the 200-liter suspension tank could be raised to 0.02% without any fiber flocculation occurring. With dacron fibers, it was necessary to stay at 0.01% solids in order to minimize flocculation. (2) This flocculation observed with dacron fibers could be the cause of unusually large ΔP, and thus k. It was visually estimated that 5 to 10% of the dacron fibers in the forming tube above the mat were flocculated.

In spite of the marked difference in levels of experimentally calculated k between nylon and dacron fiber mats, the newly derived streaming current model was applied with equal success to individual runs with both types of fibers. It is concluded that the variations between runs in mat formation were not large enough to explain between-run zeta potential changes, which were large with nylon fiber mats.

Nonreproducibility with Nylon Fiber Mats

A discussion of results with nylon fibers is appropriate because it was nonreproducibility with nylon fibers that caused the change to the more hydrophobic dacron fibers. It is difficult to explain the reproducibility problems with nylon fibers. As seen from the data presented in Table II, variations in zeta potentials of as high as 60% were found between consecutive runs using the same KCl solution and fibers from the same 200-liter suspension.

When the change was made to dacron fibers, the range of ζ values from four consecutive runs (8-9 to 8-12, Table I) was about 10%. This remarkable improvement using the same set of electrodes indicates that the nylon fibers were the source of the reproducibility problems.

The reason for the problem with nylon fibers is not clear. However, two observations which might lead to an explanation were made. (1) The nylon fibers showed appreciable swelling (5% increase in diameter after soaking in water for two weeks). (2) The second of two consecutive runs consistently produced the lower streaming currents (refer to Runs 6-22A to 6-30B, 7-26 to 7-29 in Table II). Fibers in the first run were equilibrated in 1×10^{-4} M KCl for about 20 hours, while the time extended to 30-40 hours for fibers in the second run of each two-run series.

Summary of Reproducibility Discussion

It appears that the streaming current data were obtained with electrodes functioning close to equilibrium conditions and thus gave a meaningful measure of the electrokinetic properties of the dacron fibers. The reproducibility of zeta potentials at various electrolyte concentrations (Fig. 9) and the absence of electrode polarization in most runs support the preceding conclusion. The six

TABLE II

SUMMARY OF STREAMING CURRENT RESULTS WITH NYLON FIBERS[a]

Run	Calc'd. Zeta Potential -ζ, mv.	Coeff. of Variation[b]	Empirical Exponent, h[c]	Permeant (KCl Solution) pH at 25.0°C.	Moles/l. x 10,000
11-7-65	3.6+	5%	2.8		1
12-21	2.6	6	1.7		1
12-30	3.7	9	3.6		1
1-13-66	2.8	7	2.5		1
1-21[d]	3.2	9	4.0		1
1-31	1.3	7	3.0		
5-25[d]	3.5	5	2.5		1.13
5-31[d]	6.6	8	2.6	6.0	1.13
6-9	4.5	3	2.8	6.3	1.15
6-22A[d,e]	11.9	6	2.6	6.5	1.13
6-22B[d,e]	10.1	3	2.9	6.5	1.12
6-30A[d,e]	8.0	3	2.8	6.7	1.21
6-30B	6.8	6	3.1	6.5	1.21
7-26[d,e]	7.8	2	2.8	6.2	1.15
7-27[e]	4.9	5	3.2	6.2	1.11
7-28[e]	5.4	5	2.7	--	1.15
7-29	3.0	5	3.1	6.3	1.15
			Av. = 2.9		
Results at High Electrolyte Concentrations					
6-14A[d,e]	4.7	16	4.1	6.0	7.1
6-14B	4.2	13	3.8	5.7	8.0
7-21A[d,e]	1.4	9	3.5	6.2	10.1
7-21B[e]	2.7	29	5.2	--	10.1
7-23A[e]	3.2	27	5.3	--	10.8
7-23B	3.0	27	5.3	6.2	10.8

[a] No correction for the flow current was made for any run; all fibers were extracted with 95% ethanol prior to forming mat; for nylon fibers: diameter = 32.3 μm., α = 0.96 cc./g., length = 2.9 mm.; see Appendix V for tables of ζ calculations.

[b] Coefficient of variation = sigma x 100/zeta.

[c] Determined for porosity $\leq$ 0.80; Biefer and Mason found that $h = 1.5$.

[d] Single spacing between runs indicates that the same KCl solution was used to permeate the beds during those runs.

[e] Fibers in this run and the following run were from the same 200-liter suspension, i.e., approximately 90 liters were used to form each bed.

points below the curve in Fig. 10 may indicate a lack of equilibrium conditions in the structure of Ag-AgCl electrodes which are newly anodized or have been stored for more than two weeks.

The between-run variation in mat formation, as measured by the Kozeny factor, was relatively small; but the magnitude of the Kozeny factor was unusually large with dacron fiber mats. No adequate explanation can be given for the large between-run zeta potential variation with nylon fiber mats.

MONO- AND DIVALENT COUNTER IONS

Calcium counter ions were more effective than potassium ions in reducing ζ values (Fig. 9), as would be expected. However, the ζ reduction by calcium ions was not as large as one might expect if a very rough analogy is made to coagulation concentration ratios of $1:(1/\underline{z}_i)^{\epsilon}$ (or 1:1/64) in the Schulze and Hardy rule, or Overbeek theory (20, p. 306). In explanation, it is noted that even the calcium ion concentration is less than that ($\sim 5 \times 10^{-4}$ molar) which usually produces coagulation (20). Secondly, as Overbeek (20) pointed out, for relatively low zeta potentials, which is the case here with $\zeta < 15$ mv., a ratio lower than Schulze and Hardy's will hold. The concentration ratio to produce coagulation could drop to $1:(1/2)^2:(1/3)^2$ for concentrations of mono-, di-, and trivalent counter ions, respectively (20).

For lack of a theoretical prediction of ζ vs. $\underline{c}$ behavior for different ions, a comparison with other electrokinetic results will be made. Overbeek (20) states that the ζ vs. $\underline{c}$ relationship in many cases can be represented as follows:

$$\zeta = k_2 - k_3 \log c \qquad (25),$$

where $\underline{k}_2$ and $\underline{k}_3$ are constants. Plots in the literature of ζ vs. $\underline{c}$ show that ζ

becomes nearly independent of c at very low concentration ($\leq 5 \times 10^{-5}$ M for 1:1 electrolyte) (20). Thus, Equation (25) is restricted to $c \geq 5 \times 10^{-5}$ M.

The data plotted in Fig. 9 indicate that ζ was independent of c below about 1×10^{-4} M for KCl solution. The streaming current results of Neale and Peters (21) show that the ζ vs. c curves were independent of c at $c \leq 4 \times 10^{-4}$ M NaCl for nylon fiber mats. Therefore, the ζ results in Fig. 9 are fairly similar to previous results (20, 21) at $c \leq 10^{-4}$ M KCl and show the expected ζ decrease at $c \geq 10^{-4}$ M KCl. However, too few points were obtained in this study at $c > 10^{-4}$ M to confirm Equation (25). The range of c was kept $<10^{-3}$ M KCl due to the previously discussed viscosity variation effect (15).

In addition, the backcurrent correction (see p. 93) was large unless c was less than 4×10^{-4} M KCl since the resistance was quite low ($\sim$250 ohms) at electrode separations as small as 0.10 inch and $c = 4 \times 10^{-4}$ M KCl.

EFFECT OF FIBER ORIENTATION IN MAT

Referring back to Curve 2 in Fig. 8, it is noted that Biefer and Mason's corrected equation [Equation (3)] does not give a constant zeta potential, even at porosities < 0.80. Instead of a value of $h = 1.5$ as in Equation (2), h averaged 3.7 with dacron fiber mats and 2.9 with nylon fibers for the present streaming current data at mat porosities < 0.80 (Tables I and II). Thus, a distinct difference exists between the present streaming current variation as a function of mat porosity and that observed by Biefer and Mason (26).

An explanation for this difference is based on the fiber orientation factor which results from an edge effect when a mat is formed (refer to Experimental, p. 35). It is safe to assume that the 3-inch diamter mats used here

had a larger percentage of fibers oriented perpendicular to the approaching flow in comparison to the 1-inch diameter mats of Biefer and Mason.

It is recalled that Equation (23) was derived from Happel's model for flow perpendicular to cylinders. Applying Happel's model (25, 31) for flow parallel to cylinders, the following counterpart to Equation (21) was obtained.

$$I = N \int_o^{2\pi} \int_a^{a+\tau} \rho(r)\, u(r)\, r\, dr\, d\theta \tag{26}$$

$$I = \frac{A}{\pi b^2} \frac{D\kappa^2 \psi_\delta U}{8 K K_o(\kappa a)} \int_a^{a+\tau} K_o(\kappa r)[(a^2 - r^2) + 2b^2 \ln (r/a)]r\, dr \tag{27}$$

where b = radius of the fluid envelope,

$K = [4a^2b^2 - a^4 - 3b^4 + 4b^4 \ln (b/a)]/8b^2$,

and all other terms have been defined previously (see Symbols and Abbreviations).

In Fig. 11, curves for the streaming current variation with porosity are given for the three cases of interest:

Curve 1 – Flow perpendicular to cylinders according to Equations (21) and (23),

Curve 2 – Biefer and Mason's experimentally observed variation, which was adjusted to the scale of Curves 1 and 3 (refer to Table III, Column 5), and

Curve 3 – Flow parallel to cylinder according to Equation (27), the Fortran computer program for which is listed at the end of Appendix IV.

It is obvious from Fig. 8 on p. 41 that considerable discrepancy exists between the magnitude of the zeta potential that is predicted by the new model and that based on the capillary model. As a result, a scale adjustment was made for Curve 2, but this adjustment will not change the relative value of the I/U

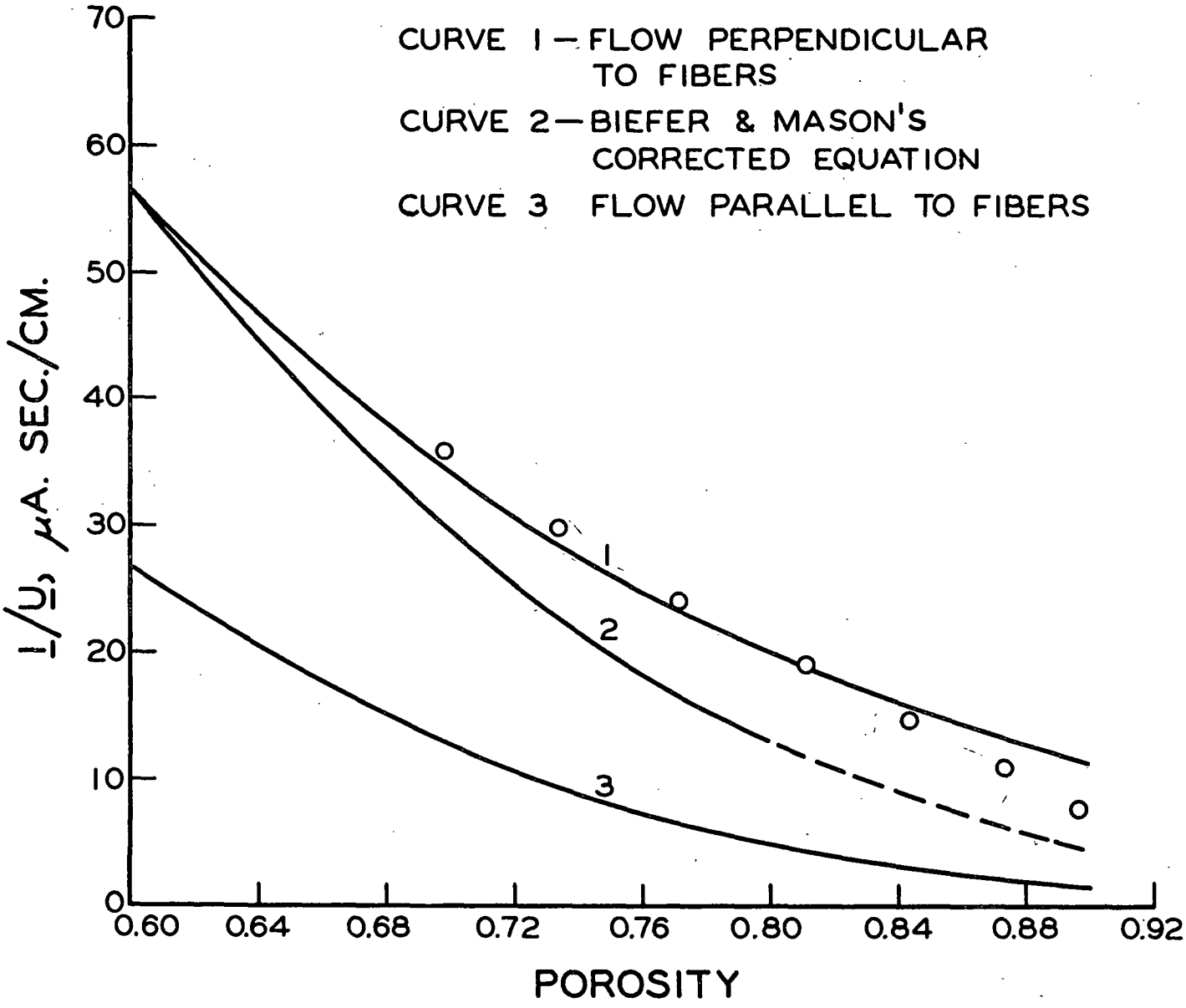

Figure 11. Streaming Current Slopes ($\underline{I}/\underline{U}$) as a Function of Fiber Mat Porosity (Refer to Table III; Data Points from Run 9-22)

vs. ϵ variation. A listing of the I/U values used to plot Fig. 11 is given in Table III.

TABLE III

I/U VS. ϵ VALUES USED IN FIGURE 11[a]

	Slopes (I/U), μa, sec./cm.			
	Using Happel Model			
	Flow Perpendicular to Fibers, Equation (21)	Flow Parallel to Fibers, Equation (27)	Biefer and Mason's Corrected Equation, Equation (3)	
Porosity (ϵ)	--	--	b = 1.0	b = 3.24[b]
0.92	9.7	0.9	1.0	3.2
0.88	12.8	1.9	1.8	5.8
0.84	16.3	3.2	2.7	8.9
0.80	20.3	5.0	4.0	12.9
0.76	25.1	7.3	5.7	18.4
0.72	30.9	10.5	7.9	25.4
0.68	37.9	14.5	10.6	34.4
0.64	46.4	19.8	13.9	45.0
0.60	56.9	26.8	17.5	56.9

[a]The experimental conditions of Run 9-22 are used as an example: 0.000145M KCl, 24.4°C., ζ = 9.2 mv., dacron fiber radius = 8.7 μm.

[b]Adjustment factor = 56.9/17.5 = 3.24 since most fibers in either a 3-in. or a 1-in. diameter mat should be oriented perpendicular to flow under the high compacting force needed to obtain 0.60 porosity. The I/U values in Columns 4 and 5 for $\epsilon > 0.80$ should be somewhat smaller than those shown here since b was less than 1.0 at $\epsilon > 0.80$ (26); hence, the dashed line at $\epsilon > 0.80$ in Fig. 11.

Referring to Fig. 11 again, one sees that the streaming current – vs. – porosity relationship of Curve 2 deviates farther from Curve 1 as the porosity increases. Thus, increased fiber orientation toward the direction of flow in 1-inch diameter mats compared to that in 3-inch diameter mats offers a reasonable explanation for the difference between the I/U vs. ϵ relationship observed by Biefer and Mason (26) and that observed in this work.

The data points in Fig. 11 for Run 9-22 also indicate a deviation from Curve 1 at $\epsilon \geq 0.85$. Since this deviation was typical of streaming current data at $\underline{c} < 1.0 \times 10^{-4}$ $\underline{M}$ KCl (Appendix V), it is likely that fiber orientation at high porosity was a factor in this work.

However, the fiber orientation effect at high porosities was not as pronounced at $\underline{c} > 1 \times 10^{-4}$ $\underline{M}$ KCl, nor at $0.5 - 2 \times 10^{-4}$ $\underline{M}$ $CaCl_2$. In these runs (10-5 to 10-14B), fairly good agreement with Curve 1 was obtained. An adequate discussion of the role of fiber orientation at high porosity cannot be given until there is a better understanding of the ion transport process within a fiber mat at various electrolyte concentrations (see discussion p. 29 and in Appendix II). The electrolyte concentration (i.e., thickness of the diffuse layer) appears to influence the extent of the deviations from Curve 1 at high mat porosities.

Additional evidence which indicates the sensitivity of streaming current data to fiber orientation in the mat is obtained by comparing the different averages for $\underline{h}$ in Tables I and II. The significantly lower value of 2.9 for nylon fiber mats when compared to 3.7 for mats of dacron fibers indicates that the nylon fiber mats contained a larger proportion of fibers oriented toward the direction of flow ($\underline{x}$-direction). Comparing length-to-diameter ratios ($\underline{\ell}/2\underline{a}$) for the two fibers, it is seen that the ratio (6000/17.4 = 345) for dacron fibers was almost four times that (2900/32.3 = 90) for nylon fibers. Elias (50) found that glass fibers with the lower $\underline{\ell}/2\underline{a}$ ratio will have the larger average $\underline{x}$-direction orientation. Fiber stiffness is a factor which must be considered when comparing glass, dacron, and nylon fibers — glass being the most stiff, nylon the least. Even though the stiffer dacron fiber should show a greater proportion of $\underline{x}$-direction orientation than nylon fibers at comparable $\underline{\ell}/2\underline{a}$ ratios and mat-forming conditions, it appears safe to conclude from the four-times-larger ratio in this work that dacron

fibers would have a smaller x-direction orientation. The small amount of flocculation noted with dacron fibers (see p. 48) might increase x-direction orientation; however, this conjecture cannot be supported by experimental evidence at this time.

A question that arises at this point involves the possible difference in average coefficients of variation between nylon and dacron fiber mats. Comparing results in Tables I and II, it is clear, even though some scatter is present, that the average coefficient of variation is less for nylon than for dacron. This is the opposite of what one would expect. However, the probable answer to the conflict lies in the fact that only data at $\epsilon < 0.80$ were used to calculate h, while the coefficient of variation included data at $\epsilon > 0.80$, where the deviation from average ζ_c was the largest. A considerably larger proportion of readings were at $\epsilon > 0.80$ for dacron fibers in comparison to nylon fibers. This fact, along with the various changes in electrolyte concentration for runs with dacron fibers, produced the larger coefficients of variation in runs with dacron fiber mats.

In summary, the following observations indicate an x-direction orientation effect: (1) The discrepancy between the results of Biefer and Mason and those of the present study points toward an orientation effect, which resulted from a difference in mat-forming technique. (2) The difference between average h values very possibly relates to the large difference in length-to-diameter ratios between nylon ($\ell/2a = 90$) and dacron ($\ell/2a = 345$). (3) The discrepancy between theory and experiment at porosities ≥ 0.85 could result from a fiber orientation effect, but the occurrence of the discrepancy mainly at $c < 10^{-4}$ M KCl raises doubt about this last hypothesis.

REVIEW OF LIMITATIONS

ASSUMPTIONS IN THEORETICAL DEVELOPMENT

The assumptions used to derive the streaming current relationship in Equation (23) can be expressed in the following general terms.

(1) It is assumed that the Gouy-Chapman theory for the diffuse part of the electrical double layer under static, nonflow conditions can be applied to the dynamic conditions of electrokinetics (refer to discussion on p. 40).

(2) The flow equations from Happel's free-surface model are assumed to give an adequate description of the velocity very close to the surface of cylindrical fibers which are arranged in concentrated assemblages and are oriented perpendicular to the approaching liquid velocity (see p. 24).

(3) It is assumed that the dominant means of counter ion transport in the fiber mats is by liquid flow, i.e., the rate of charge transport to the fiber surfaces from the bulk liquid by ion migration in an electric field, or by ion diffusion in a concentration gradient, is small compared to the rate of ion transport by liquid flow (refer to Appendix II).

In specific terms, these general assumptions imply that:

(a) Charge is uniformly distributed on the fiber surface with the same charge distribution on each fiber;

(b) The dielectric constant ($\underline{D}$) within the diffuse layer is the same as in the bulk of the solution (15);

(c) $\underline{z_i}\ \underline{e}\ \psi/\underline{k_1}\ \underline{T}$ is small, i.e., $\psi_\delta < 10$ mv., or $\psi_\delta < 50$ mv. according to Rice and Whitehead (42); refer to p. 32.

(d) $\kappa r > 10$ (discussion on p. 34);

(e) Creeping flow of an incompressible liquid is occurring; thus inertia terms can be omitted from the equation of motion (51);

(f) Viscosity within the diffuse layer is the same as that in the bulk of the solution (refer to p. 9); and

(g) Mat porosity > 0.4 to 0.5 for Happel model (31).

EXPERIMENTAL LIMITATIONS

Limitations which can be attributed to the experimental method for measuring streaming current include the following.

(1) An electrode system operating close to equilibrium conditions and measuring all excess charge passing the electrode is required (see discussion on p. 47).

(2) The supporting septum for the fiber mat should have only negligible influence on the velocity pattern through the fiber mat (refer to discussion of Kozeny factor differences between nylon and dacron fiber mats on p. 49).

(3) A mat-forming technique which arranges all fibers with their axes perpendicular to the approaching flow is needed (discussion on p. 36).

CONCLUSIONS

The new streaming current relationship in Equation (23), which is based on the Happel flow model, represents a marked improvement over the usual capillary model approach to the streaming current/potential phenomenon in fiber mats. It was demonstrated that Equation (23) gave a satisfactory treatment of experimental data at various porosity levels with both dacron fiber mats (0.70 to 0.85 porosity; fiber diameter = 17.4 μm.) and mats of nylon fibers (32.3 μm. diameter; mat porosities 0.60 to 0.80) at electrolyte concentrations of about 1 to 4 x 10^{-4} molar KCl and 0.5 to 2 x 10^{-4} M $CaCl_2$.

The major difference between the new approach and the capillary-model approach to the streaming current phenomenon involves the model for flow through fiber mats. By using the Happel model for flow through assemblages of cylinders, (1) a good estimate of the velocity profile at the fiber surface is obtained, and (2) a better understanding of the counter-ion transport process between fibers results.

The same Gouy-Chapman theory for a diffuse layer at equilibrium was used in both the new streaming current model and the classical theory, which is based on the capillary flow model. However, as has been stated in the literature, an improved understanding of the electric double layer under the nonequilibrium conditions of electrokinetics is needed (refer to p. 12).

The application of the Happel flow model to streaming current theory appears to be a better approach to solving the discrepancies between streaming current theory and experiment than the varying tortuosity explanation of Biefer and Mason (26). Improving the flow model was suggested by Biefer and Mason as an alternative approach.

There is agreement, however, with Biefer and Mason's conclusion that zeta potentials calculated from electrokinetic data with porous media are not absolute

values. Additional work should be done to independently determine the zeta potential of fibers used in streaming current studies and/or to confirm the assumptions concerning ion transport and the Happel flow model in the streaming current model presented here.

The streaming current data appear to be quite sensitive to fiber orientation in the mat. A difference between average value of $\underline{h}$, an empirical measure of streaming current variation as a function of porosity, for mats of dacron fibers and mats of nylon fibers may result from a large difference in the length-to-diameter ratios between these two types of fibers. Differences in fiber orientation due to an edge effect during mat formation appear to explain why Biefer and Mason (26) found a smaller $\underline{h}$ value (1.5) with 1-inch diameter mats than was found with the 3-inch diameter mats of the present study ($\underline{h}$ = 2.9 to 3.7).

Some variability between runs was observed in the streaming currents (1) from the first two trials with electrodes which were newly anodized or had been idle for several weeks, (2) with mats of nylon fibers, and (3) from five runs in which some polarization was noted. The general conclusion is, however, that the experimental system was reproducible at various concentrations of KCl and $CaCl_2$ solutions when dacron fiber mats were used. Reasonable explanations were offered for the variability due to electrodes. Furthermore, the new calculation of the relation between the zeta potential and streaming currents at various fiber mat porosities was quite consistent within any particular run for both dacron and nylon fiber mats, despite between-run variability.

FUTURE WORK

One area for future work would involve additional experimental studies to test the streaming current model presented in this report. A layer of non-contacting, uncut cylindrical fibers could be arranged in a frame, which could then be inserted horizontally into the permeation cell between the two electrodes. The porosity would be varied by decreasing the separation between fibers. The advantage of this technique lies in the fact that the number of fibers contributing to the streaming current is easily determined.

Electrophoresis studies with dilute suspensions of fibers [see Henry (41)] could be used to determine the zeta potential of the same fibers used for streaming current measurements. If the zeta potentials were found equal, there would be additional support for the new streaming current model.

Another area for future work involves extending the present approach to the streaming current phenomenon to noncylindrical fibers such as pulp fibers. Fibers with elliptical cross sections of various aspect ratios would be a logical first step in this direction. The difficulty, however, is that equations are presently unavailable for flow past assemblages of "elliptical fibers" (25). Even if flow equations were not available, it might be possible to approximate the streaming current, I, from "elliptical fibers" by using the model for cylindrical fibers. It is recalled that I was determined using the velocity profile very close to the solid surface at $\theta = \pi/2$ and $3\pi/2$. This velocity profile under conditions of creeping flow and at low aspect ratios is more likely influenced by separation between fibers (i.e., mat porosity) than it is by the cross-sectional shape of the fibers.

The fiber orientation effect on the streaming current from mats with fibers of various length-to-diameter ratios merits further study. The object would be

to theoretically predict $\underline{I}$ as a function of fiber orientation in the direction of approaching flow. Experimentally, the edge effect could be eliminated by by forming 5-inch diameter mats which would be frozen and cut to 3 inches in diameter. Care would have to be taken to avoid aeration of the mat.

SYMBOLS AND ABBREVIATIONS

$\underline{A}$ = cross-sectional area of bed, cm.^{2}

A. = Ångström unit

$\underline{A}_e$ = cross-sectional area available for flow within bed

$\underline{a}$ = radius of swollen fiber, μm.

$\underline{a}_1$ = constant in conductance equation

$\underline{b}$ = radius of Happel's fluid envelope; proportionality constant assigned a value of 1.0 at $\epsilon < 0.80$

$\underline{C}$, $\underline{D}_1$, $\underline{E}$, $\underline{F}$ = constants in Happel's equations

$\underline{C}_3$ = 9.0×10^8, a constant for converting units in streaming current equation from capillary model (see Computer Program in Appendix IV)

$\underline{C}_4$ = 9.0, a constant for converting units in streaming current equation developed from Happel model (listed as C2 in Computer Program)

$\underline{c}$ = electrolyte concentration in bulk of solution, moles/liter

$\underline{c}_1$ = uniform bed density, g./cc.

$\underline{D}$ = permittivity (dielectric constant) of the bulk of the liquid, (statcoulomb)^2/(dynes cm.^{2})

$\underline{D}_2$ = diffusion coefficient, cm.^{2}/sec.

$\underline{e}$ = electronic charge

$\underline{h}$ (or $\underline{H}$) = empirical exponent to correct streaming current equation developed from capillary model

$\Delta\underline{h}$ (or $\Delta\underline{H}$) = overall frictional pressure drop across mat, cm. in a carbon tetrachloride-water manometer

$\underline{I}$ = streaming current from a porous bed, μa.

$\underline{I}_o$ = symbol for zero-order modified Bessel function of the first kind

$\underline{I}_f$ = flow current between electrodes when bed removed, μa.

$\underline{I}_r$ = residual current, i.e., current between electrodes when liquid flow was zero, μa.

$\underline{I}_s$ = measured streaming current without correction for $\underline{I}_f$, μa.

$\underline{i}$ = identification of type of ion; streaming current from a single capillary

K = Darcy factor in Equation (27)

K_o = symbol for zero-order modified Bessel function of the second kind

k = Kozeny factor, dimensionless

k_o = shape factor, dimensionless

k_1 = Boltzmann constant

L = overall thickness of porous bed, inches

L_e = length of a pore or capillary

L_e/L = tortuosity factor, dimensionless

ℓ = fiber length, cm.

M = moles per liter (molar)

m = mean hydraulic radius

N = number of capillaries in a porous mat; number of fibers contributing to streaming current

$n_i(\infty)$ = number of ions of type i per cc. at zero potential in the bulk of the liquid

O.H.P. = outer Helmholtz plane in electric double layer

ΔP = overall frictional pressure drop across mat, dynes/cm.^{2}

p_s = compacting pressure on bed, p.s.i.

dp/dl = pressure gradient in porous bed

q = tortuosity factor in electrical conductance through porous media

R = radius of capillary; correlation coefficient

r = radial distance coordinate

S_o = specific surface area per unit volume of porous bed, cm.^{2}/cc.

S_v = specific surface area per unit volume of particle, cm.^{2}/cc.

T = absolute temperature, °K.

T_1, T_2, T_3, T_4 = terms used in streaming current equation

U = superficial approach velocity above porous bed, cm./sec.

$\underline{u}$ = mean velocity in a capillary, cm./sec.

$\underline{u}_e$ = point velocity in a capillary, cm./sec.

$\underline{u}_\theta$ = angular velocity for case of a fluid moving perpendicular to a stationary cylinder

$\underline{v}_\theta$ = angular velocity in Happel equation

$\underline{x}$, $\underline{y}$, $\underline{z}$ = coordinates

$\underline{z}_i$ = ion valency

α = fiber specific volume, cc./g.

δ = thickness of immobile layer, A.

ϵ = porosity or void fraction, dimensionless; $\epsilon = 1 - \alpha\underline{c}_1$

ζ = zeta or electrokinetic potential which is the experimentally obtained estimate of ψ_δ, mv.; ζ = average $\zeta_{\underline{c}}$

$\zeta_{\underline{c}}$ = zeta potential calculated at each mat porosity, mv.

η = viscosity of the bulk of the liquid, centipoises

θ = angular component in cylindrical coordinates

κ = Debye-Hückel constant, $(\mu m.)^{-1}$; κ^{-1} is proportional to diffuse layer thickness (τ)

π = 3.1416

ρ = excess charge per unit volume, ions/cc.

τ = thickness of diffuse layer, $\mu m.$

ψ = average electrical potential at distance $\underline{r}$ (or $\underline{x}$) from solid surface

ψ_o = surface potential of solid

ψ_δ = average electrical potential at plane of closest approach of ion centers (O.H.P.), mv.

ACKNOWLEDGMENTS

The guidance and assistance of Dr. Dale G. Williams, the Chairman of my faculty Advisory Committee, along with that of the late Dr. William L. Ingmanson and Mr. John W. Swanson, the other Committee members, is gratefully acknowledged. Dr. Ingmanson's death in November, 1966, removed an able advisor from those who study flow through porous media.

The discussions with Mr. Heribert Meyer and Dr. Richard W. Nelson were very helpful in the development of the streaming current model. Assistance with the experimental apparatus and techniques by Messrs. Bruce D. Andrews, Julian Conkey, Keith Hardacker, Harold H. Heller, and Orlin C. Kuehl was appreciated. In addition, my appreciation is extended to Miss Olga Smith and Messrs. John J. Bachhuber, Marvin C. Filz, Jr., John D. Hankey, and Paul F. Van Rossum for their staff services. The assistance of Mrs. Elizabeth Cary in typing the report, along with that of Mrs. Nancy Ciriacks during the rough draft stage, is gratefully acknowledged.

Finally, sincere appreciation is given to the many other Institute staff members who have aided me and my family. This includes those in the Office of the Dean, the Librarians, and many people in the Engineering and Plant Service Departments.

LITERATURE CITED

1. Reuss, F. F., Mem. Soc. Imperiale Natural (Moscow) 2:327(1809).

2. Sennett, P., and Olivier, J. P., Ind. Eng. Chem. 57, no. 8:32-50(Aug., 1965).

3. Kitchener, J. A., and Haydon, D. A., Nature 183:78-80(1959).

4. Haydon, D. A. In Danielli, Pankhurst, and Riddiford's Recent progress in surface science. Vol. 1. p. 94-158. New York, Academic Press, 1964.

5. Delahay, P. Double layer and electrode kinetics. New York, Interscience, 1965. 321 p.

6. Davies, J. T., and Rideal, E. K. Interfacial phenomena. New York, Academic Press, 1961. 468 p.

7. Helmholtz, H., Wied. Ann. 7:337(1879).

8. Gouy, G., J. Phys. Rad. 9:457(1910).

9. Chapman, D. L., Phil. Mag. 25:475(1913).

10. Stern, O., Z. Elektrochem. 30:508(1924).

11. Grahame, D. C., Chem. Revs. 41:441(1947).

12. Devanthan, M. A. V., Trans. Faraday Soc. 50:373(1954).

13. Bell, G. M., Mingins, J., and Levine, S., Trans. Faraday Soc. 62, no. 4: 949-59(1966).

14. Levine, S., Mingins, J., and Bell, G. M., Can. J. Chem. 43, no. 10:2834-66 (1965).

15. Lyklema, J., and Overbeek, J. Th. G., J. Colloid Sci. 16:501-12(1961).

15a. Stigter, D., J. Phys. Chem. 68:3600-2(1964).

16. Sparnaay, M. J., Trans. Faraday Soc. 53:306-14(1957).

17. Buff, F. P., and Stillinger, F. A., J. Chem. Phys. 39:1911-23(1963).

18. Morimoto, T., Bull. Chem. Soc. Japan (In Engl.) 37, no. 3:386-92(1964).

19. Seno, M., and Yamabe, T., Nature 202, no. 4937:1110-11(1964).

20. Overbeek, J. Th. G. In Kruyt's Colloid science. Vol. 1. p. 195-244. London, Elsevier, 1952.

21. Neale, S. M., and Peters, R. H., Trans. Faraday Soc. 42:478-87(1946).

22. Goring, D. A. I., and Mason, S. G., Can. J. Research 28B, no. 6:307-38(1950).

23. Mossman, C. E., and Mason, S. G., Can. J. Chem. 37:1153-64(1959).

24. Neale, S. M., Trans. Faraday Soc. 42:473-8(1946).

25. Happel, J., and Brenner, H. Low Reynolds number hydrodynamics. Englewood Cliffs, N. J., Prentice-Hall, 1965. 553 p.

26. Biefer, G. J., and Mason, S. G., Trans. Faraday Soc. 55:1239-45(1959).

27. Sullivan, R. R., and Hertel, K. L. In Kraemer's Advances in colloid science. Vol. I. p. 38. New York, Interscience, 1942.

28. Brown, J. C., Jr. Determination of the exposed surface area of pulp fibers from air permeability measurements, using a modified Kozeny equation. Doctor's Dissertation. p. 103-12. Appleton, Wis., The Institute of Paper Chemistry, 1949; Tappi 33, no. 3:130-7(1950).

29. Carman, P. C. Flow of gases through porous media. New York, Academic Press, 1956. 182 p.

30. Scheidegger, A. E. The physics of flow in porous media. p. 93. Toronto, University of Toronto, 1957.

31. Happel, J., A.I.Ch.E. Journal 5, no. 2:174-7(1959).

32. Boyack, J. R., and Giddings, J. C., Arch. Biochem. Biophys. 100, no. 1:16-25 (1963); C.A. 61:7746d(1964).

33. Ghosh, B. N., and Pal, P. K., Trans. Faraday Soc. 57:116-22(1961).

34. Ghosh, B. N., Bandopadhyay, S., and Moulick, S. P., Proc. Natl. Inst. Sci. India Pt. A, 27:193-200(1961).

35. Ghosh, B. N., Moulik, S. P., and Sengupta, S. K., J. Electroanal. Chem. 9:372-9(1965).

36. Stigter, D., J. Colloid Sci. 19:252-67; 268-78(1964).

37. Jacquelin, G., and Bourlas, H., Tech. Rech. Papet no. 3:49-58(March, 1964).

38. Hastbacka, K., and Nordman, L., Paperi ja Puu 45, no. 6:353-8(1963).

39. Ingmanson, W. L. Private communication.

40. Debye, P., and Hückel, E., Phyzik Z. 24:185(1923).

41. Henry, D. C., Proc. Roy. Soc. (London) 133:106-40(1931).

42. Rice, C. L., and Whitehead, R., J. Phys. Chem. 69, no. 11:4017-24(1965).

43. Flügge, W. Four-place tables of transcendental functions. New York, Pergamon Press, 1954. 136 p.

44. Ives, D. J. G., and Janz, G. J. Reference electrodes. New York, Academic Press, 1961. 633 p.

45. Zucker, G. L. Critical evaluation of streaming potential measurements. Ann Arbor, Mich., University of Michigan Microfilms, 1959. 156 p.

46. Han, S. T. The status of the sheet-forming process – a critical review. Appleton, Wis., The Institute of Paper Chemistry, Dec. 31, 1965. 342 p.

47. Brown, A. S., J. Am. Chem. Soc. 56:646-7(1934).

48. A.S.T.M. standards on textile materials, Part 24. D 629-59T. Philadelphia, American Society for Testing Materials, 1964.

49. Ingmanson, W. L., and Whitney, R. P., Tappi 37, no. 11:523-34(1954).

50. Elias, T. C. An investigation of the compression response of ideal unbonded fibrous structures by direct observation. Doctor's Dissertation. Appleton, Wis., The Institute of Paper Chemistry, 1965.

51. Bird, R. B., Stewart, W. E., and Lightfoot, E. N. Transport phenomena. New York, J. Wiley and Sons, 1960. 780 p.

52. Farrar, N. O. Streaming current – a method of measuring zeta potential. Problem 186-C, Course A300. Appleton, Wis., The Institute of Paper Chemistry, 1964. 23 p.

53. Daniels, F., and Alberty, R. Physical chemistry. 2d ed. New York, J. Wiley and Sons, 1961. 744 p.

APPENDIX I

DERIVATION OF THE STREAMING CURRENT EQUATION USING CAPILLARY MODEL

FLOW IN A SINGLE CAPILLARY

The point velocity for laminar flow of an incompressible fluid in a cylindrical tube is given by (51):

$$u_e = - \frac{dP}{dL_e} \frac{1}{4\eta} (R^2 - r^2) \qquad (28),$$

where u_e = point velocity,

dP/dL_e = pressure gradient,

η = viscosity,

R = radius of the capillary (or tube), and

r = radius at any point.

The mean velocity, u, in the capillary is given by the well-known Hagen-Poiseuille law (51):

$$u = \frac{\int_0^R u_e \, 2\pi r \, dr}{\int_0^R 2\pi r \, dr} = - \frac{R^2}{8\eta} \frac{dP}{dL_e} \qquad (29).$$

Defining x as the radial distance from the plane of shear, which is very close to the capillary wall (see Fig. 1),

$$x = R - r$$

Substituting into Equation (28)

$$u_e = - \frac{dP}{dL_e} \frac{1}{4\eta} (2Rx - x^2)$$

If $x \ll R$,

$$u_e = - \frac{dP}{dL_e} \frac{1}{2\eta} Rx \qquad (30).$$

Equation (30) expresses the velocity close to the capillary wall where $x \ll R$.

If the flowing fluid carries away the charged particles, which are located near the plane of shear, then the current is as follows:

$$i = \int_0^R \rho u_e \, 2\pi R \, dx$$

where ρ = the volume charge density, and

i = the current.

Since the functions are continuous in the interval 0 to R, the integral may be expressed as:

$$i = \int_0^\tau \rho u_e \, 2\pi R \, dx + \int_\tau^R \rho u_e \, 2\pi R \, dx.$$

If the thickness of the diffuse portion of the electric double layer is τ, then by definition $\rho = 0$ at $x = \tau$ and $\rho = 0$ at $x = R$.

Then

$$\int_\tau^R \rho u_e \, 2\pi R \, dx = 0$$

and

$$i = \int_0^\tau \rho u_e \, 2\pi R \, dx \qquad (31).$$

The Poisson electrostatic equation for a flat surface is (4):

$$d^2\psi/d^2x = -4\pi\rho/D \qquad (32),$$

where ψ = the electric potential, and

D = the dielectric constant.

Substituting Equations (30) and (32) into (31),

$$i = \int_0^\tau \frac{D}{4\pi} \frac{d^2\psi}{dx^2} \frac{dP}{dL_e} \frac{Rx}{2\eta} 2\pi R \, dx.$$

If D and η are independent of ψ,

$$i = \frac{R^2 D}{4\eta} \frac{dP}{dL_e} \int_0^\tau \frac{d^2\psi}{dx^2} \, x \, dx.$$

Integrating by parts

$$i = \frac{R^2 D}{4\eta} \frac{dP}{dL_e} \left\{ \left[\frac{x\, d\psi}{dx} \right]_0^{\tau} - \left[\psi \right]_0^{\tau} \right\}$$

Using the boundary conditions that $\psi = 0$ and $d\psi/dx = 0$ at $x = \tau$.

$$i = \frac{R^2 D}{4\eta} \frac{dP}{dL_e} \psi_{x=0} \qquad (33).$$

Defining the zeta potential, ζ, as the experimentally determined potential at $x = 0$, and substituting Equation (29) into (33) yields the streaming current equation for a single capillary,

$$i = -2\, D\, u\, \zeta \qquad (34).$$

FLOW IN POROUS MEDIA

The total current, I, through a bundle of N capillaries is:

$$I = Ni = -2\, D\, u\, \zeta\, N \qquad (35),$$

and

$$N = A_e/\pi R^2 \qquad (36),$$

where A_e = total area available for flow, and

πR^2 = area of a capillary.

The hydraulic radius concept defines the following (29):

$$R^2 = m^2\, 8/k_o,\ m = \epsilon/S_o,\ u = (U/\epsilon)\ (L_e/L) \qquad (37a, b, c),$$

where

m = mean hydraulic radius,

k_o = shape factor,

ϵ = porosity,

S_o = specific surface area per unit volume of porous medium

U = superficial approach velocity above porous medium, and

L_e/L = tortuosity.

Substituting Equations (39) and (37) into (35),

$$I = \frac{-2D\,\zeta\,U\,L_e}{\epsilon\,L}\;\frac{A_e\,k_o}{8\,\pi}\;\frac{S_o^2}{\epsilon^2} \qquad (38)$$

But

$$\epsilon = A_e L_e / A\,L$$

Substituting in Equation (38),

$$I = \frac{-D\,\zeta\,U\,k_o\,S_o^2\,A}{4\pi\epsilon^2} \qquad (39).$$

The Kozeny-Carman equation (29) represents the flow through a porous plug under conditions of laminar flow,

$$U = \epsilon^3\,\Delta P / \left[k_o\,(L_e/L)^2\,S_o^2\,\eta L\right] \qquad (40).$$

Substituting Equation (40) into Equation (39) and replacing ϵ with $(1 - \alpha \underline{c}_1)$ gives the streaming current for flow through the porous plug,

$$\frac{I\,\eta\,L}{\Delta P\,D} = -\frac{A\,\zeta}{4\pi\,(L_e/L)^2}\,(1 - \alpha c_1) \qquad (41),$$

where α = fiber specific volume, and

$\underline{c}_1$ = average density of porous medium.

Equation (41) is identical to Equation (1) on page 14 and was used by Mason and coworkers (22, 26) to treat streaming current data. Neale and Peters (21) used a relationship similar to Equation (41).

The writer wishes to thank Norman Farrar (52) for the derivation which has been presented in this appendix section.

APPENDIX II

COUNTER ION TRANSPORT TO FIBERS

The following analysis is an expansion of the discussion introduced on page 29.

It will be assumed that the diffuse layer can be described by the Gouy-Chapman theory under both dynamic and static (equilibrium) conditions. This assumption implies that there is no ion migration in the bulk of the electrolyte solution surrounding the fiber since the electric field will be zero except for the region very close to the fiber (about 0.1 μm. from fiber).

Support for the assumption is obtained from studies of the relaxation effect in electrophoresis. The relaxation effect, in which the original symmetry of the double layer is disturbed by movement of the particle and the counter ions in opposite directions, is negligible when $\kappa a \geq 100$ (20). For the present, dacron fibers (a = 8.7 μm.) and 1 x 10^{-4} M KCl (κ^{-1} = 0.03 μm.), κa is very large at 290. The electric double layer is not subjected to an external electric field in the streaming current method, as it is in electrophoresis; but this fact only reaffirms the assumption that double layers through which liquid is slowly flowing can be described by the Gouy-Chapman theory.

With migration eliminated as a cause of ion transport at distances greater than about 0.1 μm. from a fiber, liquid flow and diffusion remain to be analyzed. A few calculations, using the highly idealized fiber assemblage in Fig. 12 will show that ion transport by liquid flow predominates over that by diffusion across streamlines.

A fairly large lateral separation exists between fibers at the porosity ranges (0.90 to 0.65) considered in this study. A charge flux existed ($\rho\vec{u} > 0$)

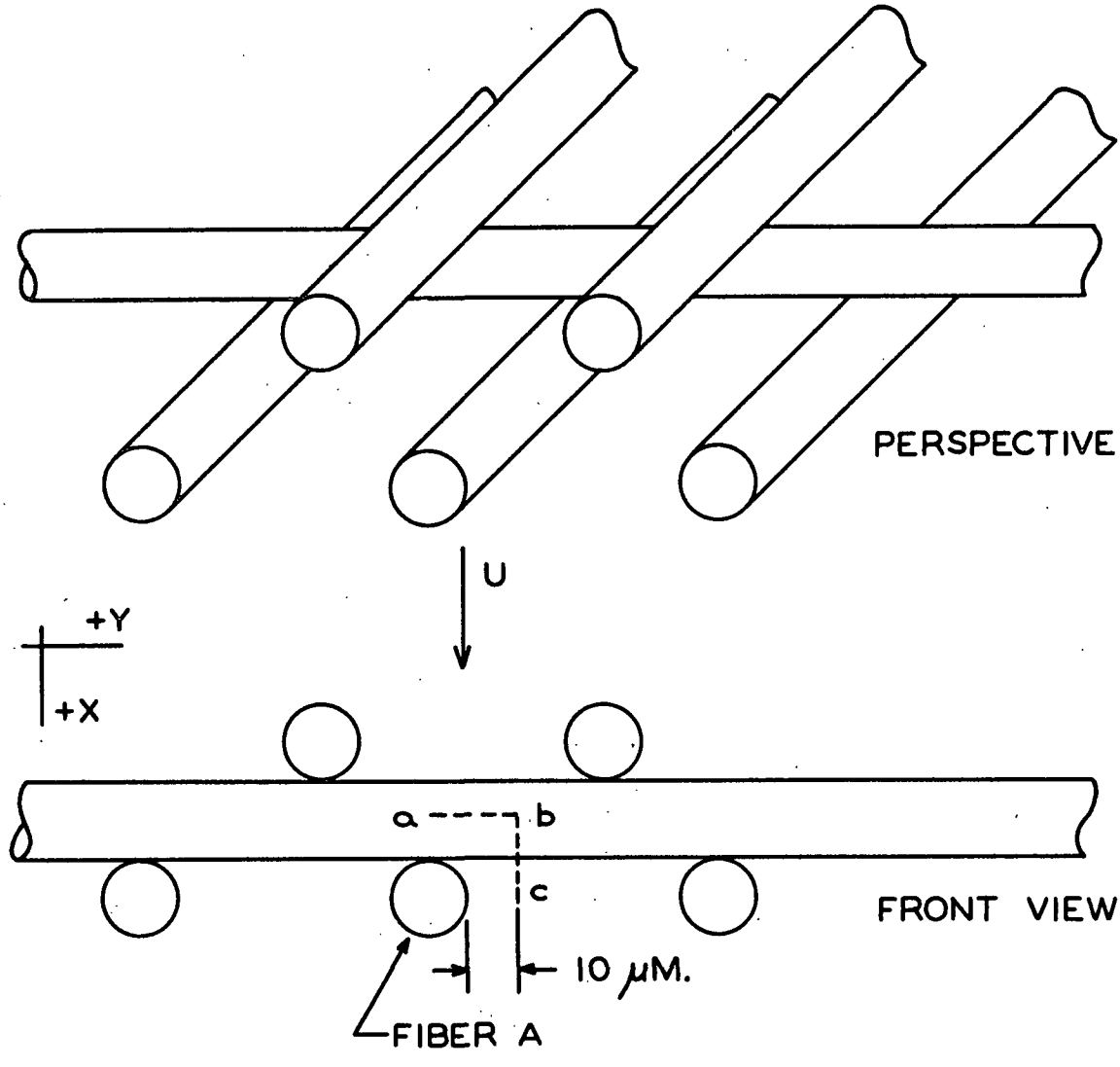

Figure 12. Idealized Views Into an Assemblage of Cylinders with Porosity = 0.80 and Diameter = 17.4 μm.

in the bulk solution between fibers if lateral transport of counter ions to the fibers was negligible. In order to show this, the upper right portion of Fiber A in Fig. 12 is used as an example.

Simplifying the diffusion equation (53) by assuming that all ion concentration gradients are constant, the charge flux is as follows:

$$\rho u_y = - D_2 \Delta\rho/\Delta y \qquad (42),$$

where

ρ = counter ion density in bulk solution,

u_y = velocity component of counter ions in y-direction toward fiber,

D_2 = diffusion coefficient, which equals 2×10^{-5} cm.^{2}/sec. for KCl at 25°C. and at infinite dilution (53), and

$\Delta\rho/\Delta y$ = change in ρ with distance in y-direction (constant ion concentration gradient).

If ρ is assumed uniform throughout the bulk solution (including along line abc in Fig. 12) but is assumed equal to zero at the outer edge of the diffuse layer, then Equation (42) is

$$u_y = - D_2/\Delta y \qquad (43)$$

$= (-2 \times 10^{-5}$ cm.^{2}/sec.$)/10 \times 10^{-4}$ cm.

$=$ -0.02 cm./sec., which is a fairly low velocity in the streaming current system.

Referring back to Equation (6),

$$I = \iint_S \rho \vec{u}\, d\vec{S}.$$

Since ρ is assumed uniform and area $ab\Delta z$ equals $bc\Delta z$, the ratio of charge transported by liquid flow in the x-direction (I_x) to that by migration in the y-direction (I_y) is

$$I_x/I_y = u_x/u_y \cong 10 \text{ to } 20. \quad (44)$$

The 10-to-20 range is based on the superficial approach velocity ($\underline{U}$) in the range 0.13 to 0.31 cm./sec. (at the lower porosity levels $\underline{U}$ ranged from 0.04 to 0.215 cm./sec.), and the liquid velocity ($\underline{u}_x$) approaching the fiber in the mat at a distance is always $>\underline{U}$ approaching the mat.

Even though this has been a very rough approximation of a complex system, the ratio $\underline{I}_x/\underline{I}_y$ is large enough to support the hypothesis that liquid flow is the predominant process for counter ion transport to the diffuse layer of each fiber. This, in turn, supports the method for obtaining $\underline{N}$, the number of fibers contributing to $\underline{I}$ (refer to page 29).

APPENDIX III

EXPERIMENTAL APPARATUS, MATERIALS, AND PROCEDURES

ELECTRODES

FABRICATION AND INSULATION

The 3.0-inch diameter disks were cut from 0.016-inch thick fine silver blank ordered from Engelhard Industries, Newark, N. J. Prior to drilling, the disks were polished with very fine grit carborundum. The perforations were 1/16-inch holes in a staggered pattern on 7/64-inch centers to give 30% cross-sectional area open to flow. A 1/4 x 3-inch "pigtail" of solid silver was left on each disk to provide electrical connection. This eliminated the need to fuse or solder a connection on the silver disk.

Insulation of the back of the disks is essential in achieving stable Ag-AgCl electrodes (22). The silicone rubber (Dow-Corning or General Electric) used to coat the silver was easily applied and stood up well after months of immersion in dilute electrolyte solution. Within 5 minutes of application, the silicone rubber was removed by suction from the perforations. As a result, most of the perforations, as well as the back, had a thin coating of silicone rubber. Coating the holes simplified the task of cleaning the silver surface for repeated anodizations. Both sides of the silver pigtails and the soldered wire connections at the end of each pigtail were coated with silicone rubber.

After waiting a day for sufficient polymerization, the face of each silver disk was polished with 320-C silicon carbide paper followed by polishing with crocus cloth. The preceding operation succeeded in removing the silicone rubber coating from about 5% of the 650 holes in each disk.

A rigid support for the silver disks was provided by 2-inch thick Plexiglas, which was drilled with about seventy 1/4-inch diameter holes. One layer of 30-mesh nylon was used to distribute flow between Plexiglas support and the silicone rubber-backed silver disk. The disks were tied to the support with three 8-lb. monofilament lines threaded through the perforations.

A slot machined in the edge of the top support provided passage for the 1/4 x 3-inch silver pigtail. In the bottom support, a hole was drilled at a 45° angle so that the pigtail could pass under the plastic surface that provided a liquid seal with the O-ring of the anodizing tube or permeation cell.

ANODIZATION

Preceding each anodization, the silver surfaces were cleaned as follows:

1. Polished with Silvo silver polish (R. T. French Co., Rochester, N. Y.) and a clean, soft cloth; rinsed with distilled water;
2. Washed with 95% ethanol and a small brush, followed by a distilled-water rinsing;
3. Washed with Alconox solution and brush with subsequent rinse and storage in deaerated distilled water.

In cases where the disks had been previously anodized, the silver chloride coating was removed with concentrated ammonium hydroxide just prior to the Silvo silver polish treatment.

The apparatus used to form the Ag-AgCl electrodes is shown in Fig. 13 and 14. All gas bubbles had to be removed from the silver surfaces and nylon mesh before anodization. This was accomplished by tapping the entire Plexiglas anodizing tube on the lab bench after it had been partially filled with deaerated 0.10N hydrochloric acid (made with reagent-grade HCl from a newly opened bottle). Moving the top electrode up and down in the liquid removed all gas bubbles.

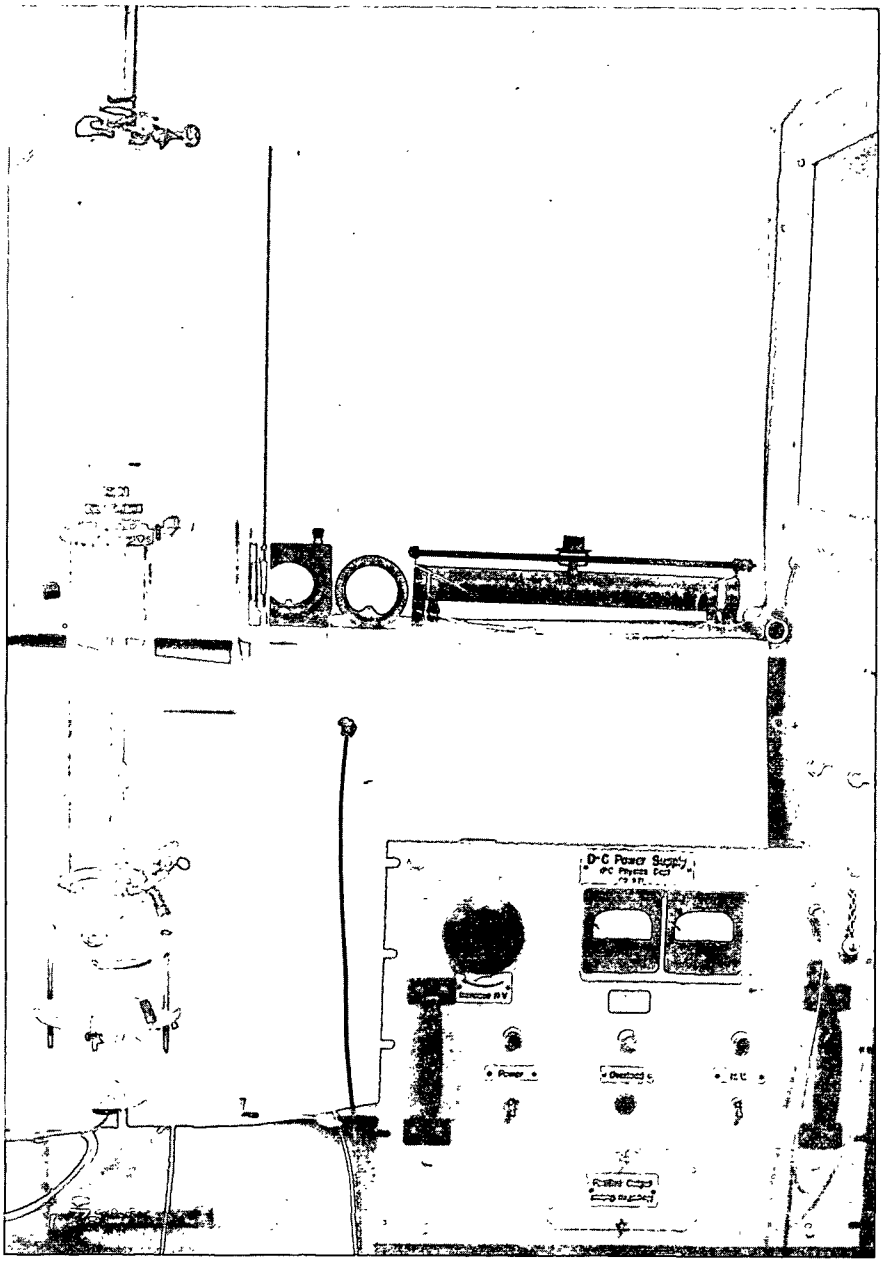

Figure 13. Plexiglas Tube and Other Apparatus for Electrolytically Forming Silver-Silver Chloride Electrodes

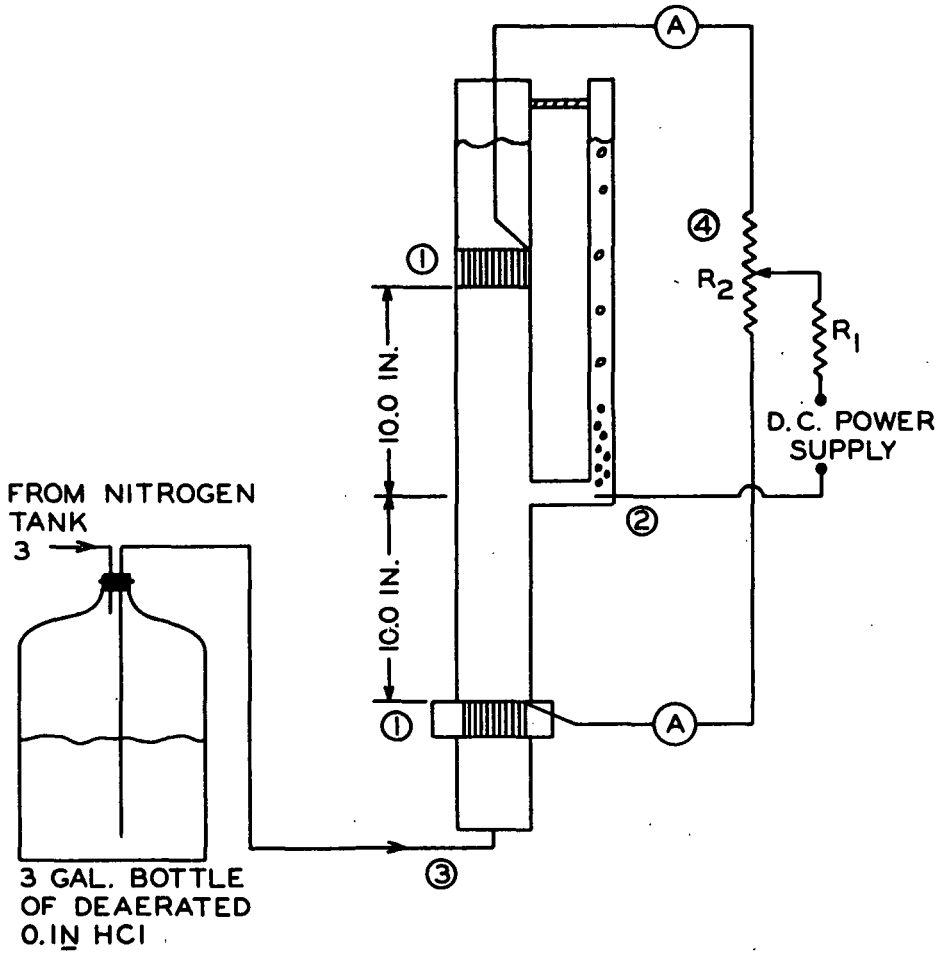

① ELECTRODE AND PLASTIC SUPPORTS (SILVER SURFACE FACING TOWARD CENTER OF ANODIZING TUBE)

② PLATINUM WIRE

③ DIRECTION OF 0.1N HCl FLOW REVERSED EVERY 5 MINUTES WITH LEVEL NEVER FALLING BELOW TOP ELECTRODE

④ SLIDE WIRE ON RESISTANCE R_2 ADJUSTED TO KEEP SAME CURRENT THROUGH EACH AMMETER (A) (R_1 = 1000 AND R_2 = 690 OHMS)

Figure 14. Apparatus for Electrolytically Forming Silver-Silver Chloride Electrodes

In order to form stable Ag-AgCl electrodes in which the residual current would decrease to 0.00 μa. it was found that the polarity of the silver disks had to be periodically reversed. This observation was also made by Neale and Peters (21) as well as Goring and Mason (22).

By reversing the current direction every fifteen minutes for 1.5 hours and then anodizing for 0.5 to 1.0 hours, a uniform, brown (milk chocolate) coating of AgCl was achieved. With the last set of electrodes (Pair No. 11), the current density was increased from 1.0 to 4.0 milliamp./cm.^{2}, the final anodizing time was increased from 0.5 to 1.0 hour, and a new batch of 0.10N HCl was prepared. These changes with Pair No. 11 did not alter the streaming current results when compared with results from previous electrodes (No. 9 and 10).

STORAGE OF ELECTRODES

The Ag-AgCl electrodes were rinsed with a dilute electrolyte solution immediately after anodization. They were then placed in the permeation cell and submerged in deaerated 1 x 10^{-4}M KCl with the electrodes shorted together. Within several days of anodization, the residual current between the electrodes usually fell to 0.0 μa.

Exposure of the electrodes to direct sunlight or indoor lighting was avoided at all times. Jacquelin and Bourlas (37) reported that light influenced the magnitude of the streaming current obtained with Ag-AgCl electrodes. Other reports state that sunlight did not affect the stability or reproducibility of Ag-AgCl electrodes (47). Ives and Janz (44) mention that photoelectric effects are likely to affect electrode kinetics rather than the equilibrium potential. It was concluded that the case for lightproof conditions was not sufficiently strong, but that care should be taken to shield the electrodes.

LIFE EXPECTANCY

The life expectancy of the Ag-AgCl electrodes is at least one month, or on a better scale, at least 20 streaming current runs. Electrode Pair No. 9 was reanodized after 25 runs (2 months old) since more scatter in the ζ values appeared in the 22nd and 25th runs (9-10 to 9-16 B in Table I and Fig. 9). Pair No. 11, which had an AgCl coating six times heavier, was used for 14 runs (a 2-week period) with very good reproducibility of streaming current results.

A word of precaution is in order while on the subject of reproducibility. Low streaming currents were observed during the first two runs with each pair of electrodes. It appears that the absence of equilibrium conditions in the structure of the Ag-AgCl surfaces caused low current readings immediately after electrodes were formed, or had been stored for several weeks (see discussion, page 48).

DISTILLED WATER

Considerable effort was made to prevent contamination of the distilled water and dilute electrolyte solutions. Polyethylene tubing and polyvinyl chloride valves were used, except for about six feet of latex tubing, which had been well rinsed. A Millipore filter (142-mm. filters with 0.45-μm. average pore size and a 124-mm. Fiberglas prefilter) was used to filter all the distilled water used in this study. In addition, the dilute electrolyte solutions permeating the fiber beds were continuously recirculated through the Millipore filter.

Distilled water was supplied by a Barnstead water still (No. SMH-10, rated at 10 gal./hr.). The feed to the still was Appleton city water which had been deionized and filtered. The use of alkaline permanganate (triply) distilled water was considered, but the 60 gallons of distilled water consumed for each run prohibited this with the stills that were available.

Variation in streaming current results between consecutive runs, particularly with nylon fibers, does not appear to be attributable to changes in distilled water quality. This conclusion is supported by data from Runs 7-26 to 8-12. Even though the entire distilled water system was thoroughly cleaned on 7-18-66, reproducible streaming currents were not obtained until the change was made from nylon to dacron fibers in the four runs from 8-9 to 8-12.

All distilled water used to suspend fibers and for permeation was deaerated by heating the water in the 500-gal. stainless steel storage tank to a boil. Cold water flowing in the stainless steel coil decreased the temperature in the lower half of the tank to 25°C., while a layer of hot distilled water remained in the top half to prevent aeration of the 25°C. water.

FIBERS

SELECTION

The criteria for selecting fibers were as follows: (1) The fibers had to be cylindrical to test the application of the Happel model; (2) they had to be compressible so that a fairly wide range of mat porosities could be achieved; and (3) nonswelling fibers would make it possible to determine the fiber specific volume from the pycnometric density.

Lustrous nylon 66 fibers from Du Pont were used initially, but, as explained previously, reproducibility was not achieved (refer to Table II and discussion on page 50). Results with dacron fiber (Du Pont Type 54, semidull polyester staple) showed much better reproducibility. A summary of data for the synthetic fibers is given in Table IV.

TABLE IV

DATA FOR SYNTHETIC FIBERS

Type	Nylon 66	Dacron
Denier	7.5	3
Av. swollen diameter, μm.	32.3	17.4
Av. length, mm.	2.9	6.0
Diameter increase on swelling, %	5	0
Specific volume (corrected for swelling), cc./g.	0.96 ± 0.02[a]	0.67 ± 0.07[a]
Extraction (48), % weight loss		
Carbon tetrachloride, %	0.27	0.13
95% Ethanol	1.4[b]	0.26[b]
Water (50°C. for nylon; 28°C. for dacron)	0.49	0.14
0.1N HCl (80°C.)	0.87	--

[a] Approximate 2 sigma value was considerably greater for dacron than for nylon, although the same technique was used to find pycnometric density. This difference may relate to more hydrophobic character of dacron fibers.

[b] Ethanol removed all the material that other solvents could remove.

EXTRACTION

The nylon fibers were extracted with 95% ethanol in a large Soxhlet extractor. Removal of all the nonfibrous surface material prevented any possible streaming current variation with time due to water removal of this material in the fiber mat.

However, the only dacron fibers extracted were those used for the first four runs (9-9 through 9-12). There was very little extractable material on the dacron fiber (Table III), and it appeared that some improvement in the extent of fiber flocculation occurred when the fibers were not extracted. There was no flocculation problem with the extracted nylon fibers.

FORMING FIBER MAT

The fibers were deaerated by suspending them in 95°C. distilled water after they had been given 300 revs. in a British disintegrator. Deaeration was completed after about 20 minutes under aspirator suction.

The deaerated fibers were carefully transferred from a clean 4000-ml. suction flask to 200 liters of deaerated electrolyte solution. The 4000-ml. flask was held below the liquid surface to prevent aeration of the fibers. The 0.01% consistency fiber slurry was slowly stirred for about 20 hours while the fibers equilibrated with the electrolyte. Electrolyte concentration was always the same as that for the streaming current run that followed.

The mat was formed upon the bottom electrode by constant-rate filtration of the dilute fiber slurry at approximately 1.6 cm. per sec. (73 ml. per sec.). A photograph of the Plexiglas forming and permeation cell was shown previously in Fig. 6 and 7. This forming method is discussed by Ingmanson and Whitney (49) and Han (46).

STREAMING CURRENT APPARATUS

The procedure for streaming current measurements was discussed in the main body of this report, and the flow system was shown in Fig. 5 (page 37).

A Scalamp galvanometer with a built-in shunt was purchased from the Ealing Corp., Cambridge 38, Mass. The sensitivity was 0.05 μa./mm. and the resistance presented to the external circuit was 25 ohms at all settings, including shorted. Unshielded, plastic-insulated wire was used to connect the electrodes to the galvanometer. Shielded wire was unnecessary since no extraneous current could be detected with a long loop of the wire.

The mat porosity was changed by periodically increasing the compacting pressure supplied by a hydraulic ram. The maximum compressive force was 1900 lb.

The temperature of the permeant in the 50-liter bottle was controlled to 25 $\pm$ 1°C. by flowing either steam or cold well water through the stainless-steel, U-tube heat exchanger.

CONSTANT FLOW RATE

Streaming currents were determined at three or four different flow rates varying from 0.04 to 0.47 cm./sec. A constant flow rate was maintained with a Maisch stainless steel metering pump, which was driven by a 1/3 h.p. Adjusto-Spede motor (Eaton Mfg. Co., Kenosha, Wis.). Flow rates were measured with a Fischer-Porter Tri-Flat flowmeter.

PRESSURE DROP MEASUREMENTS

Carbon tetrachloride-water and chlorobenzene-water manometers were used to measure the frictional pressure drops across the bed and within the bed. Pressure drop readings within the bed indicated that a constant pressure gradient was maintained as the flow rate increased, even at porosities as high as 0.88 for nylon fiber mats and 0.90 for dacron fiber mats.

The distilled water in the manometer system was kept deaerated by flushing the system with hot distilled water about once a month. The 3/16-inch i.d. glass manometer tubes were cleaned with cleanser and distilled water at the same time. Manometers were obtained from Meriam Instrument Co., Cleveland, Ohio 44102.

ELECTRICAL RESISTANCE

Mat resistance was measured after liquid flow was stopped at each porosity level. The measurement was made with a Z-Y bridge (Type 1603-A, General Radio Co.,

West Concord, Mass.) at 1000 cycles per second. These a.c. measurements did not polarize the electrodes.

Several d.c. resistance measurements were made with electrode Pair No. 6. It was found that currents greater than 14 μa. would cause appreciable electrode polarization. Therefore, d.c. measurements were discontinued since the vacuum-tube voltmeter put 100 to 400 μa. through the electrodes to measure resistances in the 10,000 to 300-ohm range of this study.

In addition, streaming currents in this work were usually less than 10 μa. with the largest being 16 μa. Thus, electrode polarization would not be a problem if the preceding polarization results apply to the other Ag-AgCl electrodes. Polarization was discussed on page 45.

ELECTROLYTE CONCENTRATION

A conductivity bridge and platinized platinum cell were used to determine the electrolyte concentration. At the end of each run, a polyethylene bottle was filled to the top with the electrolyte solution. The method was reproducible and expeditious.

APPENDIX IV

CALCULATIONS

CORRECTIONS TO ORIGINAL DATA

DEFORMATION OF APPARATUS UNDER LOAD

The highest loading of the fiber mats was about 1900 lb. Under these loads, the apparatus, as well as the fiber mat, compressed. The thin silicone-rubber insulation on the back of each electrode was the main contributor to the deformation shown in Table V.

TABLE V

APPARATUS DEFORMATION UNDER LOAD

Compressive Load, lb.	Deformation, in. July 13, 1966 First Loading	July 13, 1966 Repeat Loading	Sept. 19, 1966	Oct. 17, 1966[a] First Loading	Oct. 17, 1966[a] Repeat Loading
0	0.000	0.000	0.000	0.000	0.000
~25	0.025	0.016	0.022	0.011	0.025
100	0.043	0.036	0.044	0.046	0.044
225	0.057	0.054	0.061	0.060	0.059
425	0.072	0.070	0.076	0.076	0.076
800	0.092	0.091	0.094	0.094	0.094
1275	0.109	0.109	0.112	0.111	0.111
1900	0.131	--	0.131	0.131	0.131

[a] Readings of Oct. 17 were adjusted downward 0.009 inch since the stainless steel shaft was seating that much deeper into the plastic support for the top electrode. Hence, it is recommended that in the future a permanent, stainless-steel, threaded well be designed into the top support. The stainless steel shaft would then seat into this nonyielding steel well.

The good reproducibility between both repeat loadings and deformation tests over a three-month period indicates that the stress-strain relationship for the apparatus was in the elastic region. As a result, the error in the porosity

calculation ($\epsilon = 1 - \alpha \underline{c}_1$) due to variability in determining the electrode separation ($\underline{L}$) was fairly small, e.g., $\epsilon = 0.700 \pm 0.003$ (2 sigma limits). The mat concentration ($\underline{c}_1$) equals mat weight (oven dried) divided by ($\underline{A} \times \underline{L}$).

The error in the absolute value of porosity for dacron fiber mats is much larger ($\epsilon = 0.70 \pm 0.03$), however, due to the large error in the specific volume (α) determination (see Table IV). This large error in the value for porosity affects the magnitude of the calculated zeta potential, but it does not affect the evaluation of reproducibility between runs since the same $\alpha = 0.67$ cc./g. was used throughout.

BACKCURRENT THROUGH FIBER MAT

Since the resistance of the galvanometer which was connected across the two Ag-AgCl electrodes was only 25 ohms, the electrical resistance of the fiber mat had to drop to 1250 ohms before the backcurrent correction was even 2% of the total streaming current ($\underline{I}$). Thus, the backcurrent correction became appreciable at $\underline{c} > 1 \times 10^{-4}$ $\underline{M}$ KCl ($\underline{c} > 5 \times 10^{-5}$ $\underline{M}$ $CaCl_2$), as is shown by the resistances listed in Appendix V (e.g., Table XIXA).

The backcurrent correction was made to each streaming current reading prior to calculating the slopes of the regression lines, which are given in Appendix V. The correction was made using the following relationship:

$$I_{galvanometer} \times 25 = I_{mat} \times R_{mat} \ .$$

But $\underline{I} = \underline{I}_{gal.} + \underline{I}_{mat}$. Therefore,

$$I = I_{gal.} \ (1 + 25/R_{mat}) \qquad (45).$$

FLOW CURRENT

The flow current is defined as the current between two electrodes during liquid flow when the porous medium is not present. It is analogous to the flow potential (moto-electric effect) between electrodes in the streaming potential studies of Zucker (45). He concluded that the flow potential was an important source of error in streaming potential measurements; an error which may exceed the magnitude of the true streaming potential. Particularly large flow potentials of up to 100 mv. were found with perforated platinum electrodes, while Ag-AgCl electrodes deficient in chloride ions ($c < 10^{-5}$ M KCl) had smaller flow potentials of about 10 mv. (45). The criteria given by Zucker for eliminating the flow potential were two electrodes identical in geometry as well as in reversible e.m.f. and a sufficient concentration of ions to which the electrode system is reversible. An examination of Zucker's data and discussion indicates that the flow potential effect was minimized, but never completely eliminated.

In the present study, it was standard procedure to measure the flow current (I_f) at 3 or 4 different electrode separations immediately before and sometimes after the fiber mat was formed (see page 38). The streaming current readings (I_s) were then corrected to obtain the "true" streaming current (I) in the following manner:

$$I = I_s - I_f \qquad (46)$$

Both the I/U and I_s/U slopes of the regression lines are given in Appendix V. However, only I_s/U values were used to calculate the zeta potentials. The general conclusion after examining all the data was that an I_f effect definitely existed (note the large intercepts at the beginning of most runs), but that a test for I_f when the mat was removed did not necessarily measure the actual flow current effect that existed when the mat was present. Therefore, the most consistent manner of

handling the data was to use only $\underline{I}_s/\underline{U}$ values based on the assumption that any nonzero intercepts were caused by a relatively constant $\underline{I}_f$ at each electrode separation.

Support for the preceding approach to the flow current effect is obtained by examining several runs which typified the variable nature of the measured $\underline{I}_f$. Starting with results using the best electrode pair (No. 11), it is seen in Table XXA of Appendix V that the intercepts in Column 5 are farther from the residual current ($\underline{I}_r$) at no flow than the Column 8 intercepts, which had no correction for $\underline{I}_f$. Thus, the experimentally measured $\underline{I}_f$ did not give the expected correction to the $\underline{I}_s$ values. It is also noted in Table XXA that $\underline{I}/\underline{U} \cong \underline{I}_s/\underline{U}$, except for Run 10-14B.

The criterion that the intercept should approximately equal $\underline{I}_r$ in correcting for the flow current effect was based on the results from several runs in which $\underline{I}_f$ was very small, or even zero. For example, in Runs 5-25 and 5-31 (Table IIIA) and Run 6-9, the uncorrected intercepts were fairly close to the $\underline{I}_r$ values.

The most convincing evidence supporting a flow current correction is the experimental data from Run 11-7. An attempt was made to determine experimental reproducibility by measuring the streaming current from the same mat on consecutive days. Comparing Curves 1 and 2 in Fig. 15a, it is seen that the $\underline{I}_s$ results of 11-8-65 (Curve 1) are displaced about +0.4 μa. from the $\underline{I}_s$ line 12 hours earlier on 11-7. A comparison of Curves 4 and 5 in Fig. 15b shows that the 11-8 $\underline{I}_f$ data were 0.4 to 0.6 μa. more positive than on 11-6. Applying the respective $\underline{I}_f$ corrections to Curves 1 and 2 produced a common line with a zero intercept (Curve 3).

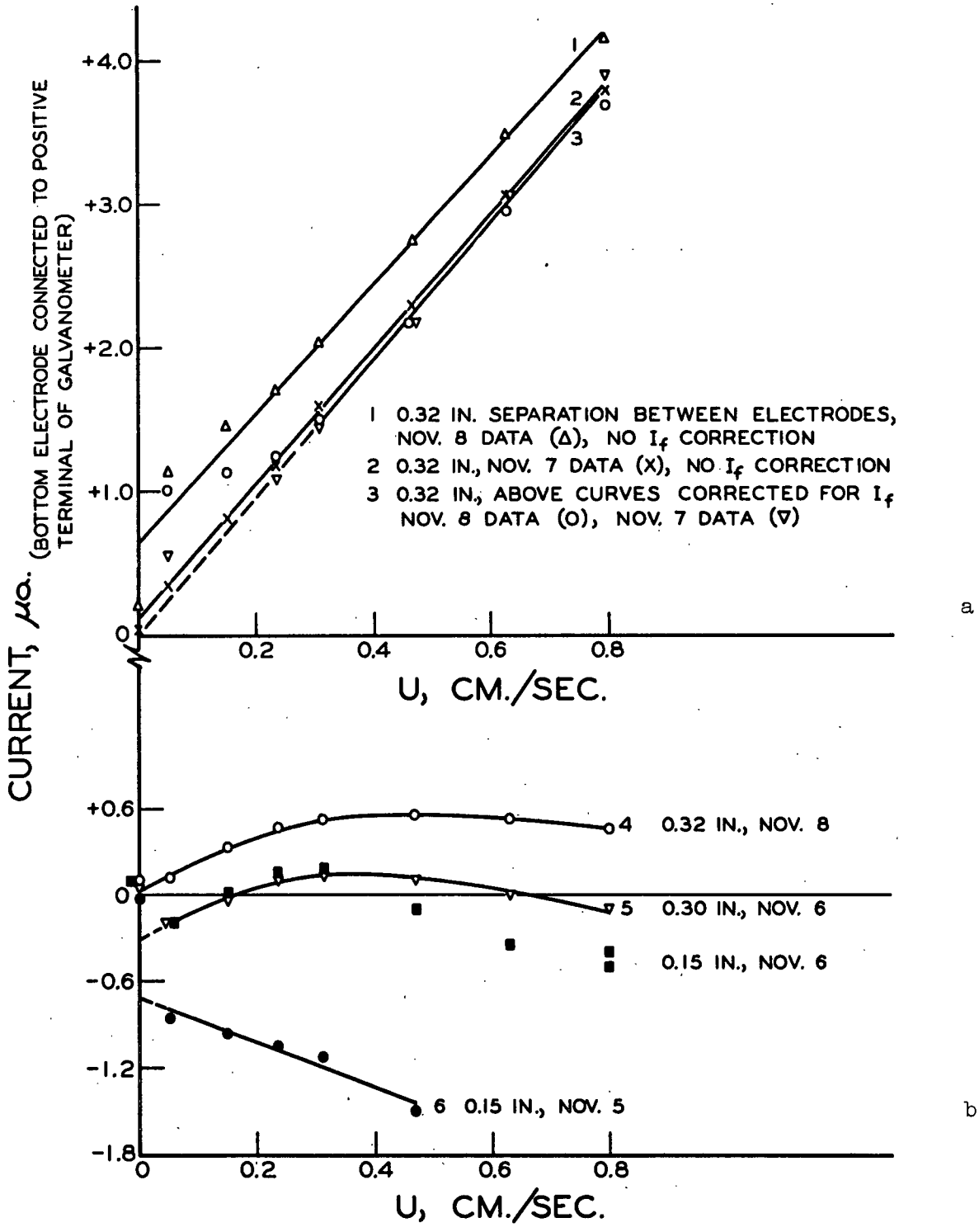

Figure 15a. Streaming Current Variation as a Function of Flow Rate; Flow Current Correction Illustrated (Run 11-7-65);
b. Flow Current (I_f) Variation as a Function of Flow Rate on Three Different Days

It is apparent, however, that I_f values at $U < 0.2$-0.3 cm./sec. were not accurate measures of the flow current effect when the mat was present. In addition, the three curves in Fig. 15b show how I_f changed from a large negative value to a moderately large positive value in three days. This I_f change from negative to positive usually occurred with freshly anodized electrodes (Pair No. 6 for Fig. 15 data was anodized Oct. 29); subsequent I_f values remained positive, had curves similar to Curve 4 in Fig. 15b, and showed less day-to-day variation than occurred with new electrodes.

The I_f data in Fig. 15 did correct the I_s values to produce the expected linear I vs. U relationship, which had an intercept of zero. As mentioned previously, I_f data generally did not correct the I_s values to yield regression lines with zero intercept. In order to explain this, it is hypothesized that the I_f measurements did not necessarily measure the actual flow current effect when the mat was present (see I values at $U < 0.25$ cm./sec. in Fig. 15a). It is also evident from Fig. 15a that the slopes of Curves 1 and 2 are similar to the slope (I/U) of Curve 3. Thus, the use of I_s/U values to calculate the zeta potentials appears to be a reasonable approach to the problem of flow current corrections.

ZETA POTENTIAL CALCULATIONS

REGRESSION LINES

The method of least squares was used to estimate the regression lines for I vs. U, I_s vs. U, and ΔH vs. U. A modified version of R. W. Nelson's Utility Program 912 – Linear multiple regression with rearrangement of variables – was used in the IBM 1620 computer to calculate the slopes, intercepts, and correlation coefficients listed in the "A" tables of Appendix V.

In several instances (Runs 1-13, 1-31, 5-31, and 6-9), the I/U slopes were not calculated since I_f was negligible. For Runs 6-14A, 6-22A, 7-21B, 7-26, and

8-30, data for the I vs. U lines were calculated using I_f values obtained both before and after the run – the after-run data being printed on the second line. This was done when the day-to-day I_f variation was large in an attempt to obtain a better estimate of I.

The temperature of the electrolyte solution permeating the mat is given in the first column of the "A" tables. In several runs (e.g., 6-14A and 16-14B) for which the same temperature is given at every porosity level, the listed value is actually the average temperature for the entire run since computer cards from these runs did not contain individual temperatures.

SECOND STEP CALCULATIONS

The values calculated for the mat porosity, Kozeny factor, and zeta potentials are listed in the "B" tables of Appendix V. The Kozeny factors from experimental data were found using Equation (24) on page 48; those in the next column were calculated from the Davis correlation (46, page 162).

The zeta potential estimates from the capillary model theory were obtained by inserting the I_s/U slopes into Equation (12) of Appendix I. The value for the shape factor (k_o) in Equation (12) was found by dividing the Davis correlation Kozeny factor by $(L_e/L)^2$, which was set equal to 2.0. The experimental pressure drop data were considered too uncertain to be used in any calculation other than the experimental Kozeny factor (see discussion, page 48).

Zeta potentials from Biefer and Mason's (26) empirically obtained correction were based on a modified form of Equation (3) on page 18.

The third column of zeta potentials was calculated from a modified form of Equation (23). Instead of $N = A/2a\ell$ as on page 29, the number of fibers contributing

to the streaming current was set equal to the physical number of fibers per layer, or

$$N \cong 2a\ A(1 - \epsilon)/(\pi a^2\ \ell) \qquad (47).$$

It is interesting to note that zeta potential variation (3rd zeta column) as a function of porosity is large (about the same as that using capillary-model theory). Thus, the assumptions concerning ion transport, which were discussed in Appendix II, are essential to the new streaming current model.

The ζ_c values in the fourth column of zeta potentials were calculated using Equation (23). The Fortran language computer program for the calculations listed in the "B" tables of the Appendix follows. A Super-go Fortran Processor from the IBM 1620 Users Group Library was used.

Several more comments about the calculations are necessary. Only I_s/U values for which $R > 0.9900$ were used to determine the zeta potentials. The viscosity and dielectric constant for pure water were used since the electrolyte solutions were very dilute. The results listed in Appendix V are one digit larger than experimental error justifies since the computer does not round off. Finally, the value for XMAX in the computer program established the upper limit of the numerical integration, while NC specified the number of divisions between XMIN and XMAX. XMAX was set equal to a + 0.6 μm. [$a + \tau$ in Equation (23)] for all electrolyte concentrations in order to accommodate the large τ at $c = 2 \times 10^{-5}$ M KCl. NC was set at 20. The values for zeta potentials calculated at higher c were not affected by the large XMAX (τ equals only 0.06 μm. at 1.9×10^{-4} M $CaCl_2$). This was demonstrated by setting XMAX equal to a + 0.06 μm. and recomputing the results for Run 10-12B.

COMPUTER PROGRAM

```
C       FLOW PERPENDICULAR TO CYLINDERS

C       NUMERICAL INTEGRATION
C            NEWTON-COTES QUADRATURE  N = 6
C       UTILITY PROGRAM  307B2  22 FEB 1965
        DIMENSION AB(7), W(7), T(4)
        DIMENSION VAR(4)
90      READ, NC, XMAX
        READ, A, SV, C2, V, C3
        CON = 0.0
        XMIN = A
        ASQ = SQRT(XMIN)
401     READ,  WT,NOO,TEM,CONCN,MONTH,MDAY,MYEAR,NPO
        K = 1
        TEMP=TEM
        AETA = .894 + .02*(25.-TEMP)
        DIEL = 80. - 0.4*(TEMP - 20.)
        AKM1=SQRT(DIEL*1.38E-16*(TEMP+273.1)/(CONCN*8.*3.14*138.70))
        IF (MONTH - 10) 621, 626, 621
626     IF (MDAY - 12) 621, 620, 620
C       CHANGING RECIPROCAL OF DEBYE-HUCKEL CONSTANT FROM CM. TO MICRONS
C       WITH CALCIUM CHLORIDE AS ELECTROLYTE
620     AKM1 = AKM1*3333.
        GO TO 109
C       WITH A 1-1 ELECTROLYTE (POTASSIUM CHLORIDE)
621     AKM1 = AKM1*10000.
         TEMP = TEM
109     IF(CONCN-CON)108, 783, 108
108     CON = CONCN
10      TEMP = XMAX - XMIN
        Z = NC
        QINC = TEMP / Z
        DELX = QINC / 6.0
        DO 150 I = 1, 7
150     AB(I) = 0.0
        W(1) = 0.29285714
        W(2) = 1.5428571
        W(3) = 0.19285714
        W(4) = 1.9428571
        W(5) = 0.19285714
        W(6) = 1.5428571
        W(7) = 0.29285714
        XS = XMIN
        X = XMIN
        Z = 0.0
        I = 1
        J = 1
        GO TO 12
1       AB(I) = AB(I) + Y
        IF (I - 6)  2, 50, 4
   50   I = I + 1
        XS = XS + QINC
        X = XS
        GO TO 12
    2   I = I + 1
        X = X + DELX
12      GO TO (100,200,300,400),K
100     VAR(1) = X*SQRT(X)
        GO TO 3
200     VAR(2) = LOG(X)/SQRT(X)
        GO TO 3
```

```
300     VAR(3) = 1.0/SQRT(X)
        GO TO 3
400     VAR(4) = 1.0/(X*X*SQRT(X))
C             COMPUTATION OF INTEGRAND
      3 Y = ASQ*EXP(XMIN/AKM1 -X/AKM1)*VAR(K)
C             END OF COMPUTATION OF INTEGRAND
        GO TO 1
      4 IF (J - NC)  5, 7, 92
5        IF(SENSE SWITCH 3) 7, 6
      7 Z = 0.0
        DO 9  I = 1, 7
9       Z = Z + AB(I)*W(I)
        Z = Z * DELX
         IF(SENSE SWITCH 3) 490,6
490      PRINT, XS, Z
      6 I = 1
        J = J + 1
        IF (J - NC)  1, 1, 92
92      T(K) = Z
        K = K+1
        IF (K - 4) 10, 10, 93
93      IF (SENSE SWITCH 1) 101, 102
101     PRINT, T(1), T(2), T(3), T(4)
        PRINT, AKM1, AETA, DIEL
        PAUSE
        IF (SENSE SWITCH 1) 90, 102
102     T1 = T(1)
        T2 = T(2)
        T3 = T(3)
        T4 = T(4)
C       PRINT OUT OF TABLE SUMMARIZING STREAMING CURRENT RESULTS
        DIMENSION BIU(3), MZ(10)
        DIMENSION ZETA(10), ZAT(10),EPS(10)
783     CONTINUE
78      SX = 0.0
        SY = 0.0
        SSY = 0.0
        SSX = 0.0
        SSXY = 0.0
        AREA = 45.24
        KN = 1
81      K = 0
11      IF(SENSE SWITCH 3) 786,787
786     PAUSE
        IF(SENSE SWITCH 3) 788,787
788     READ, NPO
787     K = K + 1
30      IF (K-1) 302, 302, 303
302     READ, MX
        N = NOO - MX + 1
        DO 460 M = MX, NOO
460     READ, MZ(M)
303     IF(NPO - 4) 870, 560, 561
870     READ,AL,IP,TEMP,BIU(2),UA,UB,APU,UC,UD
         GO TO 480
560     READ,AL,IP,TEMP,BIU(1),UA,UB,BIU(2),UC,UD,APU,UE,UF
         GO TO 480
561     READ,AL,IP,TEMP,BIU(1),UA,UB,BIU(2),UC,UD,APU,UE,UF
        READ,BIU(3),UA,UB
480     IF(K-MX) 11,461,461
461     MZZ = MZ(K)
```

```
      AIU = BIU(MZZ)
      DIEL = 80. - 0.4*(TEMP - 20.)
      AETA = .894 + .02*(25.-TEMP)
C     ADJUSTMENT FOR A CHANGE IN APPARATUS DEFORMATION
32    IF(MONTH - 10) 622, 623, 622
623   IF(MDAY - 3) 622, 624, 624
624   IF(MDAY - 12) 625, 625, 622
625   AL = AL + .009
622   CONC = WT/(AREA*2.54*AL)
      VC=V*CONC
      EPSI = 1.0 -VC
      B2=A*A/(1.0-EPSI)
      BB=B2*B2
      B=SQRT(B2)
      AA=A*A*A*A
      D=-2.0/(LOG(B/A)+0.5*(AA-BB)/(AA+BB))
      F=D*A*A*BB/(4.0*(AA+BB))
      C=-8.0*F/BB
        EE = 1.0 + F/(A*A) - 0.5*D*(LOG(A)+0.5) - 0.375*C*A*A
      T = 0.375*C*T1 + 0.5*D*T2 + T3*(EE+0.25*D) - F*T4
      ZETA(K) = C2*AIU*A*4.*3.1416*AKM1**2/(AREA*DIEL*(T3-T))
      ZAT(K) = ZETA(K)*3.1416/(4.0*(1.0-EPSI))
      AKC = 3.5*EPSI**3*(1.0+57.0*VC**3)/SQRT(VC)
      AKO = AKC/2.0
       AKD = AETA*AL*2.54E-02/(APU*580.0)
36    AK = EPSI**3/(VC*VC*AKD*SV*SV)
      ZET = C3*4.*3.1416*AIU*EPSI**2/(DIEL*SV*SV*AREA*AKO*VC*VC)
      ZE = ZET*AKO/(AKC*EPSI**1.5)
110   FORMAT(1XF6.3,F6.3,F7.2,F7.2,F6.2,F8.2,F7.2,F7.2,F6.2)
76    PRINT 110,AL  , EPSI, AIU, AK,AKC,ZET,ZE,ZAT(K),ZETA(K)
      KK = K + 1
C     EMPIRICAL FIT OF CALCULATED ZET
      EPS(K) = EPSI
      IF (EPSI - 0.8) 70, 70, 11
70    X = LOG(EPSI)
      Y = LOG(ZET)
      IF (KN - 1) 71, 71, 41
71    RUNS = NOO - K +1
      KN = KN + 1
      KZ = K
      KN = KN +1
41    SX=SX+X
      SY=SY+Y
      SSX=SSX+X*X
      SSY=SSY+Y*Y
79    SSXY=SSXY+X*Y
80    IF(NOO -K) 152,152,11
152   XB=SX/RUNS
      YB=SY/RUNS
      CSSXY=SSXY-RUNS*XB*YB
      CSSX=SSX-RUNS*XB*XB
      CSSY=SSY-RUNS*YB*YB
      R=CSSXY/SQRTF(CSSX*CSSY)
      RLOGB=(SSX*SY-SX*SSXY)/(RUNS*SSX-SX*SX)
      SLOPE=(RUNS*SSXY-SX*SY)/(RUNS*SSX-SX*SX)
      IF(KN - 2) 78, 78, 77
C     AVERAGE ZETA AND COEFFICIENT OF VARIATION
77    OBS = N
      SX=0.0
      SSX=0.0
       DO 105 K=MX,NOO
```

```
      GO TO 16
17    KK=1
      OBS=N-1
      SX = 0.0
      SSX = 0.0
       MMX=MX+1
      DO 105 K = MMX,NOO
16    X = ZETA(K)
      SX=SX + X
105   SSX=SSX+X*X
      XBAR=SX/OBS
      SIGMX=SQRT((SSX-SX*SX/OBS)/(OBS-1.0))
      COEFF=SIGMX*100./XBAR
      IF(N-KK)780,781,781
73    FORMAT(2X2HH=,F5.2,2X2HR=,F6.4,22X14HOVERALL AVE. =,F6.2,1H+,F6.2)
780   PRINT 73, SLOPE, R, XBAR, COEFF
      GO TO 17
111   FORMAT(27X28HAVE. (FIRST VALUE OMITTED) =,F6.2,1H+,F6.2)
781   PRINT 111, XBAR, COEFF
20    IF (SENSE SWITCH 1) 21,401
21    PAUSE
      IF (SENSE SWITCH 1) 90,401
      END

C     FLOW PARALLEL TO CYLINDERS

C     THE FOLLOWING CARDS WERE INSERTED INTO THE PRECEDING PROGRAM
C     IN ORDER TO CALCULATE  I/U  VALUES IN TABLE III
100   VAR(1) = A*A*SQRT(X)
200   VAR(2) = X**2.5
300   VAR(3) = LOG(X/A)*SQRT(X)
      T(4) = 0.0
      IF(K-3) 10, 10, 93
      T5 = T(1)
      T6 = T(2)
      T7 = T(3)
      READ, ZETA
C     SLOPE I/U FOR FLOW PERPENDICULAR TO FIBERS USING HAPPEL MODEL
      AIU=ZETA*DIEL*AREA*(T3-T)/(C2*A*4.*3.142*AKM1**2)
C     SLOPE I/U FOR FLOW PARALLEL TO FIBERS USING HAPPEL MODEL
      T= T5-T6+2.0*B2*T7
      DARCY= A*A/2. - A**4/(8.*B2)-3.*B2/8. + B2*LOG(B/A)/2.
      DIU = ZETA*AREA*DIEL*T/(C2*B2*DARCY*8.*3.142*AKM1**2)
C     SLOPE I/U USING CAPILLARY MODEL
      BIU= ZETA*DIEL*SV*SV*AREA*AKO*(1.-EPSI)**2/(C3*EPSI**2*4.*3.142)
C     SLOPE I/U USING BIEFER AND MASON CORRECTED EQUATION
      CIU= BIU*AKC*EPSI**1.5/AKO
76    PRINT, EPSI, AIU, DIU, CIU
```

APPENDIX V

TABLES OF CALCULATIONS WITH STREAMING CURRENT DATA

SUMMARY OF EXPERIMENTAL CONDITIONS

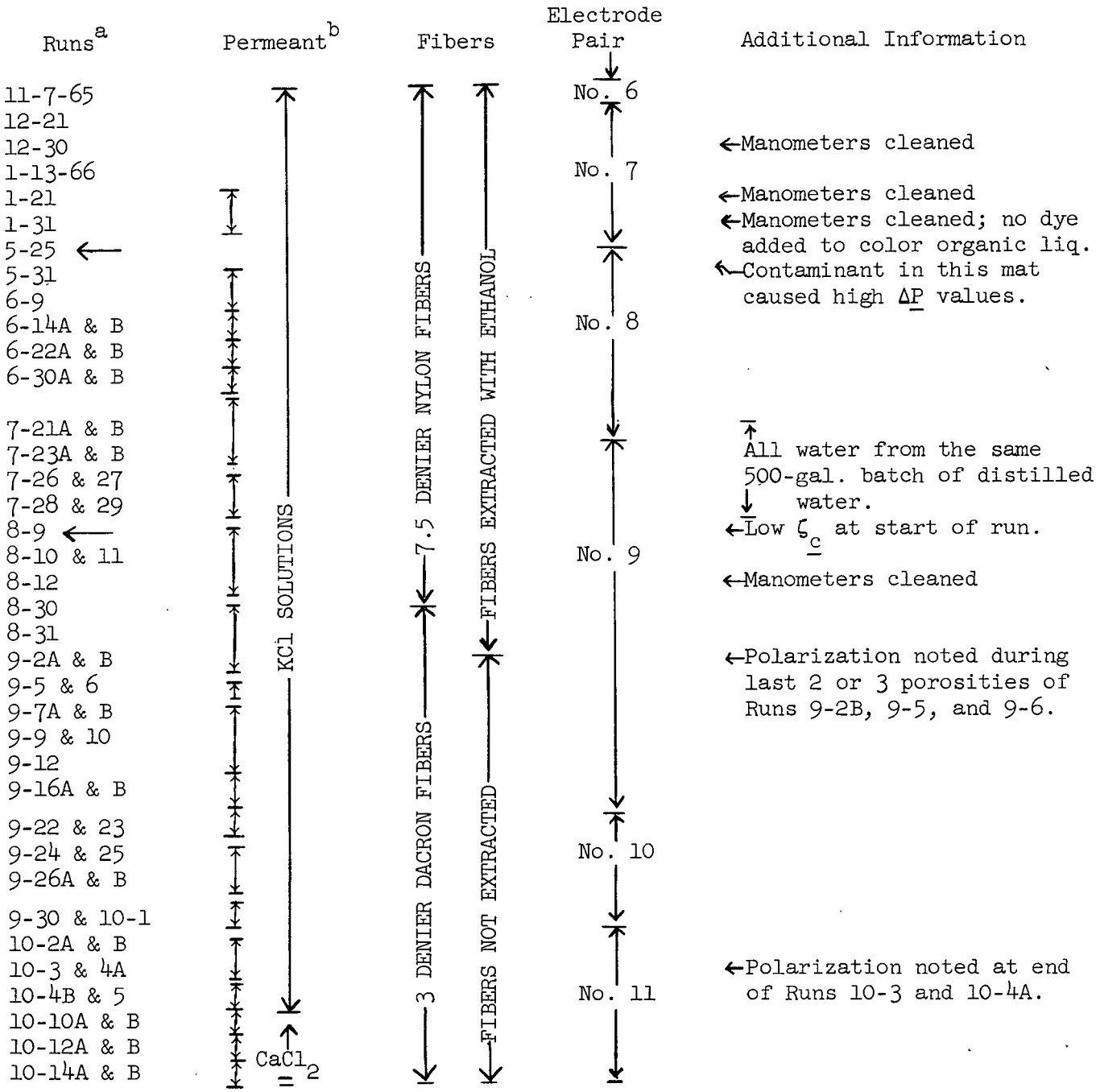

[a] Fiber mats in runs grouped together (e.g., 6-14A & B) were formed from the same 200-liter fiber suspension.

[b] The first column shows which runs used distilled water from the batch. Electrolyte concentrations are given in the tables which follow.

TABLE VIA

INITIAL CALCULATIONS WITH STREAMING CURRENT DATA

Temp., °C.	Resistance, ohms	I_r, μa.	Slope (I/U), μa.sec./cm.	Intercept, μa.	R	Slope (I_s/U), μa.sec./cm.	Intercept, μa.	R	Slope ($\Delta H/U$), cm.sec./cm.	Intercept, cm.	R
RUN 11- 7			MAT WT.= 12.12 g.			.000100M					
22.2	2400	.10	1.379	.60	.9770	1.635	.51	.9903	16.92	-.45	.9998
22.7	2200	.10	2.647	.45	.9887	3.017	.35	.9969	27.63	-.57	.9996
22.7	2200	.01	3.231	.34	.9915	3.601	.24	.9984	32.71	-.43	.9999
22.7	2200	.00	4.535	.20	.9944	4.583	.19	.9997	41.96	-.67	.9996
22.7	2200	-.03	3.735	.59	.9840	4.112	.88	.9979	43.36	-.80	.9989
RUN 12- 21			MAT WT.= 18.47			.000100M					
25.7	3570	.00	1.260	.17	.9926	1.260	.08	.9926	28.29	-.94	.9999
24.5	3400	.02	2.015	.25	.9982	2.015	.15	.9982	38.97	-.97	.9997
24.6	3220	.05	2.552	.16	.9977	2.552	.05	.9977	44.97	-1.24	.9995
24.0	3000	.05	3.032	.18	.9997	2.946	.07	.9996	51.86	-1.47	.9996
24.0	3000	.02	3.388	.17	.9998	3.321	.04	.9998	60.71	-1.77	.9994
24.3	3000	.00	4.118	.17	.9996	3.957	.02	.9997	72.55	-1.12	.9995
24.4	3000	.00	4.726	.16	.9999	4.595	.01	.9999	86.85	-1.52	.9999
24.6	3000	.00	5.441	.12	.9999	5.312	-.02	.9999	106.17	-2.30	.9999
RUN 12- 30			MAT WT.= 14.57			.000100M					
24.2	4000	.12	1.395	.33	.9980	1.663	.37	.9957	14.21	-.33	.9984
24.5	3220	.07	2.800	.13	.9956	3.020	.23	.9990	24.09	-.59	.9996
24.5	3100	.04	3.088	.25	.9888	3.256	.36	.9979	29.95	-.61	.9991
24.5	2950	.07	3.974	.01	.9957	4.077	.15	.9996	37.43	-.79	.9996
24.5	2800	.05	4.566	-.05	.9947	4.649	.09	.9998	48.10	-1.02	.9987
24.6	2800	.05	4.710	-.00	.9933	5.018	.09	.9997	60.01	-.89	.9995
24.6	2800	.03	6.057	-.10	.9951	6.340	.00	.9998	92.71	-2.03	.9991
RUN 1- 13			MAT WT.= 23.96			.000100M					
25.5	5000	.00	1.543	.01	.9888	1.829	.15	.9987	36.76	-.21	.9999
24.4	4260	.07	1.969	.01	.9962	2.256	.15	.9988	43.04	-.00	.9996
24.4	4350	.03	2.460	-.06	.9975	2.746	.07	.9993	47.95	-.51	.9997
24.1	4360	.00				2.877	.04	.9997	55.91	-.77	.9994
23.8	4300	-.01				3.684	-.02	.9997	70.23	-.64	.9996
23.5	4200	-.04				4.264	-.06	.9997	87.81	-1.66	.9994
23.5	4160	.03				4.841	-.06	.9999	105.59	-.96	.9998
23.5	4100	.00				5.414	-.08	.9998	126.95	-2.24	.9997

TABLE VIB

SECOND STEP CALCULATIONS WITH STREAMING CURRENT DATA

Mat Thickness (L), in.	Mat Porosity, ϵ	Slope, (I_s/U)	Kozeny Factor: Experimental	Kozeny Factor: Davis Correlation	Calculated Zeta Potential, mv.: Capillary Model	Bieber +Mason (26)	Assuming N Varies	ζ_c (N = Const.)	
RUN 11- 7		MAT WT.= 12.12 g.			.000100M KCl				
.520	.805	1.63	7.00	5.88	19.52	13.51	10.45	2.59	
.394	.743	3.01	6.88	5.57	18.64	14.55	10.55	3.45	
.356	.715	3.60	6.57	5.55	16.89	13.95	9.89	3.58	
.318	.681	4.58	6.51	5.57	15.51	13.78	9.46	3.83	
.318	.681	4.11	6.72	5.57	13.91	12.36	8.49	3.44	
H= 2.77	R= .9343					OVERALL AV. =		3.38±	13.85
					AV. (FIRST VALUE OMITTED) =			3.57±	5.11
RUN 12- 21		MAT WT.= 18.47			.000100M KCl				
.727	.787	1.26	7.12	5.73	12.65	9.05	6.82	1.84	
.600	.742	2.01	6.61	5.57	12.54	9.79	7.08	2.31	
.548	.718	2.55	6.31	5.55	12.43	10.21	7.23	2.59	
.507	.695	2.94	6.04	5.56	11.46	9.88	6.85	2.65	
.469	.670	3.32	5.86	5.58	10.25	9.33	6.31	2.64	
.431	.641	3.95	5.68	5.59	9.44	9.18	5.97	2.72	
.402	.616	4.59	5.62	5.58	8.81	9.11	5.67	2.77	
.372	.585	5.31	5.47	5.51	7.96	8.90	5.17	2.73	
H= 1.73	R= .9700					OVERALL AV. =		2.53±	12.32
					AV. (FIRST VALUE OMITTED) =			2.63±	5.76
RUN 12- 30		MAT WT.= 14.57			.000100M KCl				
.827	.852	1.66	8.02	6.68	34.66	22.00	18.53	3.47	
.542	.775	3.02	6.74	5.66	26.41	19.34	14.40	4.11	
.469	.740	3.25	6.32	5.56	19.79	15.52	11.20	3.70	
.414	.705	4.07	6.04	5.56	17.57	14.81	10.38	3.88	
.369	.670	4.64	5.92	5.58	14.28	13.01	8.79	3.69	
.328	.628	5.01	5.44	5.59	10.72	10.74	6.84	3.23	
.294	.585	6.34	6.09	5.52	9.56	10.66	6.21	3.27	
H= 3.63	R= .9876					OVERALL AV. =		3.62±	8.86
					AV. (FIRST VALUE OMITTED) =			3.65±	9.42
RUN 1- 13		MAT WT.= 23.96			.000100M KCl				
.778	.742	2.25	5.61	5.57	14.02	10.95	7.94	2.60	
.858	.766	1.82	5.95	5.62	14.66	10.92	8.08	2.40	
.742	.730	2.74	5.66	5.56	15.03	12.05	8.64	2.97	
.683	.706	1.00	.28	5.56	4.34	3.65	2.56	.95	
.608	.670	1.00	.27	5.58	3.07	2.80	1.90	.79	
.551	.636	1.00	.24	5.59	2.27	2.23	1.44	.66	
.508	.605	1.00	.21	5.56	1.75	1.86	1.13	.57	
.477	.580	1.00	.20	5.50	1.43	1.62	.93	.50	
H= 2.47	R= .9857					OVERALL AV. =		2.75±	6.71
					AV. (FIRST VALUE OMITTED) =			2.77±	6.81

TABLE VIIA

INITIAL CALCULATIONS WITH STREAMING CURRENT DATA

Temp., °C.	Resistance, ohms	I_r, μa.	Slope (I/U), μa.sec./cm.	Intercept, μa.	R	Slope (I_s/U), μa.sec./cm.	Intercept, a.	R	Slope (ΔH/U), cm.sec./cm.	Intercept, cm.	R
RUN 1- 21			MAT WT.= 28.18			.000100M					
24.2	5500	.15	1.830	.40	.9794	1.855	.49	.9843	36.49	-.38	.9998
25.7	5250	.00	2.601	-.02	.9988	2.627	.05	.9996	40.60	-.54	.9998
23.8	5260	.05	2.702	.06	.9975	2.889	.08	.9914	47.17	-.02	.9998
24.0	5350	.00	3.204	-.02	.9991	3.391	-.01	.9985	59.69	-.47	.9999
24.0	4950	-.01	3.678	-.06	.9989	3.858	-.04	.9996	73.08	-.50	.9997
23.8	4850	-.02	4.231	-.15	.9989	4.255	-.05	.9999	90.25	-.87	.9998
23.8	4870	-.03	4.678	-.19	.9981	4.692	-.09	.9997	108.28	-1.31	.9998
23.8	4930	-.03	5.041	-.22	.9990	5.054	-.12	.9997	127.42	-2.01	.9996
RUN 1- 31			MAT WT.= 22.39			.000100M					
23.3	5400	.05	.258	.20	.5640	.599	.19	.9502	25.43	-.57	.9994
23.5	5000	.04	.392	.09	.9436	.832	.09	.9772	27.63	-.30	.9994
23.7	4550	-.06	.346	.09	.8371	.804	.11	.9991	32.93	-.50	.9997
23.3	4200	.18	.730	.09	.9528	.998	.12	.9989	40.30	-.46	.9996
23.2	4130	.25	.816	.15	.9152	1.289	.15	.9951	50.34	-.57	.9997
23.0	4000	.02	1.260	.04	.9925	1.553	.10	.9973	62.25	-1.19	.9998
23.4	4000	.00				1.712	.07	.9999	73.27	-1.30	.9994
23.5	3900	.00				1.761	.06	.9995	89.13	-1.85	.9996
23.3	3970	.05				2.090	-.01	.9998	110.00	-2.14	.9998
RUN 5- 25			MAT WT.= 21.22			.000113M					
24.5	5000	.30	1.395	.26	.9967	1.000	.41	.9964	45.96	-.71	.9997
24.8	4700	.21	2.514	-.00	.9979	2.305	.15	.9995	62.59	-.28	.9998
25.2	4500	.50	3.029	.00	.9952	2.858	.16	.9970	75.31	.23	.9970
25.4	4400	.14	3.426	-.09	.9987	3.276	.07	.9996	86.35	-.77	.9996
25.5	4300	.38	3.914	-.08	.9999	3.830	.06	.9999	110.97	-1.13	.9998
25.6	4200	.14	4.750	-.20	.9999	4.666	-.04	.9999	139.00	-1.79	.9996
25.6	4100	.19	5.557	-.22	.9997	5.528	-.06	.9997	179.90	-1.30	.9999
25.7	4100	.15	6.128	-.24	.9999	5.960	-.05	.9995	192.29	-.39	.9998
25.8	4000	.08	6.678	-.27	.9999	6.510	-.08	.9994	213.58	-.67	.9996
RUN 5- 31			MAT WT.= 17.12			.000113M					
24.4	5100	.05				1.349	.65	.9370	15.60	-.11	.9999
24.9	4650	.09				2.162	.27	.9996	17.32	-.20	.9999
24.5	4000	.13				2.800	.29	.9983	20.41	-.13	.9999
24.9	3700	.07				3.755	.26	.9998	25.58	-.14	.9999
24.9	3500	.05				4.454	.22	.9998	30.25	-.11	.9946
24.9	3400	.05				5.248	.20	.9999	35.52	-.26	.9998
24.9	3050	.04				7.099	.17	.9999	50.08	-.41	.9999
24.9	3000	.01				8.640	.14	.9999	63.64	-.57	.9998
25.0	2950	.00				10.449	.10	.9998	82.72	-.82	.9999
25.0	2950	.00				12.083	.06	.9999	102.64	-1.20	.9997

TABLE VIIB

SECOND STEP CALCULATIONS WITH STREAMING CURRENT DATA

Mat Thickness (L), in.	Mat Porosity, ϵ	Slope, (I_s/U)	Kozeny Factor: Experimental	Kozeny Factor: Davis Correlation	Calculated Zeta Potential, mv.: Capillary Model	Bieber +Mason (26)	Assuming N Varies	ζ_c (N = Const.)	
RUN 1- 21			MAT WT.= 28.18		.000100M KCl				
1.087	.783	2.62	6.46	5.71	25.18	18.16	13.67	3.77	
.969	.757	2.88	5.78	5.59	20.75	15.75	11.56	3.57	
.850	.723	3.39	5.62	5.55	17.24	14.02	10.00	3.52	
.761	.690	3.85	5.37	5.57	14.31	12.46	8.64	3.40	
.687	.657	4.25	5.13	5.59	11.59	10.88	7.25	3.16	
.632	.627	4.69	4.93	5.59	9.86	9.92	6.32	2.99	
.589	.600	5.05	4.73	5.55	8.50	9.13	5.52	2.80	
H= 4.04	R= .9979					OVERALL AV. =		3.32±	10.32
					AV. (FIRST VALUE OMITTED) =			3.24±	9.44
RUN 1- 31			MAT WT.= 22.39		.000100M KCl				
.996	.812	.83	6.77	5.96	10.79	7.37	5.77	1.38	
.875	.786	.80	6.46	5.72	7.86	5.63	4.26	1.16	
.776	.758	.99	6.25	5.60	7.29	5.51	4.06	1.24	
.677	.723	1.28	5.89	5.55	6.57	5.33	3.81	1.34	
.613	.694	1.55	5.81	5.56	5.96	5.15	3.58	1.39	
.520	.640	1.76	5.58	5.59	4.12	4.02	2.62	1.20	
.479	.609	2.09	5.45	5.57	3.77	3.96	2.44	1.21	
.561	.666	1.71	5.57	5.58	5.06	4.65	3.14	1.33	
H= 3.03	R= .9888					OVERALL AV. =		1.28±	6.92
					AV. (FIRST VALUE OMITTED) =			1.27±	6.79
RUN 5- 25			MAT WT.= 21.22		.000113M KCl				
1.039	.829	1.00	14.23	6.20	15.83	10.48	8.43	1.83	
.798	.777	2.30	12.36	5.67	20.72	15.10	11.30	3.19	
.703	.747	2.85	11.75	5.57	18.79	14.53	10.57	3.39	
.652	.728	3.27	11.58	5.55	17.65	14.20	10.17	3.52	
.587	.697	3.83	11.84	5.56	15.36	13.17	9.18	3.53	
.536	.669	4.66	11.96	5.58	14.30	13.05	8.83	3.72	
.484	.633	5.52	11.87	5.59	12.36	12.25	7.89	3.68	
.459	.613	5.96	10.95	5.57	11.28	11.73	7.28	3.58	
.434	.591	6.51	10.32	5.53	10.32	11.34	6.71	3.49	
H= 2.54	R= .9990					OVERALL AV. =		3.32±	17.48
					AV. (FIRST VALUE OMITTED) =			3.51±	4.70
RUN 5- 31			MAT WT.= 17.12		.000113M KCl				
1.175	.878	1.34	9.95	7.49	38.94	23.65	21.33	3.30	
.970	.852	2.80	9.85	6.68	58.26	37.00	31.26	5.86	
.723	.802	3.75	7.73	5.85	43.94	30.58	23.58	5.93	
.662	.783	4.45	7.81	5.71	42.76	30.80	23.22	6.38	
.593	.758	5.24	7.45	5.60	38.62	29.21	21.48	6.59	
.484	.704	7.09	6.86	5.56	30.22	25.55	17.95	6.75	
.438	.673	8.64	6.89	5.58	27.42	24.80	16.88	7.02	
.395	.637	10.44	6.88	5.59	24.16	23.71	15.38	7.09	
.370	.613	12.08	7.11	5.57	22.74	23.66	14.70	7.23	
H= 2.61	R= .9932					OVERALL AV. =		6.24±	19.25
					AV. (FIRST VALUE OMITTED) =			6.61±	7.79

TABLE VIIIA

INITIAL CALCULATIONS WITH STREAMING CURRENT DATA

Temp., °C.	Resistance, ohms	I_r, μa.	Slope (I/U), μa.sec./cm.	Intercept, μa.	R	Slope (I_s/U), μa.sec./cm.	Intercept, μa.	R	Slope ($\Delta H/U$), cm.sec./cm.	Intercept, cm.	R
RUN 6- 9			MAT WT.= 23.16			.000115M					
24.2	5500	.15				1.049	.90	.8618	30.28	-.60	.9997
24.2	5000	.10				2.744	.32	.9999	35.10	-.16	.9998
24.8	4500	.07				3.230	.24	.9997	40.43	-.23	.9999
25.2	4150	.05				4.496	.15	.9996	57.77	-.96	.9998
25.1	3950	.05				5.010	.16	.9998	67.78	-.37	.9999
24.9	3950	.05				6.120	.10	.9999	90.93	-1.19	.9997
25.0	3950	.04				7.403	.02	.9999	116.49	-1.83	.9998
25.1	3950	.03				8.148	.03	.9998	132.34	-.38	.9999
RUN 6- 14			MAT WT.= 16.58			.000710M					
25.1	760	-.40	2.736	1.04	.9653	2.748	1.13	.9527	14.31	-.15	.9999
			2.406	.95	.9486						
25.1	678	.50	2.900	.87	.9937	2.912	.96	.9877	15.84	-.14	.9999
			2.569	.77	.9899						
25.1	530	.56	3.187	1.09	.9998	3.063	1.22	.9976	22.21	-.15	.9998
			2.744	.97	.9992						
25.1	490	.45	3.999	.96	.9992	3.801	1.09	.9963	29.69	-.21	.9999
			3.487	.84	.9992						
25.1	490	.17	4.762	.37	.9919	4.564	.50	.9868	30.87	-.33	.9999
			3.811	.49	.9972						
25.1	463	.26	4.331	.70	.9998	4.084	.84	.9987	37.07	-.25	.9998
			3.773	.59	.9998						
25.1	445	.25	5.084	.51	.9997	4.813	.66	.9993	48.83	-.57	.9997
			4.496	.40	.9996						
25.1	430	.20	6.023	.37	.9999	5.851	.49	.9990	64.98	-1.03	.9996
			5.302	.28	.9996						
25.1	423	.15	6.743	.27	.9997	6.571	.39	.9994	83.46	-.94	.9998
			6.021	.18	.9994						
25.1	420	.15	7.557	.20	.9995	7.384	.31	.9999	109.77	-2.18	.9999
			6.834	.10	.9992						
RUN 6- 14			MAT WT.= 13.49			.000800M					
24.7	700	.04	1.408	.45	.9788	1.751	.64	.9772	9.88	-.12	.9996
24.7	635	.33	1.482	.60	.9991	1.826	.78	.9963	11.21	-.10	.9998
24.7	435	.44	2.698	.63	.9998	3.201	.84	.9965	19.78	-.13	.9997
24.7	400	.45	2.750	.66	.9989	3.260	.87	.9986	23.69	-.01	.9995
24.7	380	.40	3.141	.57	.9990	3.689	.78	.9973	29.44	-.28	.9995
24.7	365	.32	3.662	.51	.9993	4.217	.72	.9990	37.12	-.40	.9992
24.7	350	.31	4.336	.46	.9988	4.892	.67	.9992	51.73	-.41	.9996
24.7	350	.25	5.262	.31	.9994	5.818	.52	.9996	72.07	-1.09	.9995
24.7	343	.18	6.185	.22	.9992	6.742	.43	.9997	98.54	-1.47	.9997

TABLE VIIIB

SECOND STEP CALCULATIONS WITH STREAMING CURRENT DATA

Mat Thick-ness (L), in.	Mat Poros-ity, ε	Slope, (I_s/U)	Kozeny Factor: Exper-imental	Kozeny Factor: Davis Corre-lation	Calculated Zeta Potential, mv.: Capil-lary Model	Bieber +Mason (26)	Assum-ing N Varies	ζ_c (N = Const.)	
RUN 6- 9			MAT WT.= 23.16		.000115 M KCl				
.926	.791	2.74	7.01	5.76	28.34	20.14	15.29	4.06	
.843	.770	3.23	6.88	5.64	26.85	19.85	14.74	4.30	
.703	.724	4.49	6.89	5.55	23.40	18.96	13.54	4.74	
.629	.692	5.01	6.29	5.57	19.00	16.49	11.44	4.48	
.557	.652	6.12	6.23	5.59	16.08	15.25	10.10	4.47	
.508	.619	7.40	6.23	5.58	14.60	14.98	9.40	4.56	
.476	.593	8.14	5.85	5.54	13.07	14.29	8.50	4.40	
H= 2.79	R= .9950					OVERALL AV. =		4.43±	4.75
				AV.	(FIRST VALUE OMITTED) =			4.49±	3.32
RUN 6- 14			MAT WT.= 16.58		.000710 M KCl				
.736	.811	3.06	7.58	5.95	39.90	27.28	21.23	5.08	
.607	.771	3.80	7.18	5.65	32.09	23.66	17.54	5.09	
.607	.771	4.56	7.47	5.65	38.54	28.42	21.06	6.12	
.530	.738	4.08	6.87	5.56	24.44	19.25	13.85	4.61	
.464	.701	4.81	6.78	5.56	19.92	16.95	11.82	4.49	
.406	.658	5.85	6.54	5.59	16.27	15.21	10.12	4.39	
.366	.621	6.57	6.36	5.58	13.23	13.50	8.47	4.08	
.339	.591	7.38	6.67	5.53	11.65	12.81	7.54	3.92	
H= 4.12	R= .9763					OVERALL AV. =		4.72±	14.82
				AV.	(FIRST VALUE OMITTED) =			4.67±	15.83
RUN 6- 14			MAT WT.= 13.49		.000800 M KCl				
1.014	.888	1.82	10.37	7.94	61.15	36.48	33.77	4.77	
.581	.806	3.20	7.81	5.89	39.04	26.97	20.81	5.14	
.507	.777	3.26	7.33	5.67	29.25	21.32	15.90	4.50	
.449	.748	3.68	7.21	5.58	24.49	18.89	13.71	4.38	
.399	.717	4.21	7.10	5.55	20.38	16.76	11.85	4.26	
.342	.670	4.89	6.92	5.58	15.09	13.74	9.27	3.89	
.303	.628	5.81	7.02	5.59	12.34	12.40	7.87	3.73	
.271	.584	6.74	6.91	5.51	10.03	11.24	6.50	3.44	
H= 3.76	R= .9949					OVERALL AV. =		4.26±	13.12
				AV.	(FIRST VALUE OMITTED) =			4.19±	13.41

TABLE IXA

INITIAL CALCULATIONS WITH STREAMING CURRENT DATA

Temp., °C.	Resistance, ohms	I_r, μa.	Slope (I/U), μa.sec./cm.	Intercept, μa.	R	Slope (I_s/U), μa.sec./cm.	Intercept, μa.	R	Slope $(\Delta H/U)$, cm.sec/cm.	Intercept, cm.	R
RUN 6- 22A			MAT WT.= 13.90			.000113M					
26.2	4000	.30	3.612	1.07	.9872	3.566	1.34	.9834	12.87	-.40	.9998
			3.342	1.22	.9928						
26.3	3300	.22	4.376	.89	.9966	4.810	1.15	.9961	15.55	-.31	.9993
			4.578	.99	.9998						
26.5	2900	.20	5.689	.66	.9992	6.279	.90	.9984	18.81	-.50	.9970
			6.042	.73	.9995						
26.6	2900	.12	5.581	.56	.9986	6.105	.80	.9995	18.56	-.26	.9998
			5.869	.64	.9995						
26.9	2700	.12	7.217	.47	.9993	7.784	.76	.9989	24.07	-.29	.9999
			7.349	.65	.9988						
27.3	2400	.14	9.135	.32	.9992	9.659	.66	.9997	28.82	-.05	.9999
			9.499	.45	.9994						
27.3	2270	.15	11.666	.15	.9990	12.133	.55	.9999	42.02	-1.45	.9987
			12.014	.33	.9993						
27.6	2160	.03	14.558	.47	.9999	16.336	.32	.9991	54.07	-.22	.9999
27.6	2140	.04	17.431	.43	.9998	19.241	.28	.9996	70.72	-.33	.9997
27.8	2160	.04	21.510	.36	.9995	23.319	.21	.9998	94.72	-.37	.9998
RUN 6- 22B			MAT WT.= 13.99			.000112M					
28.2	3800	.18	3.493	.33	.9942	3.717	.45	.9969	12.11	-.35	.9997
28.2	2950	.14	4.856	.63	.9999	5.092	.80	.9979	17.00	-.23	.9997
28.2	2520	.15	6.637	.55	.9993	6.832	.74	.9994	22.66	-.25	.9998
28.2	2350	.12	8.250	.51	.9990	8.410	.72	.9996	28.39	-.14	.9999
27.9	2320	.06	10.092	.37	.9985	10.211	.59	.9999	38.02	-.46	.9994
26.6	2160	.07	11.670	.45	.9996	13.479	.30	.9992	50.87	-.10	.9999
27.0	2150	-.04	14.080	.40	.9994	15.890	.25	.9998	66.78	-.14	.9998
27.0	2180	-.04	16.736	.41	.9988	18.883	.18	.9999	88.45	-.38	.9995
RUN 6- 30A			MAT WT.= 13.22			.000121M					
25.0	3670	.75	1.328	1.94	.9794	1.328	1.98	.9794	12.51	-.52	.9996
25.0	2840	.31	3.680	1.23	.9972	3.903	1.31	.9959	16.36	-.52	.9995
25.0	2460	.17	4.533	1.21	.9964	4.852	1.33	.9924	21.64	-.42	.9997
25.0	2200	.17	6.216	.83	.9994	6.657	1.07	.9975	28.99	-.62	.9991
25.0	2060	.10	7.712	.64	.9997	8.207	.94	.9980	37.25	-.66	.9999
25.0	1960	.07	9.716	.47	.9997	10.299	.83	.9982	51.75	-.69	.9998
25.0	1920	.05	11.587	.37	.9998	12.930	.62	.9994	69.45	-.64	.9999
25.0	1920	.05	14.398	.16	.9998	15.741	.41	.9994	94.45	-1.48	.9999
RUN 6- 30B			MAT WT.= 13.35			.000121M					
25.0	3650	.05	1.855	.78	.9915	2.067	.76	.9834	12.06	-.48	.9982
25.2	2700	.13	3.468	.69	.9994	3.827	.72	.9973	16.80	-.22	.9996
25.3	2350	.10	4.614	.67	.9999	4.986	.76	.9983	21.85	-.17	.9997
25.4	2180	.10	5.780	.61	.9997	6.195	.75	.9990	29.13	-.29	.9998
25.4	2050	.07	7.009	.53	.9996	7.435	.71	.9986	37.67	-.35	.9996
25.3	2000	.02	8.949	.37	.9999	9.359	.58	.9983	52.17	-.59	.9995
25.4	1950	.03	10.884	.29	.9993	11.284	.53	.9998	71.42	-1.09	.9997
25.2	1950	.01	13.151	.18	.9994	13.551	.41	.9997	96.74	-1.70	.9996

TABLE IXB

SECOND STEP CALCULATIONS WITH STREAMING CURRENT DATA

Mat Thickness (L), in.	Mat Porosity, ε	Slope, (I_s/U)	Kozeny Factor: Experimental	Kozeny Factor: Davis Correlation	Calculated Zeta Potential, mv.: Capillary Model	Bieber +Mason (26)	Assuming N Varies	ζ_c (N = Const.)	
RUN 6- 22A			MAT WT.= 13.90		.000113 M KCl				
.765	.848	4.81	9.21	6.57	95.86	61.35	51.28	9.91	
.651	.821	6.27	8.65	6.08	91.99	61.76	49.01	11.13	
.651	.821	6.10	8.56	6.08	89.49	60.08	47.67	10.82	
.546	.787	7.78	8.25	5.73	78.30	56.04	42.37	11.47	
.470	.752	9.65	7.50	5.58	67.69	51.81	37.86	11.91	
.408	.715	12.13	8.15	5.55	58.17	48.07	34.05	12.34	
.349	.667	16.33	7.33	5.58	49.67	45.56	30.76	13.03	
.312	.627	19.24	7.14	5.59	41.36	41.57	26.50	12.55	
.280	.585	23.31	6.98	5.51	35.58	39.73	23.16	12.23	
H= 2.64	R= .9981					OVERALL AV. =		11.71±	8.31
						AV. (FIRST VALUE OMITTED) =		11.93±	6.28
RUN 6- 22B			MAT WT.= 13.99		.000112M KCl				
1.001	.883	3.71	10.94	7.69	117.10	70.54	64.46	9.58	
.676	.827	5.09	8.51	6.16	80.10	53.24	42.66	9.39	
.544	.785	6.83	7.81	5.72	67.59	48.58	36.64	10.02	
.464	.748	8.41	7.22	5.57	56.34	43.54	31.69	10.16	
.403	.709	10.21	7.13	5.55	46.57	38.92	27.45	10.13	
.348	.664	13.47	6.54	5.58	39.63	36.61	24.63	10.53	
.311	.624	15.89	6.42	5.58	33.03	33.49	21.21	10.15	
.284	.588	18.88	6.51	5.52	29.41	32.57	19.14	10.03	
H= 2.87	R= .9947					OVERALL AV. =		10.00±	3.58
						AV. (FIRST VALUE OMITTED) =		10.06±	3.39
RUN 6- 30A			MAT WT.= 13.22		.000121M KCl				
.714	.845	3.90	9.60	6.50	74.64	48.02	39.88	7.85	
.559	.802	4.85	8.51	5.85	56.96	39.62	30.52	7.68	
.451	.755	6.65	7.66	5.59	47.16	35.94	26.31	8.20	
.393	.718	8.20	7.40	5.55	40.29	33.04	23.47	8.40	
.334	.669	10.29	7.05	5.58	31.48	28.75	19.45	8.19	
.290	.619	12.93	6.51	5.58	25.51	26.18	16.42	7.96	
.261	.576	15.74	6.44	5.49	22.19	25.33	14.45	7.78	
H= 2.84	R= .9948					OVERALL AV. =		8.01±	3.25
						AV. (FIRST VALUE OMITTED) =		8.03±	3.42
RUN 6- 30B			MAT WT.= 13.35		.000121M KCl				
.639	.825	3.82	8.09	6.14	58.17	38.78	30.96	6.88	
.521	.785	4.98	7.42	5.72	49.00	35.16	26.52	7.23	
.432	.741	6.19	6.92	5.57	38.35	30.01	21.71	7.13	
.372	.700	7.43	6.48	5.56	30.44	25.97	18.14	6.92	
.321	.652	9.35	6.25	5.59	24.63	23.36	15.46	6.84	
.282	.604	11.28	5.99	5.56	19.79	21.05	12.82	6.45	
.254	.560	13.55	5.81	5.42	16.99	20.22	11.03	6.16	
H= 3.13	R= .9922					OVERALL AV. =		6.80±	5.50
						AV. (FIRST VALUE OMITTED) =		6.79±	6.02

TABLE XA

INITIAL CALCULATIONS WITH STREAMING CURRENT DATA

Temp., °C.	Resistance, ohms	I_r, μa.	Slope (I/U), μa.sec./cm.	Intercept, μa.	R	Slope (I_s/U), μa.sec./cm.	Intercept, μa.	R	Slope ($\Delta H/U$), cm.sec./cm.	Intercept, cm.	R
RUN 7- 21 A			MAT WT.= 17.13			.001010M					
24.8	525	.52	1.166	-.23	.9897	1.166	-.07	.9897	19.06	-.73	.9999
24.8	447	.32	1.039	-.04	.9987	.976	.12	.9976	22.50	-.36	.9993
24.8	392	.37	1.179	.02	.9957	1.084	.20	.9985	27.84	-.09	.9999
24.8	365	.45	1.492	.08	.9965	1.397	.25	.9984	37.31	-.28	.9998
24.8	349	.44	1.787	.05	.9947	1.623	.22	.9972	48.40	-.61	.9997
24.8	340	.48	2.025	.08	.9963	1.862	.24	.9979	66.08	-.58	.9997
24.8	340	.47	2.410	.11	.9931	2.247	.26	.9951	93.12	-1.37	.9995
24.8	340	.48	2.735	.13	.9948	2.562	.28	.9948	125.03	-2.06	.9995
RUN 7- 21 B			MAT WT.= 15.56			.001010M					
25.9	508	.44	1.727	.41	.9958	1.727	.57	.9958	15.42	-.36	.9992
			1.995	.39	.9955						
25.9	403	.67	2.152	.59	.9949	2.089	.76	.9929	19.65	-.20	.9999
			2.288	.64	.9951						
25.9	360	.79	2.460	.59	.9995	2.334	.78	.9987	27.10	-.23	.9997
			2.492	.69	.9995						
25.9	330	.73	2.665	.56	.9964	2.537	.72	.9940	35.98	-.45	.9999
			2.684	.67	.9942						
25.9	312	.60	3.146	.38	.9998	2.981	.54	.9999	45.31	-.35	.9997
			3.135	.50	.9998						
25.9	303	.60	3.322	.31	.9999	3.156	.45	.9998	64.54	-.95	.9997
			3.342	.42	.9999						
25.9	298	.60	3.226	.29	.9992	3.056	.44	.9994	85.89	-1.08	.9999
			3.242	.42	.9997						
25.9	300	.52	3.395	.14	.9988	3.224	.27	.9988	116.13	-2.24	.9993
			3.410	.27	.9977						
RUN 7- 23 A			MAT WT.= 17.68			.001080M					
25.5	530	.50	2.633	.67	.9816	2.571	.78	.9781	18.14	-.32	.9986
25.5	445	.75	3.388	.75	.9996	3.294	.85	.9994	24.05	-.40	.9998
25.5	370	.55	3.840	.56	.9988	3.681	.64	.9971	36.02	.33	.9970
25.5	355	.42	4.075	.54	.9974	3.885	.62	.9949	49.32	-.71	.9999
25.5	350	.55	3.998	.46	.9999	3.776	.54	.9994	70.48	-1.27	.9996
25.5	348	.50	4.348	.32	.9988	4.120	.39	.9999	92.71	-1.51	.9995
25.5	348	.45	4.655	.19	.9976	4.426	.26	.9993	127.39	-3.20	.9992
RUN 7- 23 B			MAT WT.= 15.68			.001080M					
24.8	505	.63	3.175	.56	.9497	2.996	.74	.9489	16.63	-.66	.9999
24.8	402	.55	3.105	.55	.9948	2.968	.69	.9908	22.39	-.26	.9987
24.8	360	.83	3.031	.87	.9982	2.924	.99	.9942	14.92	2.46	.8816
24.8	330	.85	3.607	.86	.9993	3.462	.98	.9974	36.62	.46	.9958
24.8	322	.75	3.868	.75	.9999	3.722	.85	.9989	47.95	-.72	.9996
24.8	317	.83	3.725	.74	.9997	3.591	.84	.9987	63.56	-.69	.9999
24.8	312	.90	4.016	.63	.9999	3.881	.72	.9997	87.20	-1.36	.9998
24.8	315	.69	4.054	.51	.9998	3.883	.60	.9998	117.79	-2.05	.9997

TABLE XB

SECOND STEP CALCULATIONS WITH STREAMING CURRENT DATA

Mat Thickness (L), in.	Mat Porosity, ϵ	Slope, (I_s/U)	Kozeny Factor: Experimental	Kozeny Factor: Davis Correlation	Calculated Zeta Potential, mv.: Capillary Model	Bieber +Mason (26)	Assuming N Varies	ζ_c (N = Const.)
RUN 7- 21A			MAT WT.= 17.13		.001010M KCl			
.787	.818	.97	7.83	6.03	13.63	9.21	7.24	1.67
.648	.779	1.08	6.89	5.68	9.88	7.18	5.36	1.50
.552	.740	1.39	6.75	5.56	8.52	6.68	4.82	1.59
.480	.701	1.62	6.48	5.56	6.73	5.72	3.99	1.51
.420	.659	1.86	6.42	5.59	5.19	4.84	3.22	1.40
.372	.615	2.24	6.51	5.58	4.28	4.44	2.75	1.35
.335	.572	2.56	6.35	5.47	3.50	4.03	2.26	1.23
H= 3.46	R= .9961					OVERALL AV. =		1.46± 10.23
			AV. (FIRST VALUE OMITTED) =					1.43± 9.08
RUN 7- 21B			MAT WT.= 15.56		.001010M KCl			
1.001	.870	1.72	10.20	7.19	45.11	27.79	24.36	4.02
.756	.828	2.08	8.46	6.18	32.82	21.78	17.38	3.80
.591	.780	2.33	7.62	5.69	21.60	15.67	11.69	3.27
.502	.741	2.53	7.37	5.56	15.62	12.24	8.81	2.90
.442	.705	2.98	7.06	5.56	12.93	10.90	7.61	2.85
.384	.661	3.15	7.19	5.59	9.02	8.38	5.59	2.40
.341	.618	3.05	6.96	5.58	6.03	6.20	3.86	1.87
.309	.579	3.22	6.99	5.50	4.65	5.27	3.01	1.61
H= 5.19	R= .9982					OVERALL AV. =		2.84± 30.16
			AV. (FIRST VALUE OMITTED) =					2.67± 28.77
RUN 7- 23A			MAT WT.= 17.68		.001080M KCl			
.784	.811	3.29	7.76	5.95	42.91	29.34	22.82	5.47
.577	.744	3.68	6.59	5.57	23.31	18.16	13.12	4.27
.509	.709	3.88	6.91	5.56	17.47	14.60	10.26	3.79
.438	.662	3.77	6.92	5.59	10.90	10.10	6.75	2.90
.390	.621	4.12	6.67	5.58	8.29	8.46	5.31	2.56
.353	.581	4.42	6.81	5.50	6.48	7.31	4.20	2.24
H= 5.25	R= .9915					OVERALL AV. =		3.54± 34.37
			AV. (FIRST VALUE OMITTED) =					3.15± 27.08
RUN 7- 23B			MAT WT.= 15.68		.001080M KCl			
.680	.807	2.96	7.72	5.90	36.75	25.33	19.60	4.80
.570	.770	2.92	3.74	5.64	24.23	17.92	13.27	3.88
.479	.726	3.46	6.48	5.55	18.30	14.77	10.53	3.66
.436	.699	3.72	6.89	5.56	15.09	12.90	8.99	3.43
.383	.657	3.59	6.68	5.59	9.89	9.27	6.16	2.68
.341	.615	3.88	6.69	5.58	7.44	7.70	4.78	2.34
.309	.576	3.88	6.70	5.49	5.43	6.21	3.53	1.90
H= 5.26	R= .9977					OVERALL AV. =		3.24± 30.78
			AV. (FIRST VALUE OMITTED) =					2.98± 26.58

TABLE XIA

INITIAL CALCULATIONS WITH STREAMING CURRENT DATA

Temp., °C.	Resistance, ohms	I_r, μa.	Slope (I/U), μa.sec./cm.	Intercept, μa.	R	Slope (I_s/U), μa.sec./cm.	Intercept, μa.	R	Slope ($\Delta H/U$), cm.sec./cm.	Intercept, cm.	R
RUN 7- 26			MAT WT.= 16.20			.000115M					
26.1	4550	.33	2.452	.85	.9888	2.765	.70	.9897	15.93	-.58	.9988
			2.242	.57	.9886						
26.1	4000	.30	3.376	.64	.9998	3.701	.59	.9989	18.62	-.32	.9992
			3.073	.41	.9999						
26.1	3470	.25	4.618	.48	.9999	4.966	.50	.9991	24.27	-.35	.9998
			4.167	.29	.9997						
26.1	3100	.23	5.998	.43	.9994	6.434	.47	.9988	32.64	-.34	.9994
			5.468	.23	.9993						
26.1	2940	.18	7.424	.36	.9994	7.997	.38	.9995	41.96	-.45	.9994
			6.841	.14	.9995						
26.1	2860	.16	9.647	.30	.9997	10.313	.31	.9998	59.90	-.71	.9997
			9.040	.06	.9996						
26.1	2820	.15	11.987	.17	.9994	12.722	.17	.9998	80.84	-1.26	.9997
			11.449	-.07	.9994						
26.1	2820	.12	13.788	.33	.9999	15.300	.19	.9999	107.83	-1.00	.9998
			13.350	.07	.9996						
RUN 7- 27			MAT WT.= 14.08			.000111M					
25.0	4350	.20	1.017	.68	.9548	1.540	.81	.9721	13.17	-.56	.9996
25.0	3470	.20	1.745	.51	.9972	2.428	.72	.9910	18.07	-.48	.9998
25.0	2960	.29	2.658	.37	.9996	3.624	.61	.9977	25.01	-.34	.9994
25.0	2720	.26	3.283	.39	.9977	4.440	.63	.9992	32.68	-.37	.9994
25.0	2560	.25	3.850	.35	.9994	5.124	.61	.9982	43.76	-.43	.9998
25.0	2480	.22	5.050	.26	.9991	6.325	.51	.9993	63.20	-.92	.9996
25.0	2440	.20	6.004	.20	.9999	7.957	.32	.9988	84.41	-.93	.9999
25.0	2470	.18	7.857	-.02	.9991	9.132	.22	.9999	117.82	-2.62	.9993
RUN 7- 28			MAT WT.= 16.00			.000115M					
25.0	4800	.24	.871	.66	.9984	1.833	.80	.9774	20.05	-1.11	.9987
25.0	3840	.30	2.165	.35	.9965	3.077	.62	.9969	24.83	-.33	.9997
25.0	3450	.22	2.865	.26	.9964	3.911	.54	.9988	32.25	-.37	.9994
25.0	3180	.20	3.815	.09	.9980	4.828	.46	.9992	50.00	-3.31	.9961
25.0	2980	.15	4.534	-.03	.9990	5.605	.37	.9987	55.30	-.80	.9997
25.0	2860	.14	6.628	-.33	.9988	7.734	.12	.9981	134.25	-10.21	.9893
25.0	2860	.06	7.388	-.27	.9986	8.544	.19	.9998	158.22	-3.52	.9993
25.0	2860	.06	8.464	-.29	.9999	10.417	.05	.9998	205.53	-1.99	.9999
RUN 7- 29			MAT WT.= 19.66			.000115M					
24.8	5000	.28	1.053	.46	.9821	1.493	.77	.9846	23.49	-.72	.9998
24.8	4480	.20	1.314	.31	.9984	1.977	.60	.9959	28.28	-.38	.9996
24.8	4110	.17	1.616	.23	.9965	2.413	.53	.9957	35.88	-.39	.9997
24.8	3850	.19	1.833	.16	.9873	2.785	.45	.9992	45.71	-.54	.9991
24.8	3640	.15	2.298	.01	.9961	3.251	.37	.9983	56.98	-.48	.9999
24.8	3480	.13	3.145	-.13	.9967	4.128	.28	.9996	83.20	-1.31	.9997
24.8	3410	.10	3.854	-.26	.9975	4.837	.20	.9997	110.00	-2.01	.9998
24.8	3560	.47	4.693	-.51	.9976	5.730	-.02	.9996	143.98	-2.92	.9987

TABLE XIB

SECOND STEP CALCULATIONS WITH STREAMING CURRENT DATA

Mat Thick-ness (L),in.	Mat Poros-ity, ϵ	Slope, (I_s/U)	Kozeny Factor: Exper-imental	Kozeny Factor: Davis Corre-lation	Calculated Zeta Potential, mv.: Capil-lary Model	Bieber +Mason (26)	Assum-ing N Varies	ζ_c (N = Const.)	
RUN 7- 26			MAT WT.= 16.20		.000115M KCl				
.806	.832	3.70	8.03	6.24	60.97	40.16	32.47	6.94	
.654	.793	4.96	7.36	5.77	52.93	37.47	28.53	7.51	
.538	.748	6.43	6.84	5.58	42.78	33.04	24.05	7.70	
.467	.710	7.99	6.52	5.55	36.21	30.25	21.33	7.87	
.400	.661	10.31	6.45	5.59	29.57	27.47	18.42	7.93	
.358	.621	12.72	6.47	5.58	25.83	26.33	16.61	7.99	
.322	.579	15.30	6.28	5.50	22.17	25.12	14.44	7.72	
H= 2.75	R= .9943					OVERALL AV. =		7.67±	4.68
					AV. (FIRST VALUE OMITTED) =			7.79±	2.26
RUN 7- 27			MAT WT.= 14.08		.000111M KCl				
.711	.834	2.42	8.96	6.29	40.93	26.84	21.81	4.59	
.544	.783	3.62	7.86	5.71	34.74	25.03	18.86	5.19	
.460	.744	4.44	7.44	5.57	28.13	21.90	15.89	5.17	
.401	.706	5.12	7.43	5.56	22.29	18.76	13.19	4.92	
.347	.661	6.32	7.60	5.59	17.93	16.68	11.17	4.82	
.309	.619	7.95	7.43	5.58	15.72	16.12	10.12	4.90	
.278	.576	9.13	7.54	5.49	12.88	14.70	8.39	4.52	
H= 3.19	R= .9910					OVERALL AV. =		4.87±	5.30
					AV. (FIRST VALUE OMITTED) =			4.92±	5.04
RUN 7- 28			MAT WT.= 16.00		.000115 M KCl				
.708	.811	3.07	8.72	5.94	39.80	27.24	21.25	5.11	
.590	.773	3.91	8.18	5.65	33.58	24.68	18.39	5.30	
.505	.735	4.82	9.33	5.56	27.91	22.13	15.94	5.37	
.447	.700	5.60	7.91	5.56	23.07	19.65	13.75	5.23	
.394	.660	7.73	14.18	5.59	21.87	20.36	13.63	5.89	
.351	.619	8.54	12.25	5.58	16.85	17.30	10.85	5.26	
.321	.583	10.41	12.19	5.51	15.46	17.34	10.07	5.34	
H= 2.73	R= .9875					OVERALL AV. =		5.36±	4.64
					AV. (FIRST VALUE OMITTED) =			5.40±	4.52
RUN 7- 29			MAT WT.= 19.66		.000115 M KCl				
.842	.804	1.97	7.61	5.88	23.83	16.50	12.76	3.17	
.712	.769	2.41	7.13	5.63	19.81	14.68	10.90	3.20	
.622	.735	2.78	6.94	5.56	16.19	12.82	9.24	3.10	
.553	.702	3.25	6.71	5.56	13.63	11.56	8.10	3.06	
.477	.655	4.12	6.85	5.59	11.14	10.49	6.98	3.06	
.428	.616	4.83	6.75	5.58	9.30	9.61	6.00	2.93	
.387	.575	5.73	6.51	5.48	7.99	9.15	5.21	2.81	
H= 3.08	R= .9934					OVERALL AV. =		3.05±	4.43
					AV. (FIRST VALUE OMITTED) =			3.03±	4.50

TABLE XIIA

INITIAL CALCULATIONS WITH STREAMING CURRENT DATA

Temp., °C.	Resistance, ohms	I_r, μa.	Slope (I/U), μa.sec./cm.	Intercept, μa.	R	Slope (I_s/U), μa.sec./cm.	Intercept, μa.	R	Slope ($\Delta H/U$), cm.sec./cm.	Intercept, cm.	R
RUN 8- 9			MAT WT.= 9.70			.000130M					
24.2	3280	.38	4.015	1.80	.9937	5.119	1.83	.9835	15.00	-.45	.9999
24.2	2380	.50	7.164	1.83	.9991	7.927	1.90	.9958	20.05	-.46	.9998
24.2	1930	.35	10.628	1.17	.9997	12.253	1.08	.9993	23.07	-.18	.9995
24.2	1630	.35	13.878	1.10	.9999	15.788	1.00	.9999	28.91	-.19	.9997
24.2	1410	.28	20.896	.68	.9995	23.638	.47	.9996	46.95	-1.43	.9947
24.2	1250	.15	27.224	.54	.9996	29.200	.50	.9998	64.76	-1.24	.9998
24.2	1140	.18	33.932	.58	.9999	37.497	.34	.9999	84.53	-.39	.9996
24.2	1090	.03	41.784	.49	.9999	45.297	.27	.9999	115.33	-.63	.9988
RUN 8- 10			MAT WT.= 8.65			.000130M					
24.2	2270	.35	7.850	1.38	.9949	8.828	1.41	.9921	17.93	-1.04	.9994
24.2	1480	.20	16.253	1.26	.9983	18.533	1.09	.9979	26.64	-.26	.9997
24.2	1300	.35	21.206	1.05	.9999	23.570	.87	.9999	35.55	-.47	.9983
24.2	1180	.30	24.322	1.08	.9996	27.536	.85	.9999	42.81	-.27	.9984
24.2	1060	.24	33.878	.73	.9997	37.457	.51	.9992	64.80	-.58	.9990
24.2	1010	.15	41.623	.54	.9998	45.141	.31	.9999	90.78	-.95	.9987
24.2	985	.17	48.266	.54	.9998	51.730	.34	.9999	119.35	-.90	.9992
RUN 8- 11			MAT WT.= 9.82			.000130M					
24.1	2210	.21	9.765	1.12	.9994	11.333	1.03	.9990	22.55	-1.02	.9972
24.1	1690	.35	15.636	1.06	.9990	17.729	.92	.9987	28.49	-.45	.9993
24.1	1490	.37	19.584	1.07	.9999	22.375	.85	.9998	34.54	-.25	.9991
24.1	1350	.25	24.513	.98	.9996	27.542	.73	.9995	43.69	-.19	.9997
24.1	1220	.20	30.583	.95	.9985	34.717	.66	.9993	61.41	-.44	.9999
24.1	1140	.18	40.099	.72	.9996	43.613	.51	.9999	92.15	-1.11	.9965
24.1	1100	-.04	46.161	.79	.9999	49.672	.56	.9999	113.07	-.61	.9994
RUN 8- 12			MAT WT.= 6.53			.000130M					
24.5	2060	.50	5.958	1.64	.9999	7.527	1.55	.9994	10.57	-.50	.9982
24.5	1450	.40	10.551	1.94	.9988	12.578	1.83	.9981	15.56	-.53	.9999
24.5	1200	.39	14.939	1.64	.9955	17.328	1.46	.9943	19.03	-.24	.9982
24.5	1090	.40	19.416	1.45	.9994	22.869	1.21	.9992	24.28	-.16	.9999
24.5	935	.30	25.298	1.17	.9996	28.940	.94	.9994	33.12	-.18	.9993
24.5	843	.16	31.240	1.20	.9999	34.721	1.00	.9999	51.64	-.57	.9965
24.5	785	.16	37.380	1.13	.9999	41.452	.89	.9999	71.62	-.77	.9972
24.5	750	.07	44.625	1.00	.9998	48.703	.75	.9999	100.71	-1.09	.9965

TABLE XIIB

SECOND STEP CALCULATIONS WITH STREAMING CURRENT DATA

Mat Thickness (L), in.	Mat Porosity, ϵ	Slope, (I_s/U)	Kozeny Factor: Experimental	Kozeny Factor: Davis Correlation	Calculated Zeta Potential, mv.: Capillary Model	Bieber +Mason (26)	Assuming N Varies	ζ_c (N = Const.)
RUN 8- 9			MAT WT.= 9.70		.000130M KCl			
.680	.916	7.92	15.58	9.65	120.33	68.53	69.42	7.35
.529	.893	12.25	12.89	8.15	126.50	74.94	70.65	9.61
.424	.866	15.78	11.83	7.08	113.57	70.39	61.63	10.46
.339	.833	23.63	13.65	6.26	113.50	74.62	60.61	12.87
.269	.789	29.20	12.72	5.75	86.44	61.58	46.81	12.53
.226	.749	37.49	11.93	5.58	72.75	56.03	40.94	13.04
.196	.711	45.29	12.07	5.55	59.76	49.80	35.25	12.95
H= 3.53	R= .9992					OVERALL AV.	=	11.26± 19.48
					AV. (FIRST VALUE OMITTED)		=	11.91± 12.47
RUN 8- 10			MAT WT.= 8.65		.000130M KCl			
.631	.920	8.82	16.43	9.92	142.26	80.59	82.44	8.39
.367	.862	18.53	11.70	6.95	126.67	79.06	68.52	11.98
.307	.835	23.57	11.87	6.31	116.57	76.29	62.27	13.02
.265	.809	27.53	11.22	5.93	101.38	69.58	54.31	13.16
.219	.769	37.45	12.06	5.64	89.50	66.27	49.31	14.45
.188	.731	45.14	12.46	5.56	72.87	58.21	41.91	14.31
.168	.699	51.73	12.81	5.56	60.95	52.05	36.47	13.94
H= 4.03	R= .9999					OVERALL AV.	=	12.75± 16.51
					AV. (FIRST VALUE OMITTED)		=	13.48± 6.96
RUN 8- 11			MAT WT.= 9.82		.000130M KCl			
.589	.902	11.33	14.10	8.69	135.63	79.05	76.74	9.49
.423	.864	17.72	11.24	7.01	124.31	77.31	67.36	11.61
.351	.836	22.37	10.25	6.33	112.11	73.21	59.91	12.44
.298	.807	27.54	9.91	5.91	99.33	68.40	53.26	13.03
.249	.770	34.71	10.08	5.64	83.22	61.57	45.84	13.42
.214	.732	43.61	11.18	5.56	70.88	56.54	40.74	13.88
.191	.700	49.67	10.70	5.56	58.74	50.12	35.14	13.41
H= 3.65	R= .9970					OVERALL AV.	=	12.47± 12.10
					AV. (FIRST VALUE OMITTED)		=	12.96± 6.32
RUN 8- 12			MAT WT.= 6.53		.000130M KCl			
.600	.936	7.52	17.15	11.57	171.12	94.40	101.17	8.17
.376	.898	12.57	13.98	8.45	141.60	83.09	79.62	10.26
.296	.871	17.32	12.27	7.23	132.75	81.60	72.31	11.84
.237	.839	22.86	11.20	6.38	118.18	76.84	63.15	12.91
.200	.809	28.94	11.57	5.93	106.66	73.20	57.10	13.84
.165	.769	34.72	12.77	5.63	82.69	61.28	45.55	13.38
.142	.731	41.45	13.13	5.56	67.12	53.60	38.58	13.17
.125	.695	48.70	13.94	5.56	55.10	47.51	33.14	12.85
H= 4.02	R= .9997					OVERALL AV.	=	12.05± 15.95
					AV. (FIRST VALUE OMITTED)		=	12.61± 9.53

TABLE XIIIA

INITIAL CALCULATIONS WITH STREAMING CURRENT DATA

Temp., °C.	Resistance, ohms	I_r, μa.	Slope (I/U), μa.sec./cm.	Intercept, μa.	R	Slope (I_s/U), μa.sec./cm.	Intercept, μa.	R	Slope (ΔH/U), cm.sec./cm.	Intercept, cm.	R
RUN 8- 30			MAT	WT.= 5.44		.000120M					
25.3	2400	.25	4.954	2.00	.9675	5.623	1.97	.9685	11.95	-.57	.9993
			4.715	1.88	.9382						
25.3	1600	.40	6.521	2.30	.9937	7.583	2.27	.9904	21.42	-.99	.9987
			5.839	2.22	.9882						
25.3	1230	.15	12.509	1.21	.9989	13.517	1.20	.9976	25.27	-.33	.9999
			11.658	1.05	.9988						
25.3	1050	.18	17.438	.87	.9991	18.334	.87	.9980	40.28	-1.19	.9999
			16.636	.57	.9985						
25.3	930	.12	21.200	.57	.9991	22.317	.49	.9991	51.94	-.61	.9988
			19.640	.36	.9997						
25.3	820	.10	29.199	.24	.9998	30.729	.12	.9998	89.31	-1.26	.9970
			26.945	.06	.9985						
25.3	786	.03	34.606	.08	.9999	36.080	-.02	.9999	145.77	-2.45	.9955
			32.291	-.08	.9993						
25.3	760	-.05	37.775	.04	.9999	39.244	-.08	.9999	200.31	-2.98	.9968
			35.452	-.14	.9993						
RUN 8- 31			MAT	WT.= 6.90		.000120M					
24.8	2520	.22	5.231	1.43	.9932	5.901	1.56	.9951	14.54	-.57	.9996
24.8	1850	.22	9.442	1.06	.9989	10.437	1.23	.9976	19.67	-.65	.9996
24.8	1530	.20	13.416	.76	.9986	15.272	.80	.9982	26.72	-.83	.9999
24.8	1300	.15	18.017	.35	.9998	19.876	.51	.9999	40.88	-2.58	.9989
24.8	1150	-.03	22.810	.32	.9988	26.208	.31	.9998	45.20	-.44	.9973
24.8	1020	.05	29.964	.12	.9998	33.608	.16	.9999	67.93	-.70	.9984
24.8	973	.00	35.216	.09	.9998	38.979	.14	.9999	94.21	-1.07	.9990
24.8	935	-.05	41.391	.04	.9990	45.158	.09	.9997	132.13	-1.49	.9975
RUN 9- 2A			MAT	WT.= 3.93		.000120M					
24.5	1690	.20	4.316	2.14	.9849	6.450	2.21	.9877	10.02	-.53	.9979
24.4	1310	.37	7.408	1.92	.9993	9.546	2.10	.9975	11.29	-.32	.9990
24.3	1030	.31	13.995	1.11	.9995	17.511	1.19	.9992	14.15	-.17	.9966
24.4	830	.35	18.841	1.01	.9998	22.198	1.19	.9998	20.25	-.19	.9959
24.5	713	.38	22.780	.94	.9997	26.273	1.16	.9996	30.36	-.28	.9976
24.5	625	.29	26.622	.77	.9999	30.610	1.02	.9999	45.67	-.40	.9983
24.5	585	.20	33.937	.44	.9989	38.229	.67	.9992	79.59	-1.29	.9956
24.5	568	.50	34.592	.46	.9998	38.893	.70	.9999	105.85	-1.30	.9967
RUN 9- 2B			MAT	WT.= 2.96		.000390M					
24.7	492	.07	4.612	.93	.9999	4.898	1.11	.9994	5.00	-.05	.9994
24.6	290	.42	8.608	1.36	.9970	9.210	1.50	.9972	8.99	-.18	.9999
24.7	207	.40	13.236	1.20	.9980	13.731	1.36	.9978	16.94	-.44	.9999
24.8	180	.10	16.369	.86	.9994	16.743	1.05	.9990	26.96	-.93	.9997
24.8	153	.00	19.995	.57	.9989	21.666	.53	.9998	38.79	-.47	.9957
24.8	150	-.20	21.851	.37	.9991	23.527	.33	.9998	54.77	-.62	.9960
25.0	145	-.40	23.429	.17	.9987	25.113	.13	.9997	79.55	-1.19	.9930

TABLE XIIIB

SECOND STEP CALCULATIONS WITH STREAMING CURRENT DATA

Mat Thickness (L), in.	Mat Porosity, ϵ	Slope, (I_s/U)	Kozeny Factor: Experimental	Kozeny Factor: Davis Correlation	Calculated Zeta Potential, mv.: Capillary Model	Bieber +Mason (26)	Assuming N Varies	ζ_c (N = Const.)
RUN 8- 30			MAT WT.= 5.44		.000120M KCl			
.371	.914	7.58	29.36	9.48	111.05	63.49	63.89	6.95
.272	.883	13.51	22.89	7.70	122.19	73.58	67.45	10.01
.216	.853	18.33	26.10	6.69	112.17	71.17	60.32	11.27
.176	.819	22.31	24.33	6.05	92.51	62.31	49.43	11.34
.142	.776	30.72	28.70	5.67	79.47	58.05	43.51	12.37
.120	.735	36.08	33.65	5.56	60.96	48.30	34.90	11.74
.105	.697	39.24	34.54	5.56	45.67	39.16	27.40	10.54
H= 5.18	R= .9994					OVERALL AV. =		10.60± 16.82
					AV. (FIRST VALUE OMITTED) =			11.21± 7.50
RUN 8- 31			MAT WT.= 6.90		.000120M KCl			
.608	.933	5.90	21.37	11.26	126.31	69.98	74.58	6.28
.412	.902	10.43	17.68	8.66	124.48	72.61	70.47	8.76
.325	.876	15.27	17.34	7.41	124.90	76.14	68.47	10.79
.262	.846	19.87	19.29	6.53	111.87	71.83	60.02	11.73
.218	.815	26.20	15.86	6.00	103.22	70.08	55.26	12.98
.179	.775	33.60	16.82	5.66	85.42	62.57	46.87	13.41
.153	.737	38.97	17.13	5.56	66.61	52.63	38.11	12.76
.134	.699	45.15	18.01	5.56	53.35	45.57	31.97	12.22
H= 4.59	R= .9991					OVERALL AV. =		11.11± 22.05
					AV. (FIRST VALUE OMITTED) =			11.81± 13.54
RUN 9- 2			MAT WT.= 3.93		.000115M KCl			
.308	.925	9.54	25.02	10.41	171.39	96.23	100.12	9.48
.230	.900	17.51	21.50	8.54	201.96	118.20	113.95	14.45
.174	.868	22.19	20.93	7.13	163.36	100.95	88.83	14.89
.136	.831	26.27	21.58	6.23	123.96	81.74	66.22	14.20
.111	.793	30.61	23.03	5.78	94.58	66.89	51.12	13.43
.091	.748	38.22	27.58	5.57	73.10	56.48	41.24	13.22
.084	.727	38.89	31.09	5.55	60.09	48.45	34.77	12.07
H= 5.07	R= .9927					OVERALL AV. =		13.11± 14.10
					AV. (FIRST VALUE OMITTED) =			13.71± 7.41
RUN 9- 2			MAT WT.= 2.96		.000390M KCl			
.406	.957	4.89	28.69	14.96	200.87	107.20	119.51	6.46
.228	.924	9.21	26.00	10.29	161.31	90.76	93.65	9.02
.140	.876	13.73	25.73	7.43	113.01	68.83	61.67	9.68
.105	.835	16.74	26.65	6.31	82.98	54.31	44.15	9.23
.083	.792	21.66	25.81	5.76	65.96	46.79	35.52	9.40
.068	.746	23.52	24.97	5.57	44.14	34.24	24.84	8.02
.059	.707	25.11	26.94	5.56	32.00	26.89	18.89	7.03
H= 6.40	R= .9994					OVERALL AV. =		8.41± 14.93
					AV. (FIRST VALUE OMITTED) =			8.73± 11.52

TABLE XIVA

INITIAL CALCULATIONS WITH STREAMING CURRENT DATA

Temp., °C.	Resistance, ohms	I_r, μa.	Slope (I/U), μa.sec./cm.	Intercept, μa.	R	Slope (I_s/U), μa.sec./cm.	Intercept, μa.	R	Slope ($\Delta H/U$), cm.sec./cm.	Intercept, cm.	R
RUN 9- 5			MAT WT.= 6.84			.000390M					
24.7	600	.28	14.945	.52	.9784	16.513	.46	.9842	19.81	-.81	.9996
24.6	450	.64	13.126	1.61	.9997	14.771	1.60	.9999	24.18	-.48	.9996
24.4	390	-.50	18.747	.78	.9980	20.932	.77	.9990	32.24	-.30	.9973
24.4	352	.10	20.572	.72	.9996	22.773	.71	.9998	43.95	-.34	.9981
24.3	327	-.15	24.007	.52	.9989	26.220	.51	.9992	63.67	-.62	.9992
24.2	308	-.18	27.119	.35	.9999	29.342	.35	.9999	90.75	-.93	.9977
24.2	308	-.25	29.645	.34	.9998	32.366	.24	.9999	124.16	-1.26	.9983
RUN 9- 6			MAT WT.= 6.43			.000390M					
24.2	560	.15	10.814	.42	.9940	12.387	.36	.9967	15.26	-.46	.9997
24.2	460	.43	10.989	1.16	.9980	12.626	1.16	.9979	21.12	-.56	.9999
24.2	400	.35	12.100	1.22	.9999	13.802	1.25	.9997	27.52	-.67	.9994
24.1	348	.33	15.754	.81	.9985	17.957	.80	.9991	34.54	-.27	.9985
24.1	308	.25	18.726	.71	.9997	20.949	.70	.9998	51.26	-.37	.9984
24.1	290	.30	22.025	.56	.9996	24.759	.46	.9998	74.66	-.74	.9981
24.1	283	.25	24.685	.48	.9999	27.425	.38	.9999	104.49	-1.11	.9989
RUN 9- 7A			MAT WT.= 7.37			.000020M					
24.1	9900	.08	12.414	.20	.9999	11.858	.02	.9999	29.25	-2.00	.9956
24.2	9300	.13	15.698	.29	.9998	15.033	.06	.9998	38.69	-1.68	.9974
24.2	7700	.15	21.675	.01	.9997	20.826	-.25	.9998	44.55	-.87	.9966
24.5	7000	.00	27.806	-.04	.9998	26.601	-.30	.9998	55.95	-.68	.9986
24.5	6100	.00	38.032	.02	.9999	36.879	-.24	.9997	87.20	-1.10	.9968
24.6	5300	-.05	47.460	-.11	.9996	46.306	-.38	.9994	120.09	-1.51	.9955
24.6	5000	-.05	60.256	-.32	.9990	59.102	-.60	.9987	164.89	-1.92	.9959
RUN 9- 7B			MAT WT.= 5.41			.000020M					
24.8	8300	.04	8.461	.25	.9994	8.349	.24	.9994	18.12	-1.12	.9930
25.0	6900	.00	13.501	.08	.9997	13.388	.05	.9998	23.81	-.74	.9986
25.1	5900	.00	18.909	.00	.9999	18.795	-.04	.9999	32.48	-.84	.9998
25.1	4900	.00	25.605	-.08	.9997	25.547	-.14	.9996	40.41	-.41	.9982
25.0	4100	.14	36.085	-.17	.9995	36.426	-.25	.9992	68.40	-1.00	.9951
24.9	3800	-.07	46.049	-.41	.9995	45.822	-.45	.9996	100.15	-1.63	.9970
24.9	3450	-.11	56.597	-.50	.9991	56.368	-.55	.9991	137.07	-2.11	.9945

TABLE XIVB

SECOND STEP CALCULATIONS WITH STREAMING CURRENT DATA

Mat Thick-ness (L),in.	Mat Poros-ity, ε	Slope, (I_s/U)	Kozeny Factor: Exper-imental	Kozeny Factor: Davis Corre-lation	Calculated Zeta Potential, mv.: Capil-lary Model	Bieber +Mason (26)	Assum-ing N Varies	ζ_c (N = Const.)
RUN 9- 5			MAT WT.= 6.84		.000390M KCl			
.291	.862	14.77	13.60	6.96	101.64	63.39	54.81	9.56
.235	.830	20.93	12.99	6.21	97.33	64.33	51.79	11.19
.197	.797	22.77	13.15	5.81	73.45	51.56	39.44	10.16
.166	.759	26.22	13.85	5.60	56.46	42.63	31.31	9.57
.140	.715	29.34	13.85	5.55	40.14	33.19	23.48	8.51
.126	.683	32.36	14.89	5.57	32.65	28.89	19.85	8.00
H= 5.30	R= .9991					OVERALL AV. =		9.50± 12.01
					AV. (FIRST VALUE OMITTED) =			9.49± 13.45
RUN 9- 6			MAT WT.= 6.43		.000390M KCl			
.412	.909	12.38	15.93	9.08	164.11	94.68	93.39	10.82
.311	.879	12.62	15.07	7.54	107.52	65.19	58.91	9.04
.257	.854	13.80	14.87	6.72	84.96	53.81	45.57	8.46
.206	.818	17.95	13.11	6.03	72.51	49.01	38.64	8.95
.165	.772	20.94	13.14	5.65	51.69	38.04	28.30	8.18
.140	.732	24.75	13.81	5.56	40.14	32.03	23.00	7.84
.126	.702	27.42	15.36	5.56	33.13	28.14	19.70	7.46
H= 4.66	R= .9999					OVERALL AV. =		8.68± 12.66
					AV. (FIRST VALUE OMITTED) =			8.32± 7.44
RUN 9- 7			MAT WT.= 7.37		.000020M KCl			
.420	.897	11.85	22.77	8.39	131.09	77.06	74.78	9.74
.343	.874	15.03	22.81	7.35	120.16	73.44	66.71	10.64
.283	.848	20.82	19.75	6.57	119.28	76.35	64.96	12.55
.242	.822	26.60	19.47	6.09	113.15	75.85	61.38	13.87
.197	.781	36.87	21.23	5.70	100.45	72.64	55.61	15.44
.171	.748	46.30	22.33	5.58	89.06	68.73	51.01	16.32
.150	.713	59.10	23.28	5.55	79.75	66.16	47.71	17.40
H= 2.51	R= .9983					OVERALL AV. =		13.71± 21.05
					AV. (FIRST VALUE OMITTED) =			14.37± 17.48
RUN 9- 7			MAT WT.= 5.41		.000020M KCl			
.358	.911	8.34	23.76	9.28	116.52	66.90	67.73	7.59
.276	.885	13.38	22.15	7.80	124.82	74.87	70.07	10.19
.218	.855	18.79	21.54	6.75	117.92	74.54	64.40	11.86
.177	.821	25.54	19.30	6.08	108.21	72.63	58.65	13.30
.144	.780	36.42	22.76	5.69	98.49	71.35	54.52	15.20
.124	.745	45.82	24.92	5.57	85.50	66.40	49.11	15.90
.110	.713	56.36	26.48	5.55	75.97	63.06	45.43	16.58
H= 2.86	R= .9991					OVERALL AV. =		12.95± 25.33
					AV. (FIRST VALUE OMITTED) =			13.84± 18.02

TABLE XVA

INITIAL CALCULATIONS WITH STREAMING CURRENT DATA

Temp., °C.	Resistance, ohms	I_r, μa.	Slope (I/U), μa.sec./cm.	Intercept, μa.	R	Slope (I_s/U), μa.sec./cm.	Intercept, μa.	R	Slope (ΔH/U), cm.sec./cm.	Intercept, cm.	R
RUN 9- 9			MAT WT.= 5.91			.000050M					
24.0	4000	.32	9.251	1.18	.9955	9.479	1.20	.9968	25.61	-1.72	.9976
24.3	2950	.25	16.461	.79	.9997	17.301	.74	.9998	33.40	-.64	.9823
24.4	2550	.15	21.021	.55	.9997	21.860	.52	.9996	39.73	-1.04	.9999
24.6	2250	.07	28.941	.34	.9999	29.864	.30	.9999	50.44	.19	.9830
24.6	1950	.19	38.373	.26	.9999	39.530	.21	.9999	77.03	-.90	.9964
24.6	1850	.25	47.360	.00	.9998	47.945	.00	.9999	101.59	-1.00	.9976
24.7	1780	.08	56.160	.13	.9999	57.313	.06	.9999	145.50	-1.73	.9962
RUN 9- 10			MAT WT.= 4.01			.000081M					
24.5	1700	.45	8.733	.91	.9999	9.522	1.06	.9998	13.04	-.53	.9998
25.3	1400	.43	10.722	1.09	.9980	11.679	1.27	.9976	14.14	-.10	.9990
25.0	1170	.39	16.098	.78	.9994	17.058	.97	.9992	20.55	-.37	.9999
24.9	1010	.38	22.370	.46	.9999	23.541	.62	.9999	27.39	-.23	.9979
24.2	890	.34	30.551	.32	.9999	31.726	.48	.9999	45.96	-.43	.9991
24.1	835	.31	38.250	.20	.9999	39.556	.27	.9999	67.36	-.77	.9984
24.0	800	.23	45.357	.09	.9997	47.427	.08	.9999	95.16	-1.05	.9982
RUN 9- 12			MAT WT.= 7.00			.000115M					
24.6	1670	.75	11.867	1.48	.9969	12.652	1.81	.9963	20.57	-.60	.9995
24.5	1460	.72	18.552	.76	.9992	19.361	1.18	.9997	23.70	-.12	.9997
24.5	1320	.68	24.104	.52	.9999	24.972	.97	.9998	31.57	-.26	.9990
24.6	1200	.63	30.909	.37	.9998	31.779	.88	.9997	43.67	-.47	.9983
24.7	1100	.65	39.729	.42	.9998	41.192	.83	.9999	63.91	-.60	.9969
24.8	1010	.50	48.026	.46	.9999	49.610	.85	.9998	91.74	-.83	.9985
24.9	970	.48	58.041	.17	.9999	59.509	.58	.9998	123.36	-1.03	.9994
RUN 9- 16A			MAT WT.= 5.36			.000072M					
24.5	2200	.56	10.266	1.30	.9988	10.823	1.48	.9982	16.40	-.76	.9993
24.4	1790	.58	14.168	1.29	.9982	14.667	1.54	.9972	23.63	-1.00	.9995
24.6	1560	.50	21.667	.58	.9995	22.184	.90	.9998	25.98	-.23	.9993
24.6	1390	.46	27.640	.41	.9997	28.159	.73	.9999	35.40	-.34	.9990
24.6	1250	.43	35.561	.43	.9999	35.844	.75	.9999	52.24	-.37	.9986
24.7	1110	.40	43.521	.32	.9999	43.804	.64	.9997	78.47	-.77	.9973
24.5	1090	.53	51.447	.21	.9999	52.439	.50	.9999	109.88	-1.08	.9980

TABLE XVB

SECOND STEP CALCULATIONS WITH STREAMING CURRENT DATA

Mat Thickness (L), in.	Mat Porosity, ϵ	Slope, (I_s/U)	Kozeny Factor: Experimental	Kozeny Factor: Davis Correlation	Calculated Zeta Potential, mv.: Capillary Model	Calculated Zeta Potential, mv.: Bieber +Mason (26)	Calculated Zeta Potential, mv.: Assuming N Varies	Calculated Zeta Potential, mv.: ζ_c (N = Const.)
RUN 9- 9		MAT WT.= 5.91			.000050M KCl			
.393	.912	9.47	30.39	9.32	132.73	76.16	76.51	8.54
.264	.869	17.30	23.20	7.17	129.18	79.67	70.67	11.74
.224	.846	21.86	21.63	6.52	122.38	78.61	65.93	12.91
.182	.810	29.86	19.71	5.94	111.39	76.30	59.99	14.46
.151	.771	39.53	21.55	5.65	96.77	71.36	53.51	15.54
.130	.734	47.94	21.12	5.56	80.11	63.57	46.17	15.58
.115	.700	57.31	23.21	5.56	68.07	58.07	40.96	15.62
H= 3.62	R= .9991					OVERALL AV.	= 13.48±	19.61
				AV.	(FIRST VALUE OMITTED)	= 14.31±		11.45
RUN 9- 10		MAT WT.= 4.01			.000081M KCl			
.272	.914	9.52	23.65	9.44	137.75	78.81	79.35	8.68
.221	.894	11.67	19.86	8.21	123.28	72.89	69.11	9.30
.174	.865	17.05	20.48	7.04	121.67	75.54	66.13	11.31
.140	.832	23.54	19.53	6.26	113.22	74.46	60.60	12.88
.109	.785	31.72	21.06	5.72	89.70	64.43	48.86	13.34
.092	.745	39.55	22.26	5.57	73.69	57.20	41.77	13.51
.081	.711	47.42	23.96	5.55	62.45	52.05	36.94	13.57
H= 3.65	R= .9996					OVERALL AV.	= 11.80±	17.57
				AV.	(FIRST VALUE OMITTED)	= 12.32±		13.79
RUN 9- 12		MAT WT.= 7.00			.000115M KCl			
.345	.881	12.65	13.97	7.63	111.33	67.23	61.35	9.24
.284	.856	19.36	12.11	6.77	122.57	77.34	66.05	12.08
.239	.829	24.97	12.33	6.20	114.77	76.00	61.31	13.33
.202	.797	31.77	12.87	5.81	103.05	72.28	55.54	14.28
.167	.755	41.19	13.25	5.59	85.13	64.80	47.62	14.82
.145	.718	49.61	14.23	5.55	70.40	57.79	41.19	14.76
.130	.686	59.50	14.97	5.57	61.73	54.31	37.58	15.02
H= 3.43	R= .9985					OVERALL AV.	= 13.36±	15.66
				AV.	(FIRST VALUE OMITTED)	= 14.05±		8.10
RUN 9- 16A		MAT WT.= 5.36			.000072M KCl			
.312	.899	10.82	18.22	8.51	123.91	72.58	70.03	8.93
.248	.873	14.66	19.08	7.33	116.22	71.12	63.69	10.21
.197	.841	22.18	14.93	6.42	117.44	76.09	63.01	12.72
.164	.809	28.15	15.08	5.92	103.61	71.14	55.68	13.51
.134	.766	35.84	15.46	5.62	83.21	61.97	46.13	13.69
.117	.732	43.80	17.74	5.56	71.73	57.16	41.33	14.05
.102	.693	52.43	18.28	5.56	58.32	50.48	35.28	13.76
H= 3.55	R= .9992					OVERALL AV.	= 12.41±	16.24
				AV.	(FIRST VALUE OMITTED)	= 12.99±		11.02

TABLE XVIA

INITIAL CALCULATIONS WITH STREAMING CURRENT DATA

Temp., °C.	Resistance, ohms	I_r, μa.	Slope (I/U), μa.sec./cm.	Intercept, μa.	R	Slope (I_s/U), μa.sec./cm.	Intercept, μa.	R	Slope ($\Delta H/U$), cm.sec./cm.	Intercept, cm.	R
RUN 9- 16			MAT WT.= 6.75			.000130M					
24.4	1540	.51	9.868	.51	.9993	10.709	1.17	.9987	16.12	-.52	.9996
24.4	1300	.55	13.127	.44	.9997	14.081	1.28	.9992	19.16	-.28	.9999
24.6	1120	.67	19.506	.10	.9998	21.142	.98	.9999	24.83	-.11	.9983
24.7	980	.66	24.491	.11	.9999	26.722	1.03	.9999	32.83	-.13	.9991
24.5	860	.68	32.053	.22	.9999	34.583	1.12	.9999	50.52	-.26	.9982
24.2	810	.75	40.056	.25	.9999	42.773	1.13	.9999	70.51	-.33	.9989
24.2	790	.68	50.122	-.00	.9998	52.134	.92	.9996	95.36	-.58	.9993
RUN 9- 22			MAT WT.= 5.95			.000145M					
24.6	1200	.87	8.442	-.12	.9996	7.484	.46	.9999	17.78	-.81	.9999
24.7	1030	.59	11.937	-.30	.9994	10.860	.35	.9997	22.20	-.66	.9998
24.6	880	.53	15.877	-.34	.9999	14.738	.35	.9999	29.75	-.83	.9992
24.5	790	.48	20.216	-.44	.9997	19.014	.28	.9997	43.24	-1.43	.9999
24.4	710	.53	26.680	-.57	.9999	24.126	.40	.9997	53.11	-.40	.9995
24.3	670	.56	32.416	-.61	.9999	29.857	.37	.9993	78.20	-.76	.9980
24.1	650	.71	38.147	-.64	.9999	35.879	.31	.9993	113.30	-1.15	.9977
RUN 9- 23			MAT WT.= 5.70			.000145M					
26.0	1200	.91	8.094	.26	.9981	8.036	.66	.9979	16.71	-.84	.9965
25.8	1000	.70	11.207	.11	.9995	11.207	.55	.9995	19.47	-.57	.9990
25.0	880	.75	15.283	.10	.9983	15.457	.55	.9986	27.33	-.81	.9999
24.4	780	.85	20.400	.00	.9999	19.984	.59	.9996	33.06	-.22	.9992
24.2	700	.91	27.387	-.03	.9994	26.616	.59	.9993	51.95	-.46	.9985
24.2	670	.87	33.783	-.11	.9999	33.420	.45	.9998	76.38	-.94	.9984
24.1	650	.56	40.335	-.31	.9996	39.737	.32	.9994	112.76	-1.72	.9988
RUN 9- 24			MAT WT.= 5.71			.000019M					
23.3	9000	.16	10.357	.07	.9999	10.466	.11	.9998	16.98	-.87	.9974
23.6	7100	.14	16.052	.00	.9999	16.161	.06	.9999	24.76	-1.09	.9986
23.9	6300	.10	21.104	-.06	.9997	20.987	.05	.9995	26.81	-.28	.9963
24.5	5500	.18	29.330	-.09	.9999	29.213	.03	.9999	34.83	-.27	.9989
24.5	4750	.10	39.800	-.13	.9999	39.568	.00	.9998	51.09	-.49	.9982
24.5	4300	.14	52.741	-.44	.9997	52.452	-.28	.9996	76.74	-1.16	.9958
24.1	4000	.40	64.048	-.48	.9981	63.758	-.33	.9979	106.96	-1.44	.9952

TABLE XVIB

SECOND STEP CALCULATIONS WITH STREAMING CURRENT DATA

Mat Thickness (L), in.	Mat Porosity, ϵ	Slope, (I_s/U)	Kozeny Factor: Experimental	Kozeny Factor: Davis Correlation	Calculated Zeta Potential, mv.: Capillary Model	Calculated Zeta Potential, mv.: Bieber +Mason (26)	Calculated Zeta Potential, mv.: Assuming N Varies	Calculated Zeta Potential, mv.: ζ_c (N = Const.)	
RUN 9- 16B		MAT WT.= 6.75			.000130 M KCl				
.398	.901	10.70	14.43	8.59	125.01	73.07	70.56	8.88	
.322	.877	14.08	12.83	7.47	117.35	71.35	64.36	10.01	
.257	.846	21.14	11.97	6.54	119.47	76.65	64.03	12.48	
.213	.815	26.72	11.73	5.99	104.92	71.27	56.11	13.20	
.171	.769	34.58	12.15	5.64	82.88	61.35	45.65	13.38	
.147	.732	42.77	12.46	5.56	69.42	55.40	39.90	13.60	
.131	.699	52.13	13.09	5.56	61.29	52.37	36.69	14.03	
H= 3.15	R= .9971					OVERALL AV. =		12.22±	16.20
				AV.	(FIRST VALUE OMITTED) =			12.78±	11.34
RUN 9- 22		MAT WT.= 5.95			.000145 M KCl				
.336	.896	7.48	17.12	8.34	81.77	48.15	45.86	6.02	
.275	.873	10.86	16.23	7.32	86.03	52.65	46.97	7.54	
.221	.843	14.73	15.66	6.45	79.57	51.40	42.56	8.50	
.184	.811	19.01	16.86	5.95	71.51	48.91	38.26	9.18	
.152	.771	24.12	14.68	5.64	58.97	43.49	32.41	9.41	
.130	.733	29.85	15.82	5.56	48.91	38.96	28.07	9.53	
.115	.698	35.87	17.44	5.56	41.66	35.69	24.96	9.58	
H= 3.47	R= .9994					OVERALL AV. =		8.54±	15.54
				AV.	(FIRST VALUE OMITTED) =			8.96±	8.92
RUN 9- 23		MAT WT.= 5.70			.000145 M KCl				
.330	.899	8.03	17.93	8.48	91.94	53.90	51.71	6.63	
.275	.879	11.20	16.19	7.52	95.83	58.13	52.58	8.09	
.220	.848	15.45	16.08	6.59	89.72	57.35	48.08	9.24	
.177	.812	19.98	13.52	5.96	75.77	51.75	40.51	9.68	
.141	.764	26.61	14.04	5.62	60.08	44.95	33.24	9.97	
.122	.727	33.42	15.41	5.55	51.75	41.69	29.88	10.36	
.108	.692	39.73	17.31	5.57	43.54	37.80	26.27	10.29	
H= 3.25	R= .9991					OVERALL AV. =		9.18±	14.89
				AV.	(FIRST VALUE OMITTED) =			9.61±	8.84
RUN 9- 24		MAT WT.= 5.71			.000019 M KCl				
.342	.902	10.46	17.92	8.68	124.47	72.57	71.55	8.86	
.260	.871	16.16	18.02	7.26	124.17	76.25	68.82	11.22	
.218	.847	20.98	15.11	6.55	118.76	76.14	64.71	12.58	
.177	.811	29.21	14.21	5.95	110.42	75.47	60.10	14.39	
.149	.776	39.56	15.35	5.67	101.83	74.40	56.69	16.13	
.127	.737	52.45	16.86	5.56	90.23	71.18	52.41	17.49	
.111	.700	63.75	17.39	5.56	75.28	64.26	45.85	17.51	
H= 2.91	R= .9942					OVERALL AV. =		14.02±	23.51
				AV.	(FIRST VALUE OMITTED) =			14.88±	17.56

TABLE XVIIA

INITIAL CALCULATIONS WITH STREAMING CURRENT DATA

Temp., °C.	Resistance, ohms	I_r, μa.	Slope (I/U), μa.sec./cm.	Intercept, μa.	R	Slope (I_s/U), μa.sec./cm.	Intercept, μa.	R	Slope ($\Delta H/U$), cm.sec./cm.	Intercept, cm.	R
RUN 9- 25			MAT WT.= 5.15			.000051M					
23.3	3650	.10	7.554	.06	.9998	8.117	.19	.9996	11.14	-.29	.9965
23.9	2900	.22	11.750	-.03	.9990	12.200	.20	.9993	15.56	-.48	.9999
23.6	2300	.35	19.595	-.23	.9999	19.931	.14	.9999	23.61	-.82	.9999
23.8	1950	.31	26.897	-.25	.9994	27.536	.11	.9996	29.11	-.25	.9980
25.1	1700	.34	39.653	-.43	.9999	40.006	.01	.9999	45.42	-.41	.9999
25.2	1550	.39	51.357	-.46	.9993	52.171	-.02	.9994	63.07	-.57	.9978
25.0	1490	.47	61.933	-.41	.9999	62.754	.04	.9999	84.24	-.62	.9996
RUN 9- 26A			MAT WT.= 5.49			.000079M					
24.0	2200	.32	10.615	.09	.9999	11.232	.31	.9998	16.90	-.67	.9968
24.2	1750	.42	15.929	-.00	.9994	16.602	.32	.9992	31.09	-.87	.9999
24.0	1470	.44	22.956	-.13	.9999	23.417	.32	.9999	41.10	-.45	.9984
23.8	1320	.45	28.864	-.15	.9994	29.384	.34	.9991	54.79	-.56	.9979
24.5	1160	.44	40.260	-.33	.9996	41.131	.17	.9994	85.36	-1.08	.9991
24.8	1080	.44	51.848	-.43	.9999	52.545	.11	.9998	114.79	-1.28	.9994
24.8	1030	.50	62.899	-.47	.9998	63.479	.09	.9997	154.41	-1.78	.9981
RUN 9- 26B			MAT WT.= 5.53			.000115M					
23.3	1540	.42	10.681	-.22	.9994	10.736	.31	.9995	14.17	-.41	.9997
24.1	1280	.51	16.233	-.44	.9991	16.289	.24	.9990	19.17	-.50	.9999
24.0	1080	.56	21.211	-.30	.9994	21.620	.43	.9994	23.85	-.23	.9961
24.1	960	.65	28.895	-.31	.9997	29.306	.49	.9998	33.40	-.25	.9991
24.7	850	.68	37.940	-.33	.9999	38.236	.53	.9999	49.09	-.46	.9979
24.9	793	.65	48.901	-.57	.9996	49.607	.29	.9995	66.50	-.60	.9982
24.9	770	.65	58.338	-.60	.9999	58.933	.32	.9999	89.93	-.74	.9990
RUN 9- 30			MAT WT.= 5.49			.000048M					
24.3	3250	.99	7.557	.19	.9999	8.390	.33	.9997	19.58	-1.06	.9989
24.2	2700	.28	13.505	-.20	.9988	14.132	.05	.9999	25.10	-.32	.9954
23.7	2300	.06	18.552	-.20	.9994	19.470	.05	.9999	35.34	-.33	.9989
24.0	2000	.20	24.295	-.09	.9999	25.506	.15	.9997	48.23	-.33	.9977
23.8	1800	.27	33.537	-.23	.9999	35.212	-.00	.9997	75.62	-.85	.9971
23.8	1650	.18	42.691	-.25	.9999	44.369	-.01	.9999	109.30	-1.07	.9978
24.1	1650	.45	50.108	-.15	.9999	51.783	.07	.9997	158.60	-1.88	.9954

TABLE XVIIB

SECOND STEP CALCULATIONS WITH STREAMING CURRENT DATA

Mat Thick-ness (L),in.	Mat Poros-ity, ε	Slope, (I_s/U)	Kozeny Factor: Exper-imental	Kozeny Factor: Davis Correlation	Calculated Zeta Potential, mv.: Capil-lary Model	Bieber +Mason (26)	Assuming N Varies	ζ_c (N = Const.
RUN 9- 25			MAT WT.= 5.15		.000051M KCl			
.371	.919	8.11	16.55	9.83	127.78	72.51	74.34	7.66
.296	.898	12.20	17.46	8.44	136.53	80.15	77.21	9.97
.213	.859	19.93	16.55	6.85	129.92	81.59	70.48	12.65
.170	.823	27.53	14.40	6.10	117.95	78.94	63.33	14.24
.134	.775	40.00	15.25	5.66	102.57	75.03	56.50	16.12
.112	.731	52.17	14.89	5.56	84.80	67.71	49.05	16.74
.097	.690	62.75	14.40	5.57	67.89	59.17	41.34	16.29
H= 3.53	R= .9989					OVERALL AV.	=	13.38± 26.04
					AV. (FIRST VALUE OMITTED)		=	14.33± 18.37
RUN 9- 26A			MAT WT.= 5.49		.000079M KCl			
.332	.903	11.23	19.07	8.74	136.06	79.20	77.25	9.48
.259	.876	16.60	25.09	7.42	135.72	82.70	74.52	11.72
.200	.839	23.41	22.45	6.39	121.56	78.95	65.16	13.27
.166	.807	29.38	21.94	5.90	105.00	72.40	56.45	13.86
.135	.762	41.13	23.84	5.61	91.62	68.75	50.96	15.38
.116	.724	52.54	23.71	5.55	78.78	63.93	45.87	16.11
.101	.683	63.47	23.31	5.57	64.00	56.68	39.18	15.81
H= 3.25	R= .9981					OVERALL AV.	=	13.66± 17.67
					AV. (FIRST VALUE OMITTED)		=	14.36± 11.90
RUN 9- 26B			MAT WT.= 5.53		.000115M KCl			
.333	.903	10.73	15.55	8.71	128.74	74.99	72.91	8.98
.259	.875	16.28	15.16	7.38	131.50	80.26	71.99	11.41
.208	.844	21.62	13.59	6.50	119.10	76.67	63.82	12.59
.166	.805	29.30	13.20	5.88	103.27	71.39	55.44	13.71
.138	.766	38.23	14.06	5.62	88.42	65.90	48.90	14.54
.118	.726	49.60	13.95	5.55	76.45	61.69	44.27	15.40
.105	.692	58.93	14.55	5.56	65.24	56.56	39.40	15.40
H= 3.01	R= .9984					OVERALL AV.	=	13.15± 17.85
					AV. (FIRST VALUE OMITTED)		=	13.84± 11.57
RUN 9- 30			MAT WT.= 5.49		.000048M KCl			
.343	.906	8.39	23.22	8.93	107.01	61.97	61.22	7.27
.267	.880	14.13	21.15	7.56	121.44	73.54	67.16	10.25
.209	.846	19.47	20.53	6.54	109.49	70.25	59.03	11.51
.170	.811	25.50	20.21	5.95	95.95	65.60	51.67	12.38
.137	.766	35.21	21.39	5.62	81.05	60.40	45.08	13.41
.117	.726	44.36	22.49	5.55	67.76	54.72	39.48	13.75
.102	.686	51.78	24.14	5.57	53.56	47.11	32.79	13.10
H= 3.75	R= .9981					OVERALL AV.	=	11.67± 19.57
					AV. (FIRST VALUE OMITTED)		=	12.40± 10.66

TABLE XVIIIA

INITIAL CALCULATIONS WITH STREAMING CURRENT DATA

Temp., °C.	Resistance, ohms	I_r, μa.	Slope (I/U), μa.sec./cm.	Intercept, μa.	R	Slope (I_s/U), μa.sec./cm.	Intercept, μa.	R	Slope ($\Delta H/U$), cm.sec./cm.	Intercept, cm.	R
RUN 10- 1			MAT WT.= 6.16			.000116M					
24.6	1740	.12	8.491	.64	.9797	8.662	.49	.9840	12.28	-.05	.9998
25.0	1390	.15	13.038	.57	.9991	13.673	.27	.9998	9.93	.41	.9598
24.6	1200	.35	17.812	.58	.9973	18.739	.20	.9989	22.26	-.14	.9989
24.6	1040	.06	23.704	.58	.9999	24.866	.12	.9999	32.92	-.36	.9968
24.6	970	.02	30.374	.52	.9997	31.656	.02	.9999	48.52	-.57	.9983
24.5	920	.04	36.759	.56	.9996	38.158	.03	.9999	70.05	-.54	.9987
24.6	890	-.10	42.542	.54	.9999	44.060	-.01	.9999	95.33	-.70	.9981
RUN 10- 2A			MAT WT.= 6.31			.000060M					
24.1	3350	.06	9.104	.98	.9984	11.004	.63	.9989	12.11	.03	.9999
24.6	3000	.25	14.297	.99	.9993	16.947	.57	.9996	18.09	-.10	.9986
24.8	2100	.18	20.310	.88	.9990	23.489	.40	.9993	23.69	-.19	.9993
24.7	1920	.17	27.337	.83	.9994	30.923	.31	.9997	35.09	-.43	.9970
24.4	1720	.18	38.088	.63	.9999	42.027	.08	.9999	51.66	-.61	.9983
24.4	1620	.05	45.193	.71	.9999	49.195	.15	.9999	69.64	-.65	.9979
24.3	1590	.13	55.849	.52	.9998	59.911	-.04	.9999	104.47	-1.27	.9983
RUN 10- 2B			MAT WT.= 6.80			.000115M					
24.2	1960	.05	11.006	.50	.9686	11.985	.27	.9673	12.56	-.01	.9998
24.6	1550	.20	15.918	.79	.9994	18.000	.45	.9999	19.00	-.17	.9961
24.6	1310	.20	19.992	.85	.9984	22.660	.45	.9997	23.97	-.17	.9983
24.6	1160	.15	25.402	.94	.9997	28.601	.48	.9999	32.24	-.15	.9973
24.5	1070	.08	35.690	.57	.9994	39.245	.07	.9999	48.55	-.39	.9997
24.4	1010	.00	42.247	.58	.9991	46.216	.05	.9998	67.65	-.53	.9985
24.2	980	-.15	50.926	.54	.9999	55.246	-.02	.9998	97.05	-.78	.9985
RUN 10- 3			MAT WT.= 6.45			.000220M					
25.3	935	-.08	13.311	.34	.9995	13.015	.21	.9990	12.96	-.01	.9987
25.3	740	.10	19.793	.59	.9999	19.614	.38	.9999	21.11	-.17	.9968
25.1	655	.25	23.908	.64	.9999	23.728	.39	.9999	29.10	-.31	.9973
24.8	590	.15	28.350	.60	.9999	28.170	.32	.9999	40.81	-.42	.9976
24.6	550	-.02	33.696	.44	.9999	33.515	.14	.9999	60.11	-.55	.9982
24.7	525	-.17	39.141	.24	.9998	39.198	-.08	.9998	85.89	-.94	.9974
24.8	510	-.30	44.815	.15	.9995	44.932	-.19	.9993	116.18	-.79	.9986
RUN 10- 4A			MAT WT.= 6.13			.000420M					
23.9	450	-.20	10.186	.05	.9991	10.186	-.07	.9991	15.41	-.07	.9987
23.9	400	-.07	12.565	.12	.9999	12.565	-.03	.9999	21.41	-.14	.9992
24.0	370	.00	13.966	.22	.9999	13.966	.05	.9999	28.08	-.22	.9981
24.0	330	.01	16.594	.16	.9999	16.594	-.01	.9999	41.41	-.39	.9997
24.0	297	-.11	19.321	.05	.9997	19.321	-.15	.9997	63.36	-.56	.9983
24.0	290	-.25	20.535	-.08	.9995	20.535	-.29	.9995	91.02	-.93	.9971
24.0	285	-.45	22.803	-.19	.9997	22.803	-.41	.9997	115.66	-.62	.9996

TABLE XVIIIB

SECOND STEP CALCULATIONS WITH STREAMING CURRENT DATA

Mat Thickness (L), in.	Mat Porosity, ϵ	Slope, (I_s/U)	Kozeny Factor: Experimental	Kozeny Factor: Davis Correlation	Calculated Zeta Potential, mv.: Capillary Model	Bieber +Mason (26)	Assuming N Varies	ζ_c (N = Const.)	
RUN 10- 1		MAT WT.= 6.16			.000116 M KCl				
.299	.879	13.67	7.56	7.55	117.60	71.24	64.68	9.89	
.240	.850	18.73	12.18	6.62	110.41	70.40	59.30	11.30	
.192	.812	24.86	12.59	5.96	95.12	64.89	50.92	12.13	
.158	.772	31.65	13.11	5.65	78.22	57.58	42.99	12.44	
.135	.733	38.15	13.83	5.56	63.09	50.17	36.21	12.26	
.121	.703	44.06	14.87	5.56	53.74	45.57	32.05	12.11	
H= 3.98	R= .9994					OVERALL AV. =		11.69±	8.25
					AV. (FIRST VALUE OMITTED) =			12.05±	3.65
RUN 10- 2A		MAT WT.= 6.31			.000060 M KCl				
.388	.905	11.00	12.18	8.83	136.82	79.44	77.99	9.41	
.299	.876	16.94	12.89	7.44	139.83	85.13	76.95	12.05	
.241	.847	23.48	12.33	6.55	133.63	85.66	71.94	13.98	
.196	.812	30.92	13.06	5.96	117.50	80.25	63.16	15.09	
.158	.767	42.02	12.97	5.63	97.85	72.81	54.29	16.09	
.137	.731	49.19	13.14	5.56	79.28	63.36	45.82	15.66	
.121	.695	59.91	14.96	5.56	68.06	58.61	41.12	15.91	
H= 3.72	R= .9945					OVERALL AV. =		14.03±	17.65
					AV. (FIRST VALUE OMITTED) =			14.80±	10.45
RUN 10- 2B		MAT WT.= 6.80			.000115 M KCl				
.314	.873	18.00	12.11	7.32	142.30	87.12	77.77	12.50	
.253	.843	22.66	11.07	6.46	122.72	79.24	65.72	13.11	
.205	.806	28.60	10.55	5.89	101.98	70.38	54.73	13.47	
.168	.763	39.24	11.04	5.62	88.44	66.22	49.04	14.73	
.146	.728	46.21	11.57	5.55	72.25	58.11	41.75	14.43	
.129	.692	55.24	12.55	5.56	60.79	52.72	36.72	14.37	
H= 3.82	R= .9980					OVERALL AV. =		13.77±	6.37
					AV. (FIRST VALUE OMITTED) =			14.02±	4.94
RUN 10- 3		MAT WT.= 6.45			.000220 M KCl				
.382	.901	13.01	12.46	8.61	153.68	89.76	86.60	10.85	
.277	.864	19.61	12.97	7.00	137.66	85.67	74.39	12.86	
.230	.836	23.72	13.40	6.32	118.96	77.74	63.41	13.20	
.190	.802	28.17	13.59	5.85	95.65	66.58	51.29	12.92	
.160	.764	33.51	14.56	5.62	76.33	57.04	42.15	12.61	
.141	.733	39.19	16.19	5.56	64.44	51.31	36.90	12.53	
.123	.694	44.93	16.25	5.56	50.35	43.52	30.26	11.78	
H= 4.30	R= .9993					OVERALL AV. =		12.39±	6.55
					AV. (FIRST VALUE OMITTED) =			12.65±	3.86
RUN 10- 4A		MAT WT.= 6.13			.000420 M KCl				
.332	.892	10.18	13.40	8.11	103.86	61.60	57.70	7.91	
.278	.871	12.56	14.52	7.24	96.04	59.03	52.12	8.53	
.237	.849	13.96	15.06	6.59	80.90	51.69	43.22	8.29	
.194	.815	16.59	16.12	6.00	65.31	44.32	34.77	8.15	
.157	.772	19.32	16.94	5.65	47.42	34.93	25.94	7.52	
.138	.741	20.53	18.89	5.56	36.38	28.52	20.59	6.79	
.125	.714	22.80	19.45	5.55	30.84	25.55	18.05	6.57	
H= 5.50	R= .9948					OVERALL AV. =		7.68±	9.84
					AV. (FIRST VALUE OMITTED) =			7.64±	10.74

TABLE XIXA

INITIAL CALCULATIONS WITH STREAMING CURRENT DATA

Temp., °C.	Resistance, ohms	I_r, μa.	Slope (I/U), μa.sec./cm.	Intercept, μa.	R	Slope (I_s/U), μa.sec./cm.	Intercept μa.	R	Slope $(\Delta H/U)$, cm.sec./cm.	Intercept, cm.	R
RUN 10- 4B			MAT WT.= 6.74			.000048M					
23.6	4500	.18	9.889	.80	.9993	11.326	.64	.9992	11.99	-.00	.9990
24.6	3400	.20	17.916	.59	.9988	19.818	.44	.9987	21.18	-.25	.9989
24.8	2800	.15	26.351	.58	.9999	28.778	.45	.9998	29.11	-.25	.9980
24.9	2500	.07	36.819	.35	.9999	39.939	.20	.9999	42.54	-.49	.9990
24.9	2200	-.02	47.496	.27	.9999	50.509	.16	.9999	64.77	-.82	.9971
24.6	2100	-.04	60.914	-.03	.9995	64.452	-.15	.9998	98.68	-1.64	.9946
24.3	2000	-.08	72.051	-.01	.9994	75.591	-.13	.9997	126.18	-1.15	.9987
RUN 10- 5			MAT WT.= 6.34			.000420M					
23.8	590	-.22	7.011	-.04	.9897	7.432	-.17	.9945	9.99	.05	.9999
24.2	430	-.05	11.059	.13	.9994	11.543	-.04	.9996	17.40	-.06	.9965
24.6	360	-.07	14.905	.17	.9997	15.455	-.02	.9997	25.92	-.21	.9994
24.4	320	-.08	17.559	.26	.9999	18.111	.03	.9999	36.27	-.28	.9997
24.1	290	-.18	20.364	.22	.9998	20.980	-.02	.9999	53.66	-.33	.9985
24.0	290	-.35	25.195	-.05	.9999	25.748	-.29	.9997	80.53	-.73	.9995
24.4	280	-.55	30.737	-.38	.9997	31.353	-.64	.9993	118.41	-1.34	.9968
RUN 10- 10A			MAT WT.= 6.48			.000104M					
23.2	1750	.10	14.976	1.42	.9954	15.378	.96	.9970	14.54	-.05	.9954
23.9	1350	.35	21.491	1.49	.9990	21.546	.95	.9994	22.99	-.20	.9969
24.0	1180	.40	24.868	1.54	.9997	24.689	.97	.9998	30.24	-.18	.9966
24.0	1060	.15	30.197	1.19	.9994	29.900	.59	.9997	42.51	-.40	.9972
24.0	970	.17	37.481	.94	.9991	37.529	.28	.9996	65.05	-.79	.9970
24.4	930	-.02	43.255	.79	.9999	42.838	.14	.9999	92.47	-1.73	.9999
24.9	900	-.15	52.725	.33	.9998	52.377	-.29	.9999	125.31	-1.49	.9985
RUN 10- 10B			MAT WT.= 6.72			.000370M					
24.0	480	-.28	10.393	.28	.9992	12.020	-.12	.9998	15.98	-.03	.9983
24.2	412	-.13	13.990	.38	.9990	15.569	-.02	.9996	23.68	-.17	.9978
24.3	370	-.04	14.596	.62	.9976	16.184	.20	.9976	30.02	-.18	.9984
24.3	340	-.10	17.605	.57	.9999	19.140	.14	.9999	41.28	-.22	.9989
24.3	320	-.14	20.507	.40	.9997	22.049	-.01	.9998	58.51	-.25	.9982
24.3	308	-.40	24.444	.13	.9986	25.929	-.28	.9990	83.62	-.56	.9978
24.4	300	-.50	26.669	.08	.9996	28.156	-.34	.9997	114.15	-.85	.9976

TABLE XIXB

SECOND STEP CALCULATIONS WITH STREAMING CURRENT DATA

Mat Thickness (L), in.	Mat Porosity, ε	Slope, (I_s/U)	Kozeny Factor: Experimental	Kozeny Factor: Davis Correlation	Calculated Zeta Potential, mv.: Capillary Model	Bieber +Mason (26)	Assuming N Varies	ζ_c (N = Const.)	
RUN 10- 4B			MAT WT.= 6.74		.000048M KCl				
.473	.916	11.32	13.25	9.66	171.68	97.77	99.64	10.54	
.339	.884	19.81	15.37	7.73	180.22	108.40	100.12	14.77	
.258	.847	28.77	14.23	6.56	164.39	105.31	88.65	17.19	
.206	.809	39.93	14.48	5.92	146.85	100.86	79.15	19.22	
.170	.768	50.50	15.60	5.63	120.02	89.01	66.58	19.59	
.145	.728	64.45	17.17	5.55	101.41	81.47	58.90	20.32	
.128	.692	75.59	16.54	5.56	83.48	72.35	50.70	19.82	
H= 3.49	R= .9983					OVERALL AV.	=	17.35±	20.58
					AV. (FIRST VALUE OMITTED)		=	18.49±	11.44
RUN 10- 5			MAT WT.= 6.34		.000420M KCl				
.465	.920	7.43	12.46	9.95	120.49	68.21	69.58	7.04	
.308	.879	11.54	12.67	7.56	99.01	59.97	54.20	8.28	
.241	.846	15.45	13.27	6.53	87.07	55.89	46.46	9.07	
.195	.810	18.11	13.12	5.94	67.31	46.13	35.89	8.66	
.161	.770	20.98	13.68	5.64	50.47	37.32	27.66	8.08	
.139	.734	25.74	15.30	5.56	42.51	33.79	24.27	8.21	
.123	.699	31.35	17.37	5.56	36.86	31.50	21.96	8.40	
H= 3.25	R= .9985					OVERALL AV.	=	8.25±	7.59
					AV. (FIRST VALUE OMITTED)		=	8.45±	4.26
RUN 10- 10A			MAT WT.= 6.48		.000104M KCl				
.379	.900	15.37	13.07	8.54	176.20	103.13	99.45	12.62	
.278	.864	21.54	13.61	7.00	149.88	93.30	81.25	14.06	
.229	.835	24.68	13.33	6.30	120.99	79.28	64.69	13.59	
.194	.805	29.90	14.24	5.88	104.71	72.45	56.26	13.95	
.161	.765	37.52	15.53	5.62	85.55	63.88	47.39	14.16	
.141	.732	42.83	17.07	5.56	69.44	55.43	39.97	13.63	
.125	.697	52.37	17.95	5.56	60.72	52.09	36.47	14.03	
H= 3.69	R= .9892					OVERALL AV.	=	13.72±	3.86
					AV. (FIRST VALUE OMITTED)		=	13.90±	1.69
RUN 10- 10B			MAT WT.= 6.72		.000370M KCl				
.330	.881	12.02	11.10	7.61	104.82	63.35	57.49	8.69	
.271	.855	15.56	12.41	6.75	97.37	61.53	52.21	9.61	
.231	.830	16.18	12.29	6.21	75.29	49.75	40.04	8.64	
.196	.800	19.14	12.83	5.83	63.44	44.32	33.99	8.65	
.166	.763	22.04	13.41	5.61	49.62	37.15	27.38	8.23	
.145	.729	25.92	14.59	5.56	41.06	32.93	23.58	8.11	
.130	.698	28.15	15.70	5.56	32.83	28.11	19.59	7.51	
H= 4.61	R= .9980					OVERALL AV.	=	8.49±	7.60
					AV. (FIRST VALUE OMITTED)		=	8.46±	8.28

TABLE XXA

INITIAL CALCULATIONS WITH STREAMING CURRENT DATA

Temp., °C.	Resistance, ohms	I_r, μa.	Slope (I/U), μa.sec./cm.	Intercept, μa.	R	Slope (I_s/U), μa.sec./cm.	Intercept, μa.	R	Slope ($\Delta H/U$), cm.sec./cm.	Intercept, cm.	R
RUN 10- 12A			MAT WT.= 6.20			.000051M					
24.6	1850	.17	13.670	.97	.9999	13.964	.67	.9995	13.53	.00	.9988
25.2	1430	.30	19.497	1.24	.9981	19.788	.89	.9981	19.40	-.04	.9972
25.0	1250	.38	21.233	1.34	.9987	21.523	.98	.9990	25.51	-.15	.9979
24.6	1110	.25	24.501	1.24	.9988	24.790	.85	.9991	34.13	-.00	.9980
24.5	1020	.14	30.628	1.00	.9998	30.918	.59	.9999	55.94	-.46	.9979
24.4	970	.03	37.231	.64	.9998	37.751	.20	.9999	80.47	-.86	.9972
24.5	948	-.11	43.396	.51	.9999	43.394	.09	.9999	106.20	-.79	.9988
RUN 10- 12B			MAT WT.= 6.83			.000190M					
23.2	615	-.05	7.246	.21	.9973	8.204	-.07	.9998	13.35	-.02	.9967
24.2	460	.10	10.954	.46	.9981	11.742	.15	.9995	21.13	-.07	.9994
24.4	410	.15	12.850	.56	.9999	13.521	.24	.9999	27.69	-.17	.9989
24.4	372	.00	15.486	.48	.9999	16.161	.15	.9999	37.97	-.20	.9989
24.4	347	-.12	18.305	.37	.9992	18.859	.04	.9996	53.10	-.27	.9992
24.4	333	-.25	21.078	.30	.9998	21.695	-.03	.9996	74.12	-.27	.9993
24.4	325	-.45	24.612	.08	.9999	25.229	-.25	.9999	106.18	-.65	.9982
RUN 10- 14A			MAT WT.= 6.29			.000048M					
24.3	2150	.22	9.613	1.48	.9941	10.424	1.20	.9938	11.98	-.07	.9974
24.1	1640	.39	15.626	1.39	.9968	16.264	1.08	.9969	20.42	-.29	.9949
24.1	1390	.45	19.494	1.29	.9997	20.016	.96	.9998	15.51	.62	.9513
24.1	1230	.27	25.252	1.03	.9998	25.715	.67	.9999	38.83	-.26	.9994
24.0	1110	.15	31.208	.89	.9999	31.554	.53	.9999	61.08	-.67	.9982
24.0	1030	.06	38.785	.61	.9995	39.015	.24	.9993	87.35	-.71	.9987
24.0	1000	.00	44.504	.44	.9999	44.792	.06	.9997	120.45	-1.25	.9983
RUN 10- 14B			MAT WT.= 6.32			.000092M					
24.7	1130	.02	8.934	.95	.9999	11.799	.80	.9999	11.24	-.00	.9985
24.5	880	.24	13.815	1.04	.9996	17.226	.91	.9995	18.21	-.11	.9985
24.4	765	.30	15.067	1.15	.9967	18.905	1.02	.9975	22.67	.04	.9997
24.5	680	.34	19.269	.99	.9987	23.418	.87	.9990	33.70	-.17	.9998
24.5	610	.23	23.376	.87	.9999	27.779	.76	.9999	51.65	-.32	.9979
24.5	577	.05	26.773	.74	.9999	31.305	.64	.9999	74.76	-.66	.9972
24.5	557	-.05	32.656	.38	.9999	37.611	.25	.9999	103.90	-.93	.9985

TABLE XXB

SECOND STEP CALCULATIONS WITH STREAMING CURRENT DATA

Mat Thickness (L), in.	Mat Porosity, ε	Slope, (I_s/U)	Kozeny Factor: Experimental	Kozeny Factor: Davis Correlation	Calculated Zeta Potential, mv.: Capillary Model	Bieber +Mason (26)	Assuming N Varies	ζ_c (N = Const.)	
RUN 10- 12A			MAT WT.= 6.20		.000051M $CaCl_2$				
.338	.893	13.96	11.92	8.15	144.38	85.54	80.27	10.93	
.262	.862	19.78	12.08	6.93	135.00	84.34	72.68	12.76	
.225	.839	21.52	12.53	6.38	111.49	72.49	59.34	12.13	
.185	.804	24.79	12.04	5.87	86.46	59.90	46.20	11.49	
.155	.766	30.91	14.28	5.62	71.74	53.42	39.45	11.71	
.134	.730	37.75	15.30	5.56	60.09	48.15	34.46	11.83	
.120	.698	43.39	15.88	5.56	50.69	43.39	30.23	11.59	
H= 3.73	R= .9997					OVERALL AV. =		11.78±	4.83
					AV. (FIRST VALUE OMITTED) =			11.92±	3.93
RUN 10- 12B			MAT WT.= 6.83		.000190M $CaCl_2$				
.422	.905	8.20	12.24	8.86	102.29	59.34	57.72	6.93	
.285	.860	11.74	11.46	6.88	77.97	48.86	41.83	7.44	
.235	.830	13.52	11.19	6.22	63.05	41.65	33.43	7.21	
.196	.796	16.16	11.31	5.80	51.71	36.35	27.68	7.16	
.168	.762	18.85	11.90	5.61	42.02	31.52	23.14	6.98	
.146	.727	21.69	12.50	5.55	33.51	27.01	19.24	6.68	
.130	.693	25.22	13.84	5.56	28.06	24.28	16.79	6.55	
H= 4.43	R= .9984					OVERALL AV. =		6.99±	4.41
					AV. (FIRST VALUE OMITTED) =			7.00±	4.81
RUN 10- 14A			MAT WT.= 6.29		.000048M $CaCl_2$				
.435	.915	10.42	14.14	9.57	155.11	88.51	88.97	9.55	
.306	.880	16.26	14.99	7.56	139.76	84.63	76.52	11.67	
.241	.847	20.01	8.01	6.56	114.12	73.09	60.92	11.80	
.197	.813	25.71	14.50	5.98	99.11	67.49	52.78	12.51	
.159	.769	31.55	15.52	5.63	75.03	55.59	41.17	12.09	
.136	.730	39.01	16.24	5.56	62.04	49.70	35.58	12.21	
.123	.701	44.79	17.98	5.56	53.77	45.72	31.94	12.12	
H= 3.62	R= .9999					OVERALL AV. =		11.71±	8.46
					AV. (FIRST VALUE OMITTED) =			12.07±	2.47
RUN 10- 14B			MAT WT.= 6.32		.000092M $CaCl_2$				
.417	.911	11.79	12.54	9.27	163.86	94.13	93.33	10.50	
.298	.876	17.22	12.84	7.42	140.91	85.88	76.73	12.08	
.244	.848	18.90	11.87	6.59	109.46	69.96	58.38	11.22	
.198	.813	23.41	12.65	5.98	90.50	61.62	48.13	11.40	
.160	.769	27.77	13.25	5.64	66.47	49.22	36.40	10.67	
.139	.734	31.30	14.50	5.56	52.26	41.47	29.75	10.04	
.124	.702	37.61	15.72	5.56	45.70	38.78	27.07	10.24	
H= 4.12	R= .9884					OVERALL AV. =		10.88±	6.63
					AV. (FIRST VALUE OMITTED) =			10.94±	7.02